DEPARTMENT OF COMMERCE
SINCLAIR WEEKS, Secretary

WEATHER BUREAU
F. W. REICHELDERFER, Chief

MONTHLY WEATHER REVIEW

JAMES E. CASKEY, JR., Editor

Volume 84
Number 11

NOVEMBER 1956

Closed January 15, 1957
Issued February 15, 1957

DIURNAL VARIATION OF SURFACE PRESSURE OVER THE NORTH ATLANTIC OCEAN

STANLEY L. ROSENTHAL AND WERNER A. BAUM
Florida State University, Tallahassee, Fla.
[Manuscript received November 28, 1956]

ABSTRACT

Data from the Ocean Vessel Stations have been used to determine for each month (1) the daily variations of mean surface pressure, (2) the 3-hour mean-pressure tendencies, and (3) the phases and amplitudes of the first three harmonics of the daily variations. Some implications of the results are discussed briefly.

1. INTRODUCTION

With partial support from the U. S. Weather Bureau through a contract with its Office of Climatology, a study is being made of the utilization of ship observations in the specification of climatic conditions over the oceans. A phase of this study is concerned with diurnal variations of meteorological elements over the North Atlantic Ocean. This article is concerned with the diurnal variation of one of these elements, the surface (sea level) pressure, hereafter called simply "pressure."

The observations taken aboard the Ocean Vessel Stations (OVS) permit, for the first time, an analysis of diurnal variations over the ocean without the assumption that islands may be treated as representative of oceanic conditions. While the very presence of the ship may have some disturbing influence, any such effects should be considerably less significant than the presence of an island.

The OVS take surface observations at 3-hr. intervals. Thus, eight observations per day are available.

2. DATA

The OVS data were tabulated by the National Weather Records Center in the form of 3-hourly mean pressures for each individual month of the study period. The numbers of observations used in computing these means were also provided. To obtain a grand mean for a particular observation time and particular month, over the complete study period, each of the tabulated 3-hourly means, say the 0000 GMT means for December at station A, was multiplied by the number of observations used to construct it, and the results for all years of the study period were added together and divided by the total number of observations.

TABLE 1.—*Position of Ocean Vessel Station, portion of record utilized, and average number of observations employed in computing 3-hourly mean pressures*

Station	Latitude (° N.)	Longitude (°)	Portion of record utilized	Average number of observations per 3-hourly mean pressure
A	62.0	33.0 W	Jan. 1948–June 1954 [1]	155
B	56.5	51.0 W	July 1948–June 1955 [2]	184
C	52.8	35.5 W	Jan. 1947–May 1955 [3]	241
D	44.0	41.0 W	Sept. 1949–June 1955 [4]	164
E	35.0	48.0 W	Sept. 1949–May 1955	168
H	36.7	69.6 W	May 1949–June 1954	154
J	52.5	20.0 W	June 1950–Dec. 1954 [5]	96
K	45.0	16.0 W	July 1949–Dec. 1953 [6]	92
M	66.0	2.0 E	July 1948–Dec. 1953	166

[1] Less January and March 1954.
[2] Less August and October 1948, July and December 1953, January and December 1954, and April 1955.
[3] Less March 1949, and January and April 1955.
[4] Less December 1954, and April and May 1955.
[5] Less all of 1952.
[6] Less all of 1952, and May 1950.

TABLE 2.—*Mean monthly pressures (mb.) and mean departures from the mean monthly pressures. * denotes maxima of DVMP, ** denotes minima of DVMP. Time is in Local Standard (Zone) Time*

Time	Jan.	Feb.	Mar.	Apr.	May	June	July	Aug.	Sept.	Oct.	Nov.	Dec.
STATION M												
00	−0.43**	+0.31*	+0.05*	−0.54**	+0.35*	+0.05	+0.20*	−0.04	+0.25	+0.00	+0.52*	−0.30
03	−.03	+.01	−.15	−.54**	−.25	−.25**	−.20	−.24	−.05	−.10	+.12	−.30
06	−.13	−.39**	−.25**	−.34	−.45**	−.25**	−.30**	−.34**	−.25**	−.20**	−.08**	−.40**
09	+.27*	−.29	−.05	+.06	−.15	−.05	−.20	−.04	+.05*	+.10*	+.22*	+.20*
12	+.27*	+.01	+.25*	+.26	+.05	+.05	+.10	+.06	−.05	+.10*	−.08	+.20*
15	+.07	+.01	+.25*	+.46*	+.15*	+.15*	+.20*	+.26*	−.15**	−.10**	−.28**	+.10**
18	−.03	+.11	−.05**	+.46*	+.05**	+.15*	+.10**	+.16	−.15**	+.10*	−.18*	+.20
21	−.03	+.21	−.05**	+.16	+.25	+.15*	+.10**	+.16	+.35*	+.10*	−.28**	+.30*
Mean monthly pressure	1000.73	1000.79	1009.25	1003.04	1016.95	1012.65	1011.20	1008.74	1006.35	1006.40	1003.68	1000.00
STATION A												
01	−0.04	−0.33	−0.06	−0.26	−0.01	+0.07	−0.09	+0.31	+0.18	−0.07	+0.04	−0.32**
04	−.34**	−.71**	−.59**	−.66**	−.41**	−.33**	−.39**	−.39**	−.19**	−.30**	−.21**	−.51
07	−.24	−.57	−.52	−.26	−.11	−.23	−.19	−.29	−.02	−.14	+.18*	−.27
10	+.16	+.13	+.04	+.24	+.09*	+.07	+.21*	−.09	+.10*	+.11*	−.14	+.54*
13	+.26*	+.33	+.39*	+.44*	+.09*	+.17*	+.21*	+.11*	−.05	−.09	−.16	+.13**
16	−.24**	+.39	+.22**	+.14**	−.11**	−.13**	+.11	−.09**	−.27**	−.12**	−.26**	+.30
19	+.16	+.77*	+.42*	+.34*	+.09	−.13**	+.11	−.09**	−.16	+.22	+.05	+.36*
22	+.26*	−.05	+.07	+.04	+.12*	+.47*	+.01	+.51*	+.37*	+.35*	+.50*	+.28
Mean monthly pressure	992.34	995.63	1003.74	1008.76	1015.91	1010.13	1010.79	1008.99	1006.26	998.36	1000.59	993.68
STATION B												
00	+0.12	0.00	+0.03	+0.15	+0.04	+0.18	+0.24	+0.14	+0.01	+0.07	+0.02**	−0.21
03	−.28	−.50**	−.43**	−.25	−.26**	−.22**	−.16	−.26	−.29**	−.23**	+.02**	−.51**
06	−.38**	−.40	−.23	−.35**	−.16	−.12	−.26**	−.36**	−.19	−.13	+.02**	−.31
09	+.02*	+.30*	+.17*	−.05	+.14*	−.02*	−.06	−.06	+.11	+.17*	+.32*	−.01
12	+.02*	+.30*	+.17*	+.05*	+.14*	−.02*	−.06	+.04	+.21*	−.03	+.02	+.09*
15	−.18**	−.10**	−.13**	−.15**	−.06**	−.12**	−.06	+.04	−.09**	−.33**	−.28**	−.01**
18	+.22	+.20*	+.07	+.15	+.04	−.02	−.06	+.24*	+.01	−.03	+.02	+.39*
21	+.42*	+.20*	+.37*	+.45*	+.14*	+.38*	+.44*	+.24*	+.21*	+.47*	+.18*	+.39
Mean monthly pressure	1003.48	1006.40	1008.33	1011.75	1014.06	1010.62	1011.06	1009.16	1007.59	1005.13	1007.08	1004.71
STATION C												
01	+0.15	−0.21	+0.42*	−0.15	−0.24**	−0.21	+0.04	+0.14	−0.14	−0.30	−0.08	−0.26**
04	+.05	−.41**	−.28**	−.65**	−.24**	−.51**	−.36**	−.46**	−.44**	−.70**	−.28**	−.26**
07	−.25**	−.11	−.08	−.15	−.04	−.31	−.06	−.16	−.14	−.40	−.08	−.16
10	+.05*	+.29*	+.22*	+.25*	+.36*	+.09	+.14*	+.14*	+.26*	+.50*	+.42*	+.64*
13	−.25	+.29*	−.18	+.25*	+.26	+.19	+.14*	+.14*	+.16	+.20	−.18	+.04**
16	−.55**	−.11**	−.48**	+.05**	−.24**	+.19	−.06	−.16**	−.14**	−.00**	−.28**	+.16*
19	+.15	+.29*	−.08	+.15	−.04	+.29*	−.16**	+.04	+.06	+.50*	+.12	+.14
22	+.65*	−.01	+.42*	+.25*	+.16*	+.29*	+.34*	+.34*	+.26*	+.20	+.32*	+.04
Mean monthly pressure	1004.05	1008.41	1004.98	1012.25	1015.34	1010.91	1014.86	1012.86	1011.24	1006.60	1007.78	1007.26
STATION J												
02	−0.36**	−0.18	−0.14	−0.41	−0.15	−0.34	−0.10	−0.15	−0.23	−0.21	−0.66**	−0.04
05	−.36**	−.38**	−.74**	−.61**	−.55**	−.54**	−.40**	−.45**	−.53**	−.31**	−.56	−.54**
08	+.04	−.08	−.14	+.09	−.15	−.14	−.30	−.15	+.17	+.09	+.14	+.26*
11	+.84*	+.42*	+.16*	+.49*	+.15*	+.06	−.10	+.25*	+.37*	+.49*	+.84*	+.06
14	−.06**	−.18**	−.04	+.39	+.05	+.26*	+.10*	+.05	−.03	−.11	−.16**	−.44**
17	−.06**	−.18**	−.24**	−.01**	−.15**	+.26*	−.10**	−.15**	−.63**	−.31**	+.24	−.04
20	+.14*	+.32*	+.46	+.09*	+.25	+.26*	+.10	+.25	+.37	+.09	+.54*	+.46*
23	−.16	+.22	+.66*	−.01	+.55*	+.16	+.80*	+.35*	+.47*	+.29*	−.36	+.26
Mean monthly pressure	1012.76	1009.68	1010.14	1017.81	1014.75	1014.34	1014.30	1014.45	1008.23	1009.31	1005.26	1010.24
STATION K												
02	+0.05	−0.36	−0.28	−0.25	−0.22	−0.37	−0.28	−0.30	−0.26	−0.39	−0.38	−0.44
05	−.75**	−.86**	−.58**	−.75**	−.72**	−.67**	−.48**	−.80**	−.76**	−.59**	−.58**	−.74**
08	−.15	−.16	+.22	+.05	+.08	−.07	+.12	.00	+.24*	+.01	+.22	−.04
11	+.65*	+.54*	+.42*	+.55*	+.28*	+.33*	+.42*	+.10	+.14	+.61*	+.52*	+.50*
14	−.55**	−.36**	−.18	+.05	+.08	+.13	+.12**	+.20*	−.06	−.19**	−.38**	−.44**
17	+.25	+.04	−.28**	−.45**	−.22**	+.03**	+.28*	−.10**	−.16**	−.09	+.02	+.06
20	+.55*	+.64*	+.22	+.25	+.28	+.23	+.02**	+.40	+.44*	+.51*	+.32*	+.66*
23	+.45	+.54	+.52*	+.55*	+.48*	+.43*	+.42*	+.50*	+.44*	+.11	+.22	+.36
Mean monthly pressure	1019.25	1017.36	1019.88	1018.65	1015.92	1019.07	1020.98	1019.90	1017.46	1018.19	1015.18	1019.54
STATION D												
00	+0.29	+0.25	+0.35	+0.26	0.00	+0.20	+0.21	+0.14	+0.02	+0.04	+0.09	+0.24
03	−.01**	−.15	−.35**	−.54**	−.70**	−.60**	−.49**	−.46**	−.48**	−.36**	−.41**	−.06
06	+.09	−.25**	−.15	−.34	−.30	−.30	−.19	−.26	−.38	−.06	−.11	−.20**
09	+.89*	+.45*	+.35*	+.16*	+.30*	.00	+.21*	+.14*	+.32*	+.44*	+.59*	+.44*
12	−.51	−.05	+.25	+.06	+.30*	+.10*	+.11	+.04	+.22	−.06	−.11	−.36
15	−.01**	−.75**	−.65**	−.34**	.00**	.00**	−.19**	−.06**	−.28**	−.56**	−.61**	−.56**
18	−.31	−.05	−.25	−.04	.00**	.00**	−.19**	−.06**	+.02	+.14	+.09	+.04
21	+.59*	+.55*	+.45*	+.76*	+.40*	+.60*	+.51*	+.54*	+.52*	+.34*	+.49*	+.54*
Mean monthly pressure	1014.61	1014.85	1008.55	1016.34	1014.40	1018.30	1021.99	1019.66	1018.18	1016.06	1018.11	1016.16

TABLE 2.—*Mean monthly pressures (mb.) and mean departures from the mean monthly pressures. * denotes maxima of DVMP, ** denote minima of DVMP. Time is in Local Standard (Zone) Time*—Continued

Time	Jan.	Feb.	Mar.	Apr.	May	June	July	Aug.	Sept.	Oct.	Nov.	Dec.
STATION H												
01	−0.28	+0.11	−0.14	−0.26	−0.20	−0.14	−0.30	−0.21	−0.06	−0.15	−0.41	−0.36
04	−.58**	−.59**	−.74**	−.76**	−.50**	−.54**	−.50**	−.61**	−.46**	−.45**	−.61**	−.46**
07	−.18	+.21	+.36	+.34	−.30	+.26	+.20	+.19	+.24	+.35	+.29	+.34
10	+.92*	+.81*	+.96*	+.84*	+.40*	+.46*	+.60*	+.69*	+.74*	+.75*	+1.19*	+1.24*
13	−.38**	−.49	+.06	+.14	+.30	+.16	+.30	+.19	+.04	−.35	−.41	−.66**
16	−.18	−.79**	−.84**	−.56**	−.30**	−.34**	−.30**	−.31**	−.46**	−.65**	−.51**	−.46
19	+.12	+.21	−.04	−.16	.00	−.24	−.30**	−.21	−.36	+.05	+.19	+.24*
22	+.22*	+.51*	+.36*	+.44*	+.60*	+.36*	+.30*	+.29*	+.34*	+.45*	+.29*	+.14
Mean monthly pressure	1020.08	1016.49	1015.34	1016.26	1014.40	1016.44	1018.90	1017.21	1017.46	1017.35	1017.31	1019.06
STATION E												
00	+0.11	+0.34	+0.24	+0.24	+0.35	+0.25	+0.32	+0.44	+0.26	+0.15	+0.32	+0.25
03	−.19	−.36	−.66**	−.66**	−.85**	−.65**	−.58**	−.46**	−.54**	−.65**	−.38	−.15
06	−.59**	−.96**	−.56	−.56	−.45	−.45	−.38	−.26	−.44	−.55	−.48**	−.45**
09	+.61*	+.54	+.44	+.44	+.25	+.25	+.22	+.34	+.36	+.55*	+.62*	+.65*
12	+.41	+.64*	+.64*	+.54*	+.55*	+.45*	+.42*	+.44*	+.46*	+.45	+.32	+.25
15	−.69**	−.66**	−.46**	−.26**	−.05	+.05	−.08	−.16	−.44**	−.45**	−.68**	−.75**
18	+.01	−.16	−.16	−.26**	−.25**	−.35**	−.38**	−.36**	−.24	−.05	−.18	−.25
21	+.31*	+.64*	+.54*	+.54*	+.45*	+.45*	+.42*	+.64*	+.56*	+.55*	+.42*	+.45*
Mean monthly pressure	1022.69	1018.26	1015.46	1020.16	1019.05	1022.35	1024.08	1023.06	1020.94	1019.85	1021.28	1018.85

During World War II, the German submarine menace forced the OVS to be more transient than stationary. Under the circumstances, it is impossible completely to isolate temporal from spatial variations; therefore, OVS observations taken prior to 1946 were excluded from the computations. The OVS included are those for which at least three years of postwar records per month are available. The final selection of data is shown in table 1. Certain intervals within the study period have been excluded, as shown by the footnotes to the table; in some cases, there were obvious tabulation errors; in others, the stations were temporarily abandoned for one reason or another.

Eight mean pressures were computed for each month for each OVS, for 0000 GMT and each 3 hours thereafter. Thus, a total of 96 mean pressures was calculated for each OVS. The last column of table 1 gives the average number of individual observations used in constructing these 96 means.

3. DAILY VARIATION OF MEAN PRESSURE

Table 2 gives, for each OVS, the mean monthly pressures for each month of the year and the differences between the 3-hourly mean pressures and the mean monthly pressures (hereafter called "departures"). In this table, the time has been converted to Local Standard (Zone) Time. The tables are arranged according to decreasing latitude of the OVS.

Northernmost stations.—Stations M (66° N.) and A (62° N.) show erratic and complicated month-to-month changes of the daily variation of mean pressure (DVMP). At M, the times of the maxima and minima wander, in an apparently unsystematic fashion, from hour to hour during the course of the year Seven months show double maxima, five display a single maximum.

At A, while less complicated, the annual course of the DVMP is still far from systematic. All months, except December, show a minimum at 0400 LST. All months, except July, display an evening maximum at 1900 or 2200 LST. Most months show another maximum and minimum at hours varying through the year.

Moderately northward stations.—The annual changes of the DVMP at B (56.5° N.) and C (52.8° N.) are complicated but appear to be somewhat more systematic than those found at the northernmost stations. Station B (table 2) shows a definite tendency for the primary maximum to occur at 2100 LST. The time of the primary minimum appears to oscillate between 0300 and 0600 LST. The hours of the secondary maxima and minima vary erratically from month to month. Some preference is found, however, for a secondary maximum (minimum) at 0900 (1500) LST. The double structure vanishes in July and August.

At C, maxima occur fairly consistently at 1000 and 2200 LST. Minima tend to occur at 0400 and 1600 LST, the former hour being preferred for the primary minimum. The double structure disappears only in June.

Station J (52.5° N.) shows less erratic behavior than any of the four stations discussed thus far. A morning maximum appears at 1100 LST in nine months. The evening maximum occurs at 2000 LST in six months, at 2300 LST during the other six months. The primary maximum appears with about equal frequency in the morning and evening. Minima occur at 0500 and 1700 LST in almost all months, the former hour being strongly preferred for the primary minimum. The double structure vanishes only in June.

The three stations in this group show, generally, larger departures from the mean monthly pressures than do the two "northernmost" stations.

Moderately southward stations.—Stations K (45° N.) and D (44° N.) show generally larger departures than do the stations previously discussed. At K (table 2), the primary minimum occurs at 0500 LST in all months. The secondary minimum occurs at 1700 LST in the months March through June, August, and September; from

October through February it appears at 1400 LST. A morning maximum is found at 1100 LST in all months except August and September. A nocturnal maximum appears at 2300 LST in the months March through September, and at 2000 LST during the months October through February. An interesting feature is that the afternoon minimum and the nocturnal maximum occur three hours earlier during the fall and winter months than during the remainder of the year. On careful inspection, a similar phenomenon is observed at J.

Station D exhibits a nocturnal maximum at 2100 LST. This is the primary maximum in all months except October, November, and January. A morning maximum is found at 0900 LST in all months except June. Minima consistently occur at 0300 and 1500 LST, the primary minimum occuring at the latter hour from October through March, at the former hour during the remainder of the year.

Southernmost stations.—The month-to-month changes of the DVMP at H (36.7° N.) and E (35° N.) are fairly systematic. Station H (table 2) shows an 0400 LST minimum in all months. A daytime minimum occurs at 1600 LST from February through November; in December and January it appears at 1300 LST. The daytime minimum tends to be the secondary one in the warm months, the primary one in the cold months. A 1000 LST maximum occurs in all months. Another maximum is found at 2200 LST in all months except December.

Station E shows a 2100 LST maximum in all months. A morning maximum occurs at 1200 LST from February through September, and is displaced to 0900 LST during the rest of the year. Neither morning nor evening is preferred for the primary maximum; in fact, five months have equal strength of the two maxima. A nocturnal minimum is found at 0300 LST from March through October, three hours later during the remainder of the year. It is the primary minimum except in November, December, and January. A second minimum occurs at 1800 LST from May through August, three hours earlier in all other months.

Summary.—The data show that the month-to-month changes of the DVMP tend to become more systematic as the latitude decreases. It is also clear that, generally, the magnitudes of the departures become greater with decreasing latitude.

Possibly this latitudinal variation of the departures can partially explain the erratic annual variations of the DVMP in the higher latitudes. Results of statistical studies of this type are subject to sampling and round-off errors. In these computations, the same absolute error will, on the average, be a larger percentage error in the higher latitudes than in the lower ones. The higher percentage error in the higher latitudes may then be a partial explanation of the relatively greater erratic behavior of the DVMP in higher latitudes.

Diurnal variation of mean annual pressure.—Table 3 summarizes the mean annual pressures and the mean annual departures for each observation hour at each OVS. Time is given in GMT. The bottom row gives the correction in hours, which will convert GMT to LST.

TABLE 3.—*Mean annual pressures (mb.) and mean annual departures from the mean annual pressures. *denotes maxima of DVMP, **denotes minima of DVMP. Time is in* GMT. *Δt is the correction, in hours, which will convert* GMT *to* LST

Time	Station								
	M	A	B	C	J	K	D	H	E
00	−0.01	+0.33*	+0.29*	+0.27*	+0.29*	+0.39*	+0.53*	−0.03	+0.46*
03	−.21	−.02	+.06	−.08	−.23	−.29	+.16	+.35*	+.38
06	−.33**	−.35**	−.27**	−.38**	−.51**	−.67**	−.37**	−.19	−.33**
09	−.02	−.13	−.22	−.16	−.01	+.04	−.21	−.58**	−.46
12	+.07*	+.18	+.09*	+.29*	+.33*	+.44*	+.36*	+.19	+.43
15	+.04**	+.21*	+.08	+.08	−.01	−.12	.00	+.79*	+.49*
18	+.34*	+.04	−.12**	−.16**	−.10	−.15**	−.42**	−.08	−.07**
21	+.09	−.33**	+.10	+.11	+.27	+.37	−.07	−.46**	−.23
Mean annual pressure	1006.64	1003.76	1008.68	1009.81	1011.19	1018.52	1016.44	1017.14	1020.46
Δt	0	−2	−3	−2	−1	−1	−3	−5	−3

Except at M, there is a marked double structure of the DVMP. M being neglected, all stations have minima at the observation hours closest to 0400 and 1600 LST. All but M and E have maxima at the observation hours closest to 1000 and 2200 LST. At E, one maximum is found at the observation hour closest to 2200 LST, another at 1200 LST; however, the departure at 1200 LST is only 0.03 mb. greater than that at 0900 LST. Thus, the disagreement with the pattern at the other OVS is not great.

Of considerable interest is the fact that only H (M again being neglected) shows a pronounced forenoon maximum. At A, B, and D, well-developed primary maxima occur in the evening. At C, J, K, and E, the two maxima are about equal in intensity.

Pronounced primary minima are found at the observation hour closest to 0400 LST at B, C, J, and K. Other stations showing clearly defined primary minima at this time, although not as pronounced, are H and E. At A and D, the two minima are about equal in intensity. No station shows a strongly marked afternoon minimum, and only D shows a tendency for a primary minimum in the afternoon.

4. THREE-HOUR MEAN-PRESSURE TENDENCIES

Table 4 gives, for each OVS, the mean 3-hour mean-pressure tendencies (hereafter called "tendencies") for each observation hour of each month. Times in these tables are Greenwich Mean Time. The tendencies are computed as the net change of the mean pressure during the 3-hour period ending at the stated observation hour. Numerical values are given in units and tenths of millibars.

As expected from the preceding discussion, the magnitude of the tendency is clearly dependent on latitude, larger magnitudes being found at lower latitudes. Variations with month of the year and time of day are also in evidence. These variations, however, are more complicated than the latitudinal ones and, in some cases, appear to be almost random. The annual variation seems to favor smaller tendencies in the warm months and larger

TABLE 4.—*3-hour mean-pressure tendencies in units and tenths of millibars*

Time (GMT)	Jan.	Feb.	Mar.	Apr.	May	June	July	Aug.	Sept.	Oct.	Nov.	Dec.
STATION M												
00	−04	+01	+01	−07	+01	−01	+01	−02	−01	−01	+08	−06
03	+04	−03	−01	00	−06	−03	−04	−02	−03	−01	−04	00
06	−01	−04	−01	+02	−02	00	−01	−01	−02	−01	−02	−01
09	+04	+01	+02	+04	+03	+02	+01	+03	+03	+03	+03	+06
12	00	+03	+02	+02	+02	+01	+03	+01	−01	00	−03	00
15	−02	00	00	+02	+01	+01	+01	+02	−01	−02	−02	−01
18	−01	+01	−03	00	−01	00	−01	−01	00	+02	+01	+01
21	00	+01	00	−03	+02	00	00	00	+05	00	−01	+01
STATION A												
00	+01	−08	−04	−03	+03	+06	−01	+06	+05	+01	+05	−01
03	−03	−03	−01	−03	−01	−04	−01	−02	−02	−04	−05	−11
06	−03	−04	−05	−04	−04	−04	−03	−07	−04	−02	−03	+03
09	+01	+01	+01	+04	+03	+01	+02	+01	+02	+02	+04	+02
12	+04	+07	+06	+05	+02	+03	+04	+02	+01	+03	−03	+08
15	+01	+02	+04	+02	00	+01	00	+02	−02	−02	00	−04
18	−05	+06	−02	−03	−02	−03	−01	−02	−02	00	−01	+02
21	+04	+04	+02	+02	+02	00	00	00	+01	+03	+05	+01
STATION B												
00	+02	00	+03	+03	+01	+04	+05	00	+01	+05	−02	−03
03	−03	−02	−03	−03	−01	−02	−02	−01	−02	−04	+02	−06
06	−04	−05	−05	−04	−03	−04	−04	−04	−03	−03	00	−03
09	−01	+01	+02	−01	+01	+01	−01	−01	+01	+01	00	−02
12	+04	+07	+04	+03	+03	+01	+02	+03	+03	+03	+03	+03
15	00	00	00	+01	00	00	00	+01	+01	−01	−03	+01
18	−02	−04	−03	−02	−02	−01	00	00	−03	−03	−03	−01
21	+04	+03	+02	+03	+01	+01	00	+02	+01	+03	+03	+06
STATION C												
00	+05	−03	+05	+01	+02	00	+05	+03	+02	−03	+02	−01
03	−05	−02	00	−04	−04	−05	−03	−02	−04	−05	−04	−03
06	−01	−02	−07	−05	00	−03	−04	−06	−03	−04	−02	00
09	−03	+03	+02	+05	+02	+02	+03	+03	+03	+03	+02	+01
12	+03	+04	+03	+04	+04	+04	+02	+03	+04	+09	+05	+08
15	−03	00	−04	00	−01	+01	00	00	−01	−03	−06	−06
18	−03	−04	−03	−02	−05	00	−02	−03	−03	−02	−01	+01
21	+07	+04	+04	+01	+02	+01	−01	+02	+02	+05	+04	00
STATION J												
00	−03	−01	+02	−01	+03	−01	+07	+01	+01	+02	−09	−02
03	−02	−04	−08	−04	−07	−05	−09	−05	−07	−05	−03	−03
06	00	−02	−06	−02	−04	−02	−03	−03	−03	−01	+01	−05
09	+04	+03	+06	+07	+04	+04	+01	+03	+07	+04	+07	+08
12	+08	+05	+03	+04	+03	+02	+02	+04	+02	+04	+07	+02
15	−09	−06	−02	−01	−01	+02	+02	−02	−04	−06	−10	−05
18	00	00	−02	−04	−02	00	−02	−02	−06	−02	+04	+04
21	+02	+05	+07	+01	+04	00	+02	+02	+10	+04	+03	+05
STATION K												
00	−01	−01	+03	+03	+02	+02	+04	+01	00	−04	−01	−03
03	−04	−09	−08	−08	−07	−08	−07	−08	−07	−05	−06	−08
06	−08	−05	−03	−05	−05	−03	−02	−05	−05	−02	−02	−03
09	+06	+07	+08	+08	+08	+06	+06	+08	+10	+06	+08	+07
12	+08	+07	+02	+05	+02	+04	+03	+01	−01	+06	+03	+06
15	−12	−09	−06	−05	−02	−02	−03	+01	−02	−08	−09	−10
18	+03	+04	−01	−05	−03	−01	+02	−03	−01	+01	+04	+05
21	+08	+06	+05	+07	+05	+02	−03	+05	+06	+06	+03	+06
STATION D												
00	+09	+06	+07	+08	+04	+06	+07	+06	+05	+02	+04	+05
03	−03	−03	−01	−05	−04	−04	−03	−04	−05	−03	−04	−03
06	−03	−04	−07	−08	−07	+08	−07	−06	−05	−04	−05	−03
09	+01	−01	+02	+02	+04	+03	+03	+02	+01	+03	+03	−02
12	+08	+07	+05	+05	+06	+03	+04	+04	+07	+05	+07	+07
15	−14	−05	−01	−01	00	+01	−01	−01	−01	−05	−07	−08
18	−05	−07	−09	+04	−03	−01	−03	−01	−05	−05	−05	−02
21	+07	+07	+04	+03	+04	00	00	00	+03	+07	+07	+06
STATION H												
00	+03	+10	+08	+04	+03	+01	00	+01	+01	+07	+07	+07
03	+01	+03	+04	+06	+06	+06	+06	+05	+07	+04	+01	−01
06	−05	−04	−05	−07	−08	−05	−06	−05	−04	−06	−07	−05
09	−03	−07	−06	−05	−03	−04	−02	−04	−04	−03	−02	−01
12	+08	+08	+11	+11	+02	+08	+07	+08	+07	+08	+09	+08
15	+07	+06	+06	+05	+07	+02	+04	+05	+05	+04	+09	+09
18	−13	−13	−09	−07	−01	−03	−03	−05	−07	−11	−16	−19
21	+02	−03	−09	−07	−06	−05	−06	−05	−05	−03	−01	+02

TABLE 4.—*3-hour mean-pressure tendencies in units and tenths of millibars*—Continued

Time (GMT)	Jan.	Feb.	Mar.	Apr.	May	June	July	Aug.	Sept.	Oct.	Nov.	Dec.
STATION E												
00	+01	+03	+04	+06	+06	+06	+06	+05	+07	+04	+01	−01
03	−05	−04	−05	−07	−08	−05	−06	−05	−04	−06	−07	−05
06	−03	−07	−06	−05	−03	−04	−02	−04	−04	−03	−02	−01
09	+08	+08	+11	+11	+02	+08	+07	+08	+07	+08	+09	+08
12	+07	+06	+06	+05	+07	+02	+04	+05	+05	+04	+09	+09
15	−13	−13	−09	−07	−01	−03	−03	−05	−07	−11	−16	−19
18	+02	−03	−09	−07	−06	−05	−06	−05	−05	−03	−01	+02
21	+03	+10	+08	+04	+03	+01	00	+01	+01	+07	+07	+07

ones in the cold months; this, however, is a gross generalization and several of the tendencies do not conform with it.

From the synoptic point of view, the tendencies in the vicinity of the "northernmost" and "moderately northward" stations are probably negligible in comparison to the error made in correcting tendencies reported by moving ships. If one considers the strong horizontal pressure gradients usually observed in the vicinity of the "moderately southward" stations, it seems reasonable to suspect that the tendencies in the regions of these stations can also be neglected with respect to the motion error.

Stations H and E, the "southernmost" stations, show generally larger tendencies, than do the other OVS. Also, these stations are in areas where weak horizontal pressure gradients are more frequently observed. For these two reasons, the tendencies in the vicinity of these stations are more likely to be important in comparison with the error due to correction for ship motion.

Table 5 is presented to complete the overall picture of the 3-hour pressure tendencies. It gives, for each observation hour at each station, the tendency as obtained from the mean annual pressures.

For comparison of the tendencies at the OVS with those at continental stations at corresponding latitudes, the reader may utilize data published by the U. S. Weather Bureau [14, 15].

5. HARMONIC ANALYSIS OF THE DIURNAL VARIATION OF MEAN PRESSURE

In recent years there has been a considerable revival of interest in pressure oscillations and harmonic analysis of

TABLE 5.—*3-hour mean annual pressure tendencies in units and tenths of millibars. Time is in* GMT

Time	Station								
	M	A	B	C	J	K	D	H	E
00	−01	+06	+02	+02	+00	+00	+06	+04	+07
03	−02	−04	−02	−04	−05	−07	−04	+04	−02
06	−01	−03	−03	−03	−03	−04	−05	−05	−08
09	+03	+02	+01	+02	+05	+07	+02	−04	+00
12	+01	+03	+03	+05	+03	+04	+06	+08	+09
15	−00	+00	−00	−02	−03	−06	−04	+06	+00
18	+03	−02	−02	−02	−01	−00	−04	−09	−09
21	−03	−03	+02	+03	+04	+05	+04	−04	+02

the DVMP (for examples, see [4, 6, 7, 8, 12, 13, 16]). Included among these new works has been a discussion of the magnitudes of the harmonic constants under a purely oceanic regime by Haurwitz [8]. However, to the knowledge of the writers, no one has utilized the OVS data for computation of these harmonic constants. It was therefore deemed worthwhile to extend this investigation to include computations of the amplitudes and phase angles of the first three harmonics of the DVMP. Computations were made for all months of the year at each station, the results being summarized in tables 6 through 11.

In performance of such analyses, the generally preferred procedure, which was also employed here, is use of a sine series in the form

$$p=p_0+\sum_n p_n \sin\left(\frac{n\pi}{12}t+\phi_n\right),$$

where p is the mean pressure at time t, p_0 the pressure averaged over all hours and a complete month, n the harmonic, p_n the amplitude of the n'th harmonic, t the time in hours on a 24-hour clock, and ϕ_n is the phase angle, in radians of the n'th harmonic. Evaulation of p_n and ϕ_n is straightforward but tedious. For computational details, the reader is referred to Brooks and Carruthers [2].

The values of ϕ_n, given in tables 7, 9, 11, and 12 have been converted to local mean (*not* standard) time in hours. For the second and third harmonics, the times shown are those of the first maximum. The p_n, given in tables 6, 8, 10, and 12 are in millibars.

The primary objective here is to make these harmonic constants available to investigators primarily interested in pressure oscillations. However, it is of some interest briefly to compare these results with those of other empirical studies and with theoretical expectations.

First harmonic.—Most writers (for examples, see [4, 8, 9, 10, 16]) feel that the 24-hour oscillation is almost entirely due to the alternate heating and cooling of the air during the course of the day. If so, strong local, seasonal, and synoptic effects would be expected in p_1 and ϕ_1, and there is some confusion in the literature concerning representative values of ϕ_1. Chapman [4] states that the first harmonic has its maximum at about local noon. Humphreys [9] claims, without producing evidence, that at low elevations the maximum of the first harmonic occurs during the coldest hours, while at high elevations it is found during the warmest hours. Bartels [1] found the maximum near 0800 local time at Washington, D. C. At Bermuda, Haurwitz [8] found the maximum to be around local noon during the summer, between 1000 and 1100 local time during the winter.

The OVS show (table 7) large annual and spatial variations of ϕ_1. There is no evidence to support the choice of a particular ϕ_1 as representative of all months and/or all locations considered. This is consistent with the thoughts of Jenkins [10], who states that the first harmonic varies between oceans and continents, with latitude, and over the ocean between the major divisions thereof.

TABLE 6.—*Amplitude (mb) of the 24-hour harmonic of the DVMP*

Station	Jan.	Feb.	Mar.	Apr.	May	June	July	Aug.	Sept.	Oct.	Nov.	Dec.
M	0.25	0.27	0.17	0.53	0.28	0.21	0.22	0.26	0.16	0.08	0.23	0.28
A	.16	.41	.46	.45	.16	.13	.24	.23	.12	.16	.19	.30
B	.25	.26	.18	.25	.10	.15	.21	.26	.11	.11	.14	.20
C	.33	.25	.22	.32	.17	.11	.08	.14	.16	.42	.05	.04
J	.32	.12	.33	.40	.25	.38	.32	.19	.05	.07	.48	.18
K	.23	.39	.09	.16	.22	.32	.14	.34	.24	.26	.18	.23
D	.46	.20	.11	.25	.28	.29	.11	.19	.05	.06	.05	.20
H	.18	.16	.26	.26	.19	.17	.28	.26	.24	.17	.24	.23
E	.04	.16	.20	.21	.27	.23	.15	.08	.11	.20	.02	.11

TABLE 7.—*Local Mean Time (hours) of the maximum of the 24-hour harmonic of the DVMP*

Station	Jan.	Feb.	Mar.	Apr.	May	June	July	Aug.	Sept.	Oct.	Nov.	Dec.
M	22.9	20.6	15.1	15.3	19.2	17.4	18.2	17.0	22.6	16.8	3.7	8.8
A	16.9	15.3	15.6	15.2	17.8	20.1	14.9	20.5	.8	19.1	23.3	14.8
B	19.3	15.4	16.5	19.5	15.7	20.8	20.9	18.4	16.6	21.7	7.0	17.6
C	23.4	14.1	.6	16.6	11.8	16.5	16.3	18.1	15.8	15.5	19.6	15.9
J	12.5	17.4	19.4	13.5	19.0	15.7	20.4	17.9	18.6	11.6	13.7	18.7
K	20.4	18.4	7.2	16.5	17.3	16.8	11.4	17.8	18.2	15.8	15.6	17.6
D	3.3	1.0	2.4	20.2	15.6	18.6	19.2	18.7	11.7	23.4	.6	18.4
H	12.1	3.6	9.4	10.8	16.6	10.6	11.2	11.6	8.9	6.6	10.4	9.2
E	12.5	17.8	15.3	15.3	15.5	15.3	15.7	17.8	16.7	15.5	2.5	3.8

The amplitude of the first harmonic (p_1) is, according to Chapman [4], larger in summer than in winter. Bartels [1] and Haurwitz [8] have verified this with data for Washington and Bermuda, respectively. At the OVS (table 6), the months of maximum and minimum p_1 vary considerably from station to station. At all of the stations, there are several months of maximum and minimum p_1, so that no simple seasonal variation may be specified.

Second harmonic.—It is generally accepted (for examples, see [4, 7, 12, 16]) that the 12-hour pressure oscillation is produced by an interaction of the 12-hour component of the daily variation of mean air temperature and the 12-hour component of the solar tidal potential.

TABLE 8.—*Amplitude (mb) of the 12-hour harmonic of the DVMP*

Station	Jan.	Feb.	Mar.	Apr.	May	June	July	Aug.	Sept.	Oct.	Nov.	Dec.
M	0.20	0.15	0.16	0.13	0.21	0.07	0.13	0.06	0.21	0.11	0.18	0.18
A	.26	.16	.16	.19	.26	.29	.13	.30	.24	.24	.22	.32
B	.24	.33	.29	.22	.17	.19	.20	.13	.20	.31	.10	.25
C	.30	.20	.37	.28	.25	.18	.25	.29	.30	.35	.33	.28
J	.31	.34	.47	.28	.26	.13	.30	.30	.54	.37	.43	.38
K	.57	.56	.50	.59	.44	.36	.41	.40	.45	.36	.46	.52
D	.63	.49	.52	.48	.38	.34	.39	.33	.43	.45	.53	.40
H	.53	.71	.73	.66	.46	.43	.43	.48	.50	.62	.73	.70
E	.53	.77	.66	.61	.57	.50	.50	.55	.59	.63	.62	.58

TABLE 9.—*Local Mean Time (hours) of the first maximum of the 12-hour harmonic of the DVMP*

Station	Jan.	Feb.	Mar.	Apr.	May	June	July	Aug.	Sept.	Oct.	Nov.	Dec.
M	9.1	0.4	0.7	7.3	11.6	10.6	11.7	11.2	10.6	10.0	11.8	9.4
A	10.3	8.7	11.1	10.0	10.0	10.9	10.6	11.2	10.4	9.6	9.0	8.6
B	9.6	10.1	9.5	9.9	9.9	9.8	10.3	10.2	10.0	9.3	9.0	8.2
C	9.6	9.4	10.1	9.4	9.8	9.5	10.4	10.3	9.7	9.3	9.2	9.2
J	9.7	9.8	10.2	10.4	10.4	10.0	11.0	10.4	10.0	10.1	8.6	8.9
K	10.1	9.8	10.0	10.5	10.4	10.4	10.6	10.3	9.8	10.5	9.4	9.6
D	9.3	9.8	10.3	10.0	10.1	10.2	10.2	10.1	10.0	9.2	9.3	10.2
H	9.5	9.7	10.0	10.1	10.7	10.3	10.4	10.3	10.4	9.6	9.4	9.1
E	9.9	10.3	10.0	10.1	10.3	10.4	10.4	10.3	10.0	9.8	9.9	9.8

The resulting oscillation is supposedly greatly amplified by a resonance phenomenon. It has been shown [11] that the solar semidiurnal tidal potential (SSTP) exhibits maxima of almost equal strength in March and October, a primary minimum in June, and a secondary minimum in December. The SSTP is also strongly dependent on latitude, being largest at the equator and decreasing poleward in each hemisphere.

Spar [13,] in an empirical study, found the strongest variation of p_2 over the United States to be with latitude. He found a seasonal variation in fair agreement with that discerned by Hann [5] for Montevideo, Uruguay.

It is possible to identify, at almost all of the OVS (table 8), maxima and minima which appear to correspond to the maxima and minima of the SSTP. However, as was the case in the studies by Spar and Hann, these maxima and minima are sometimes displaced as much as two months relative to each other. Inspection of table 8 shows that the annual variation of p_2 is limited to two maxima and minima only at the two "southernmost" stations, the others showing additional maxima and minima which do not correspond to extremes of the SSTP.

Possible worthiness of further investigation of these additional maxima and minima must be left to the judgment of investigators more familiar with the results of p_2 computations. No attempt has been made here to evaluate the thermal effects on p_2. It is possible that further investigation would show many of the discrepancies between our results and the annual variation of the SSTP to be explicable on thermal grounds.

Time-space sections of p_2 were constructed along curves joining various combinations of the OVS. Values of p_2 for February and August were picked off these sections, plotted on maps, and subjected to isopleth analysis. The results are displayed in figures 1 and 2. These charts show strong meridional gradients of p_2 which apparently correspond to the latitudinal variations of the SSTP. Some fairly strong zonal gradients are also indicated. Also of interest is the marked change in the isopleth pattern between February and August. These features appear to be worthy of investigation by authorities in the field of pressure oscillations.

The phase angle of the second harmonic of the DVMP is relatively uniform over the earth's surface [4]. Almost everywhere, the first maximum occurs about 1000 local time. Chapman [3] has presented a theoretical explanation of this worldwide relative uniformity of ϕ_2. His theory, however, is far from complete, and there has been some conflicting empirical evidence [8, 12].

Spar's result for the United States [13] showed ϕ_2 to be latest in June and earliest in January. Haurwitz [8] and Chapman [4] found the annual variations of ϕ_2 at Bermuda and Kunamoto (33° N., 131° E.), respectively, to be similar to those found by Spar.

Table 9 shows that the annual variations of ϕ_2 differ considerably from one OVS to the next. The only consistency among stations appears to be a tendency for latest ϕ_2 to occur during summer and for earliest ϕ_2 to occur around November and December. Only M does not fit this pattern.

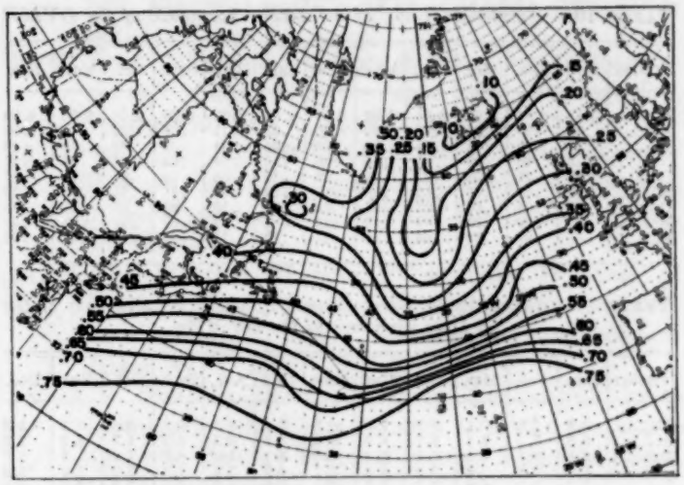

FIGURE 1.—Amplitude (mb.) of 12-hour harmonic of daily variation of mean pressure (DVMP) in February.

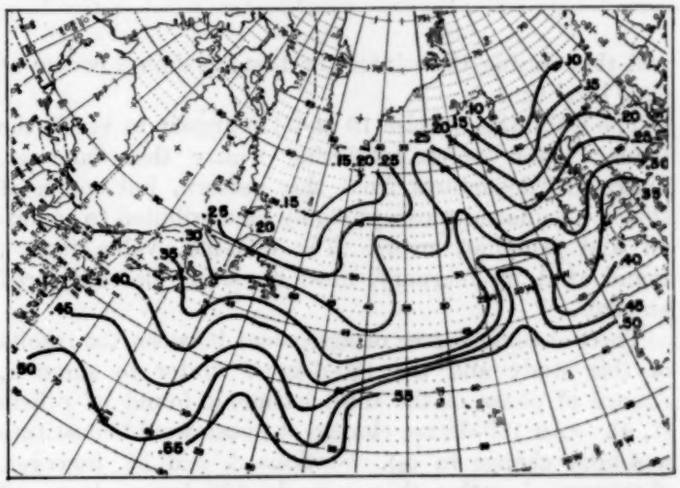

FIGURE 2.—Amplitude (mb.) of 12-hour harmonic of DVMP in August.

Third harmonic.—The 8-hour harmonic of the DVMP has been subject to less investigation than have the first two harmonics. The sun's tidal action has no appreciable component with an 8-hour period [4]. Therefore, the 8-hour pressure oscillation is usually assumed to be entirely a thermal phenomenon. Chapman [4] claims that p_3 resembles, in geographical and seasonal variation, the third harmonic of the daily variation of mean air temperature. Haurwitz [7] indicates that resonance also plays a small part in amplifying the thermally produced 8-hour oscillation.

There is evidence [1, 4, 8] that the 8-hour oscillation is largest in winter, has opposite phases north and south of the equator, and has opposite phases in summer and winter. Humphreys [9] states that p_3 reaches maxima at 30° latitude in each hemisphere, is zero at the equator,

TABLE 10.—*Amplitude (mb) of the 8-hour harmonic of the DVMP*

Station	Jan.	Feb.	Mar.	Apr.	May	June	July	Aug.	Sept.	Oct.	Nov.	Dec.
M	0.12	0.04	0.04	0.04	0.08	0.04	0.06	0.03	0.00	0.08	0.22	0.09
A	.10	.85	.09	.04	.06	.10	.07	.11	.07	.02	.15	.08
B	.07	.10	.04	.05	.02	.06	.06	.04	.03	.04	.15	.09
C	.15	.10	.08	.05	.03	.26	.11	.04	.04	.16	.08	.17
J	.22	.12	.04	.02	.13	.06	.19	.03	.10	.04	.27	.17
K	.30	.16	.07	.02	.08	.07	.09	.12	.11	.18	.16	.19
D	.15	.14	.05	.07	.07	.14	.11	.10	.05	.09	.11	.15
H	.23	.19	.04	.09	.13	.14	.12	.08	.09	.07	.21	.32
E	.31	.29	.09	.03	.14	.14	.13	.13	.07	.10	.17	.20

TABLE 11.—*Local Mean Time (hours) of the first maximum of the 8-hour harmonic of the DVMP*

Station	Jan.	Feb.	Mar.	Apr.	May	June	July	Aug.	Sept.	Oct.	Nov.	Dec.
M	3.4	2.6	7.1	3.9	7.9	6.3	7.5	0.2	6.7	2.5	7.2	3.3
A	3.9	7.5	2.4	6.7	6.3	6.0	1.5	6.8	6.7	4.7	6.2	7.7
B	2.6	1.8	4.5	3.5	1.2	5.9	6.1	1.4	4.2	4.4	.3	2.9
C	3.7	2.8	.6	7.2	4.2	3.7	6.5	7.2	5.2	2.2	1.9	2.2
J	2.7	2.9	6.8	7.2	6.5	6.2	6.5	4.3	5.0	3.3	2.4	2.3
K	2.4	2.2	.1	6.1	6.3	6.3	6.2	7.1	7.9	2.9	1.7	2.4
D	1.6	2.7	4.0	5.9	5.9	5.6	6.9	6.7	3.6	2.4	1.9	1.9
H	1.6	1.9	2.0	7.9	5.3	6.0	6.7	7.7	.0	1.6	2.1	2.0
E	2.3	2.5	3.2	4.4	6.3	6.2	6.1	5.8	3.9	2.3	2.0	2.3

and that during the winter the first maximum occurs at 0200 local time.

The OVS data (tables 10 and 11) appear to verify the tendency for larger p_3 during winter than summer. There are departures from this pattern, but much of this non-conformity can probably be attributed to round-off and sampling errors. The 0.85-mb. value for p_3, found at A in February, must obviously be considered an error.

There is some degree of agreement between the results of this study and the 180-degree, winter to summer, change of phase of the third harmonic found by others [1, 4]. (An 180-degree change of phase would constitute a 4-hour change in ϕ_3). Stations A and M, however, show several, rather than a single, 180-degree change of phase during the course of the year. A winter ϕ_3 of approximately 0200 local time, consistent with the findings of Humphreys [9], appears at B, D, E, H, J, and K.

A time section along the curve joining A, C, D, and E (not reproduced here) shows no evidence of the latitudinal variation of p_3 suggested by Humphreys.

Analysis of mean annual pressure.—Table 12 gives the harmonic constants for the first three harmonics of the diurnal variation of mean annual pressure.

The amplitude of the first harmonic (p_1) is apparently not a function of the latitude. The data show a tendency for larger p_1 to occur closer to land masses. (A rough isopleth analysis indicates a trough in the p_1 field which extends from the vicinity of A to the region just to the west of E.) The phase angle of the first harmonic (ϕ_1) appears to have complicated variations with both latitude and longitude. It is interesting to note that the western stations (B, D, E, and H) have ϕ_1's which roughly coincide with maxima of the second harmonic, while the eastern stations (M, A, C, J, and K) have

TABLE 12.—*Harmonic constants for the first 3 harmonics of the annual DVMP. Phase angles are tabulated as the Local Mean Time (hours) of the first maximum*

Station	p_1	ϕ_1	p_2	ϕ_2	p_3	ϕ_3
M	0.23	17.4	0.06	9.4	0.11	2.1
A	.12	14.7	.26	11.0	.14	6.6
B	.14	23.5	.20	9.2	.02	2.6
C	.13	16.1	.28	9.7	.03	2.5
J	.19	16.8	.33	10.0	.03	1.9
K	.22	17.2	.46	10.0	.06	1.9
D	.10	22.0	.44	9.8	.02	2.0
H	.17	10.6	.56	10.0	.07	1.8
E	.11	10.1	.59	10.1	.05	2.7

ϕ_1's which roughly coincide with minima of the second harmonic.

The latitudinal variation of p_2 is well pronounced. South of 55° N., no longitudinal variation is indicated. North of 55° N., the value at M of 0.06 mb. suggests an appreciable longitudinal variation in p_2. The exact, or even approximate, form of this variation cannot be determined on the basis of the data presented here. ϕ_2, on the whole, appears to have no strong spatial variations. The importance of the value of 11.0 LMT at A is difficult to estimate.

All stations except A show ϕ_3 in the vicinity of 0200 LMT. The value of 6.6 LMT at A is approximately 180 degrees out of phase with the other values. The largest values of p_3 occur to the northeast. Except for an immediate decrease to the south and west of the region of A and M, it is difficult to determine spatial variations of p_3.

ACKNOWLEDGMENTS

The writers wish to record their appreciation for assistance being rendered by Dr. H. Landsberg and Mr. Wm. Haggard of the Office of Climatology, U. S. Weather Bureau, and Messrs. L. Smith and N. Canfield of the National Weather Records Center, in pursuit of the study of which this analysis constitutes a phase.

REFERENCES

1. J. Bartels, "Tides in the Atmosphere," *Scientific Monthly*, vol. 35, 1932, pp. 110–130.
2. C. E. P. Brooks, and N. Carruthers, *Handbook of Statistical Methods in Meteorology*, H. M. Stationery Office, London, 1953, 412 pp.
3. S. Chapman, "The Semidiurnal Oscillation of the Atmosphere," *Quarterly Journal of the Royal Meteorological Society*, vol. 50, 1924, pp. 165–193.
4. S. Chapman, "Atmospheric Tides and Oscillations," *Compendium of Meteorology*, American Meteorological Society, Boston, 1951, pp. 510–530.
5. J. Hann "Die jährliche Periode der halbtägigen Luftdruckschwankung," *Sitzungs-Berichte, Akademie der Wissenschaften, Wien*, IIa, vol. 127, 1918, pp. 263–365.

6. M. F. Harris, "Pressure-Change Theory and the Daily Barometric Wave," *Journal of Meteorology*, vol. 12, No. 4, Aug. 1955, pp. 394–404.
7. B. Haurwitz, "Harmonic Analysis of the Diurnal Variations of Pressure and Temperature Aloft in the Eastern Caribbean," *Bulletin of the American Meteorological Society*, vol. 28, No. 7, Sept., 1947, pp. 319–323.
8. B. Haurwitz, "The Thermal Influence on the Daily Pressure Wave," *Bulletin of the American Meteorological Society*, vol. 36, No. 7, Sept. 1955, pp. 311–317.
9. W. J. Humphreys, *Physics of the Air*, (3d ed.), McGraw-Hill Book Co., Inc., New York, 1940, 661 pp.
10. G. R. Jenkins, "Diurnal Variation of the Meteorological Elements," *Handbook of Meteorology*, (F. A. Berry et al., eds.), McGraw-Hill Book Co., Inc., New York, 1945, pp. 746–753.
11. New York University, *Atmospheric Oscillations*, (Prog. Rep. 122–09, Contract AF19 (122)-49), New York, 1951.
12. J. Spar, "Thermal Influence in the Diurnal Pressure Wave," *Bulletin of the American Meteorological Society*, vol. 33, No. 8, Oct. 1952, pp. 339–343.
13. J. Spar, "Characteristics of the Semi-Diurnal Pressure Wave in the United States," *Bulletin of the American Meteorological Society*, vol. 33, No. 10, Dec. 1952, pp. 438–441.
14. U. S. Weather Bureau, "Ten-Year Normals of Pressure Tendencies and Hourly Station Pressures for the United States," Weather Bureau *Technical Paper* No. 1, 1943.
15. U. S. Weather Bureau, "Normal 3-Hourly Pressure Changes for the United States at the Intermediate Synoptic Hours," Weather Bureau *Technical Paper*, No. 1, Supplement, 1945.
16. M. V. Wilkes, *Oscillations of the Earth's Atmosphere*, Cambridge University Press, Cambridge 1949, 74 pp.

412896—57——2

CYCLONE FREQUENCIES IN THE UNITED STATES[1] FOR THE PERIOD 1905 TO 1954

C. L. HOSLER AND L. A. GAMAGE[2]

Department of Meteorology, College of Mineral Industries
The Pennsylvania State University, University Park, Pa.
[Manuscript received October 24, 1956; revised December 10, 1956]

Cyclone tracks as published in the *Monthly Weather Review* for the years 1905 through 1954, were used as a basis to tabulate the number of cyclones per month *passing through* each 5° grid of latitude and longitude in the United States. The number of cyclones passing through, entering, or leaving each grid for each month during the 50-year period was recorded and monthly means computed. The month-by-month data were scrutinized to discover whether, in addition to seasonal shifts in cyclone frequency, there might have been any systematic variation in frequency of a period longer than one year, or any trends in cyclone frequency that might have been related to extraterrestrial phenomena. The occurrence of any systematic latitudinal or longitudinal shift of the area of maximum frequency was also investigated. No true periodicities or trends were indicated and no tendency for a shift of the region of maximum frequency was noted.

The maps of figure 2 are reproduced here to illustrate the monthly pattern of cyclone frequency as revealed by the 50-year monthly means. The 5° grids are not everywhere equal in area so that different latitudes are not exactly comparable. The frequencies along the borders of the States are not as reliable as those inside the States due to the sparcity of data in these regions in the early years. These figures are not presented as an original contribution, but as a tabulation covering a longer period of time than could be considered by earlier investigators interested in cyclone frequencies. Discussion of these charts will be omitted, and the reader is referred to a paper by Klein [1] for a comprehensive treatment of cyclone tracks and frequencies in the Northern Hemisphere and for a complete bibliography on the subject.

Figure 1 shows a plot of the total number of cyclones for each year (1905–1955), obtained when the sums are taken of all grids for which data are available. The great variations in cyclone frequency shown in this chart do not seem to be correlated to sunspot number or earth magnetic character. It is interesting that the *variability* in cyclone frequency has increased throughout the 51-year period, and that this is paralleled by a similar increase

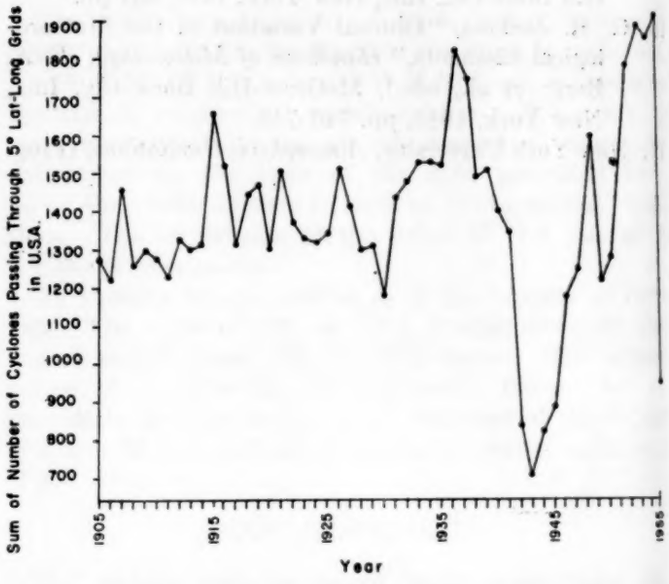

FIGURE 1.—Annual sums of number of cyclones counted in all 5° latitude-longitude grids in United States, for each year 1905 through 1955.

in the variability of sunspot numbers during the same period. The greatest deterrent to placing any interpretation on the variation in cyclone frequency from year to year lies in the fact that responsibility for defining and tracking the cyclones for charting in the *Monthly Weather Review* has changed hands frequently in the past 51 years, and the increased variability in cyclone frequency may be more closely related to the frequency with which the task of charting the cyclones changed hands than to any extraterrestrial influences. A basis for concluding that these variations are real might be the fact that since 1949 the WBAN Analysis Center (now National Weather Analysis Center) has applied a criterion defined on page 66 of the *Monthly Weather Review* for February 1949, and yet the variability in the frequencies has been nearly as great during the period 1949–1955 as during the preceding years.

The year-to-year changes in frequency are common to all areas; i. e., when the total for the United States increases, the number increases at all latitudes and all longitudes. This seems to indicate that the year-to-year

[1] Mineral Industries Experiment Station Contribution No. 56-27.
[2] L. A. Gamage, Major, U. S. A. F., presently stationed in London, England.

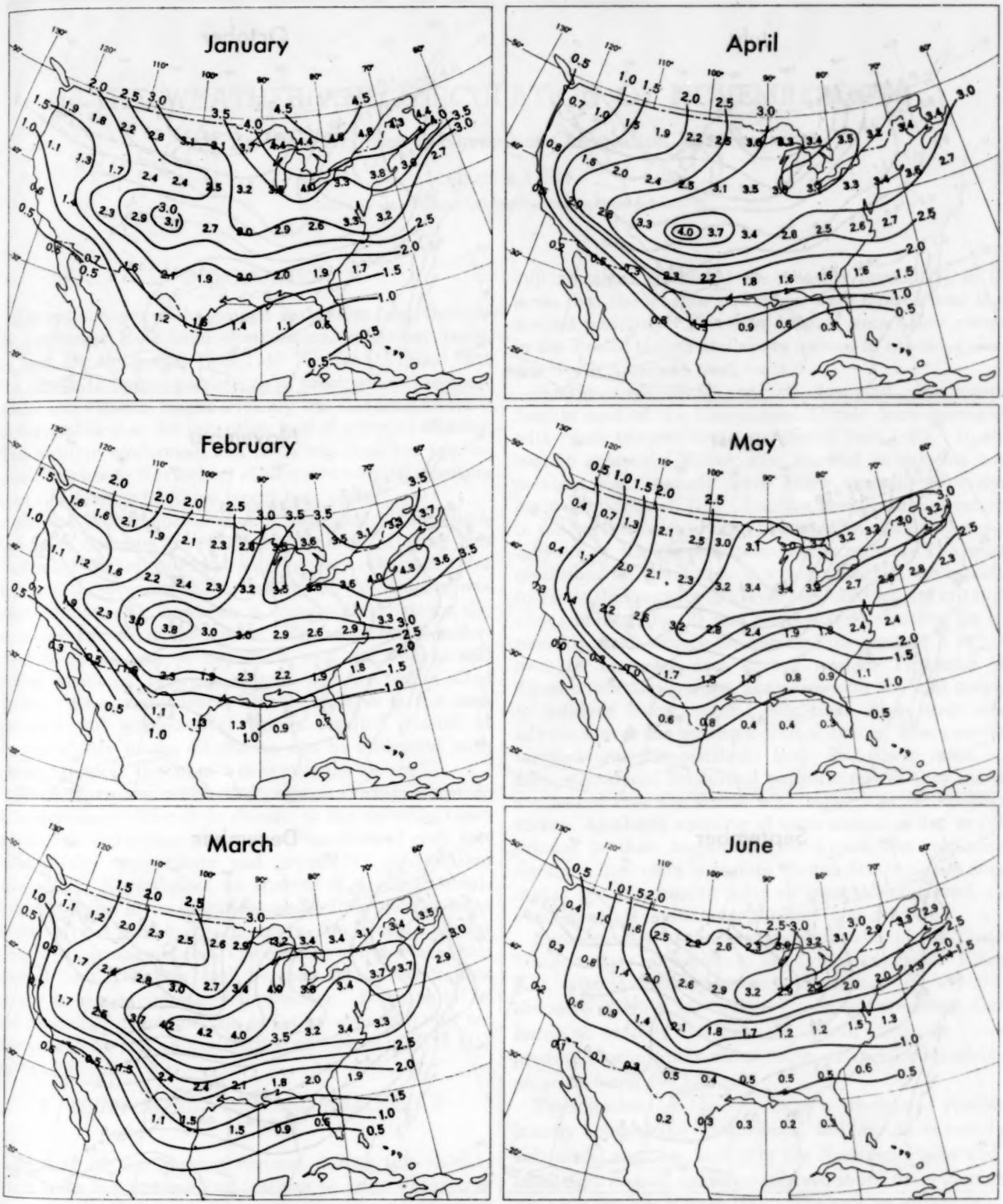

FIGURE 2.—Number of cyclones *passing through* each 5° latitude-longitude grid in the United States, by months, 1905 through 1954.
(Charts continued on following page.)

change in number cannot be attributed to lack of data in some particular area during one year or for a period of years.

The authors wish to acknowledge the help of Mr. Edward Epstein and Mr. Norman Richardson in tabulating these data.

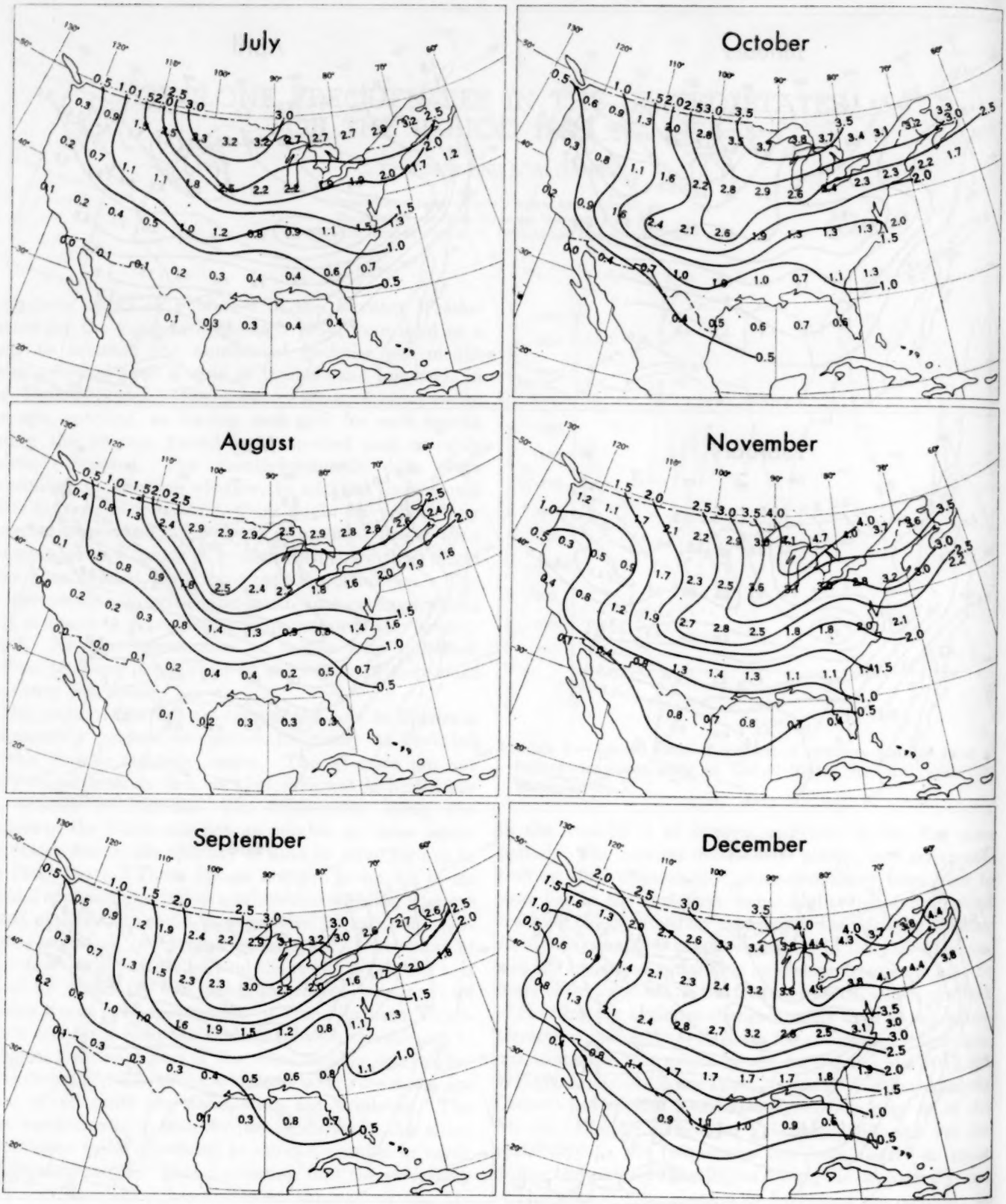

FIGURE 2—Continued.

REFERENCE

1. William H. Klein, "Principal Tracks and Mean Frequencies of Cyclones and Anticyclones in the Northern Hemisphere," U. S. Weather Bureau: *Research Paper* No. 40. (In press)

THE WEATHER AND CIRCULATION OF NOVEMBER 1956

Another October to November Circulation Reversal[1]

CARLOS R. DUNN

Extended Forecast Section, U. S. Weather Bureau, Washington, D. C.

1. INTRODUCTION

Abrupt changes of the general circulation from October to November have been characteristic of recent years. In fact, for the period 1942–1950 Namias [1] found that the month-to-month persistence of precipitation, temperature, and 700-mb. height anomaly was less from October to November than for any other pair of adjacent months. This autumn conformed, and there was even less persistence (October to November) of all meteorological elements than the average for these recent nine years.

Namias also indicated that intramonthly fluctuations had been common in recent Novembers. During this November several different regimes were observed. For the first three weeks the variability of the weather was most pronounced; however, a more stable pattern did exist near the end of the month. The mean waves underwent large changes in amplitude, and the troughs and ridges oscillated between eastern and western United States. As a consequence, notable changes in the temperature and precipitation regimes resulted. Much of the variability in the circulation can be associated with prior changes in the mean waves over the Pacific.

When there are contrasting regimes during a month, it is sometimes difficult to discern in the monthly mean circulation underlying physical explanations of each feature of the temperature and (especially) precipitation anomalies. Nevertheless, an analysis of the mean circulation in terms of its height departure from normal helps to reveal the components of mean flow responsible for these weather anomalies. The concept of departure from normal flow (DN flow) will be used extensively in this review to relate circulation to weather. Hawkins [2] in the preceding article of this series gave justification for this procedure and an explanation of how to use the DN flow at 700 mb.

2. MEAN CIRCULATION AND WEATHER OF THE MONTH

Because of the varying regimes during this month, there were few outstanding features or large departures from normal of the monthly mean maps in the Western Hemisphere (fig. 1 and Charts I, II, III, and XI). The 700-mb. chart resembled the monthly normal [3], in the sense that the troughs and ridges were located near their normal positions. However, heights were below normal in the Pacific trough and above normal in the ridge along the North American west coast.

Rather weak, ill-defined DN flow and near normal heights east of the Continental Divide were associated with small temperature anomalies (Chart I–B). In this eastern area only Miami, Fla., reached an extreme temperature class, namely much below normal. (For class limit definitions cf. [1].) Positive temperature anomalies in the northern tier of States resulted from a deficiency of cold air in the northwestern source region. The warm conditions for the month in western Canada are attested by mean thickness for the layer 1000–700 mb. up to 140 ft. above normal (fig. 2) and by positive anomalies for the monthly mean surface temperature (as great as +16° F.) over an extensive area in the western Provinces [4]. These anomalously warm airmasses were not cold enough to produce below normal conditions when they were advected over the northern United States, where normal temperatures are relatively low. But these same airmasses produced subnormal temperatures as they moved southward into the States with higher normal temperatures. Adiabatic warming of these airmasses due to subsidence in their trajectories southward was minimized since the flow aloft in eastern United States was cyclonic during the invasions of polar air from the northwest and even averaged cyclonic for the month as a whole.

Temperatures in the western mountains of the United States, where anticyclonic conditions prevailed (Chart XI), were lowered by radiational cooling. This will be discussed further in section 4. In southwestern California an easterly DN flow (fig. 1 and Chart XI, inset) produced foehn winds whose warm, dry properties created an acute forest fire hazard.

Precipitation for the month as a whole was predominantly light, as the West, South, and Southeast received subnormal amounts, and only the Northern Plains and a small area around Arkansas received much more than the monthly average (Chart III). The arid conditions in the West can be associated with the northerly DN flow observable in figure 1, while the heavier but conservative

[1] See Charts I–XVII following p. 419 for analyzed climatological data for the month.

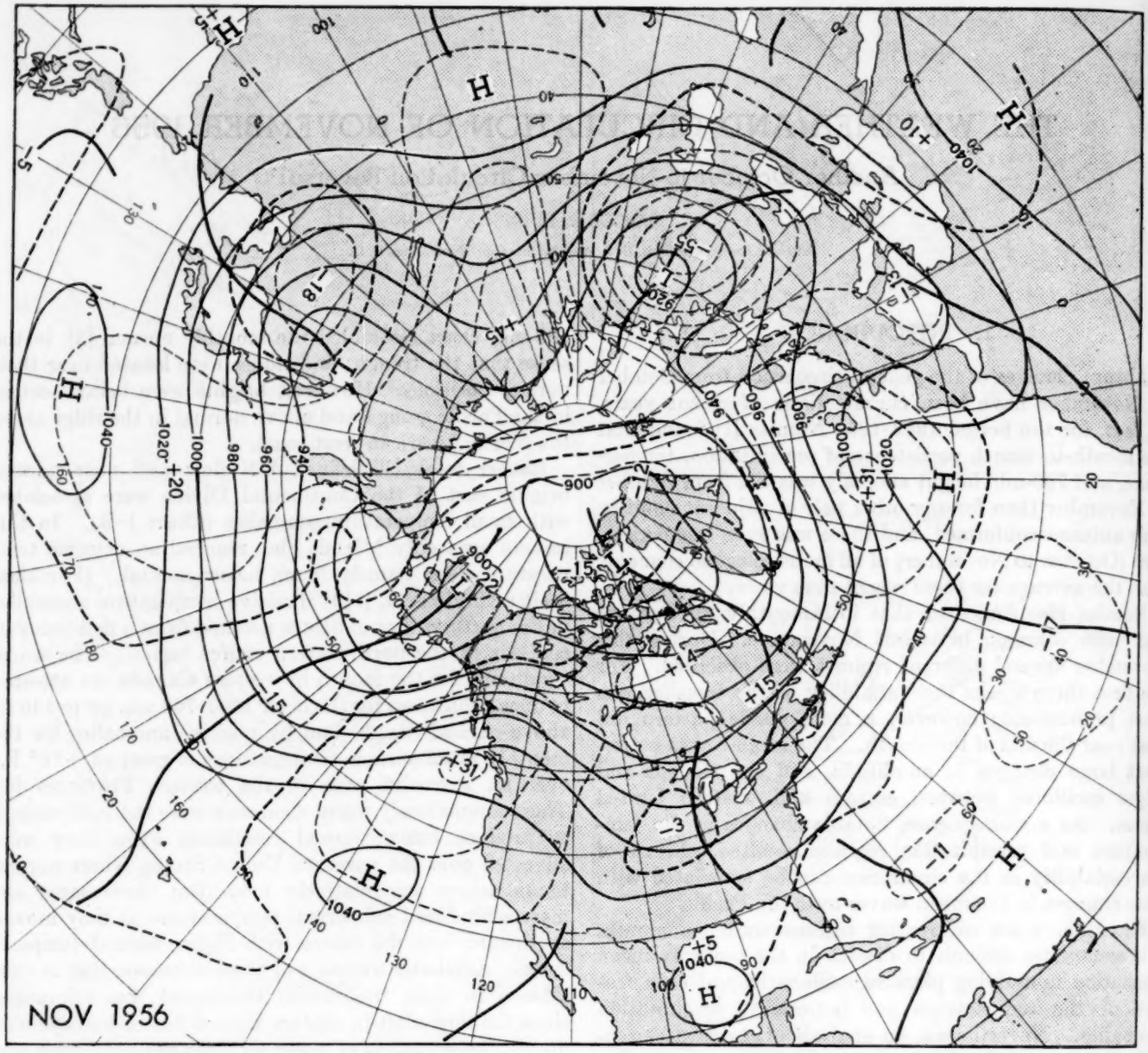

FIGURE 1.—Mean 700-mb. contours and height departures from normal (both in tens of feet) for November 1956. In the Western Hemisphere troughs and ridges were near the normal locations. Stronger than normal ridge in the West and weak trough in the East resulted in dry, cool weather in the United States.

amounts in the East occurred with a shallow mean trough and a deficiency of DN flow from the moisture sources.

3. REVERSAL FROM OCTOBER TO NOVEMBER 1956

The latitudinal wind speed profile for November (averaged over the Western Hemisphere) was similar to that of October since they both showed a northward displacement of the westerlies. This month the zonal winds were approximately 3 m. p. s. above normal north of 52° N., but roughly 3 m. p. s. below normal south of 52° N. (fig. 3). Also noteworthy was the emergence of a new relative maximum at about 38° N. which continued to develop and acted as a mechanism for displacing the westerlies southward in a discontinuous manner.

The similarity between October and November 1956 ends with the wind speed profile. Table 1 indicates that the absence during recent years of persistence from October to November was continued this fall. This reversal was most manifest in the 700-mb. lag correlation

TABLE 1.—*Measures of persistence of monthly mean anomalies in the United States area from October to November*

	1956	Average 1942–1950
700-mb. height (lag correlation)	−0.54	−0.30
Temperature (0 or 1 class change, percent)	51	58
Precipitation (0 class change, percent)	22	31

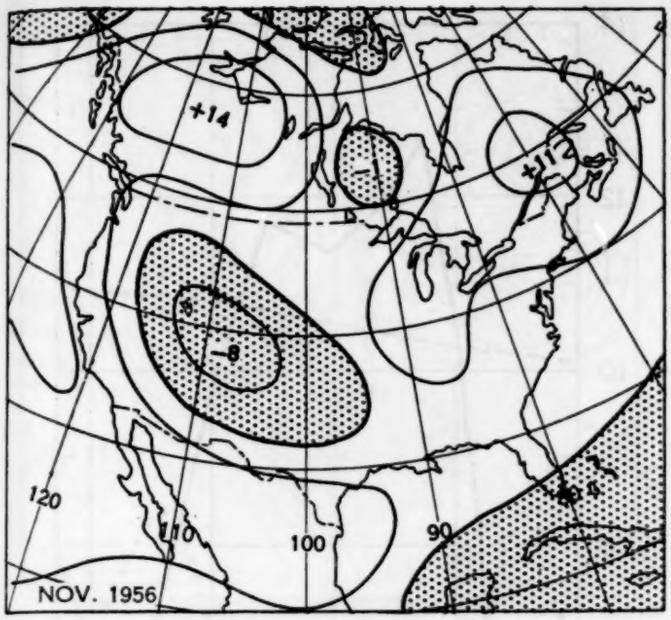

FIGURE 2.—Departure from normal (in tens of feet; 50-ft. isoline interval) of mean thickness of the 1,000–700-mb. layer for November 1956. Subnormal areas are stippled. Airmasses in the Canadian source region were abnormally warm.

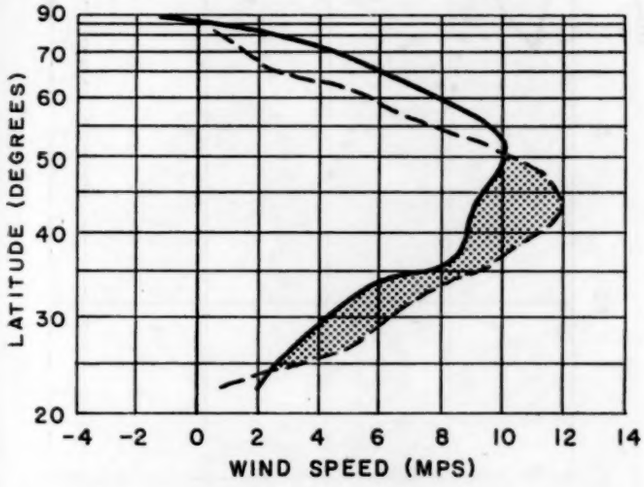

FIGURE 3.—Mean 700-mb. zonal wind speed profiles in the Western Hemisphere for November 1956 (solid) and November normal (dashed). Similar to October, the westerlies were above and below normal (stippled) north and south of 52° N., respectively.

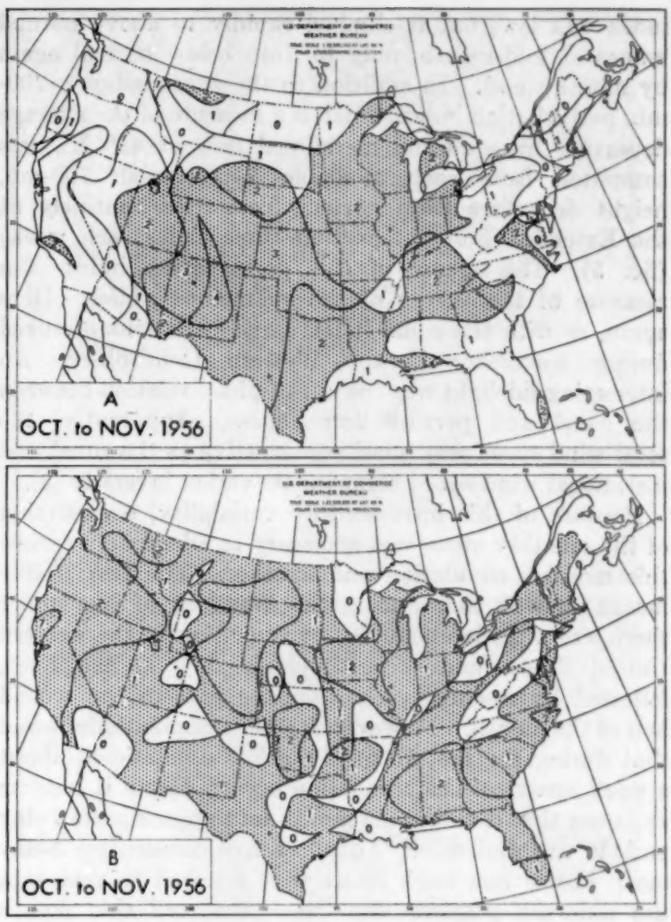

FIGURE 4.—Number of classes the anomaly of temperature (A) and precipitation (B) changed from October to November 1956. Lack of persistence observed during recent autumns was also characteristic of this year. Temperature anomalies changed notably in the Central Plains, and precipitation changed class in most areas.

of −0.54, but it was also reflected in the temperature and precipitation anomalies, which showed less than the expected small persistence for this time of year. The precipitation class changed at 78 percent of the stations in the United States. The temperature variation was not outstanding, but nevertheless it was greater than Namias' short-period average and what would be expected by chance. Unsmoothed charts of the class change of temperature and precipitation anomalies from October to November are shown in figure 4. There were only small scattered areas in which the precipitation class did not vary. The temperature class changes occurred mainly in the central portions of the country. Largest changes in temperature anomaly (from much above to below and much below normal) occurred in the southern Great Plains, where the DN flow reversed its direction from October to November. In some areas temperatures persisted from October, even though there was a change in circulation. A relevant example is the northern Great Basin area, which was cooled in October by an influx of cold maritime air under generally cyclonic conditions aloft [2], and remained cool in November under anticyclonic conditions, which enhanced radiational cooling (fig. 1 and Chart XI).

4. ANALYSIS BY WEEKLY PERIODS

Integrated with the October to November change in regime were the short-period, contrasting circulation and weather patterns of November. Variations of the 5-day mean zonal index (fig. 5) suggested that large circulation changes took place this month. Early in November the

index was low, but it climbed rapidly to above normal values at mid-month, only to drop below normal again by month's end. In addition to the zonal index, a 700-mb. perturbation index, which is a measure of the average departure from normal meridional flow at 45° N., was computed from each available 5-day mean 700-mb. height departure from normal (computed routinely at the Extended Forecast Section three times each week) (fig. 5). The square of this perturbation index is a measure of the energy of the anomalous eddies. Here again, as with the zonal index, large variations occurred during November in the Western Hemisphere. An interesting sidelight was the out-of-phase relation between the zonal and perturbation indices. Apparently, the total wind speed was quasi-conservative as the zonal and meridional wind speed components varied inversely [5].

Because of this intramonthly variability, a dissection of the monthly mean was necessary to adequately review this month's circulation and weather. The two 15-day means showed that during the first half of November there was a predominance of cyclonic flow in the western United States and of anticyclonic flow in the East, followed by essentially the opposite pattern the second half of the month. However, further examination showed that during the first 15 days marked oscillations (about a week apart) of the circulation occurred, and it became apparent that dividing the month into approximate 7-day periods was desirable. Therefore five consecutive 5-day mean charts one week apart were selected to represent the different patterns that were observed this month (fig. 6). These selected periods also correspond to periods of high zonal and low perturbation indices and vice versa. The concomitant weekly mean temperature anomalies and precipitation amounts from the *Weekly Weather and Crop Bulletin, National Summary,* [6] are also displayed (figs. 7, 8).

A. First week.—This period (fig. 6, Oct. 30–Nov. 3) was characterized by a large-amplitude, short wavelength flow, as suggested by the high perturbation index (fig. 5). Anticyclonic flow in the Northeast was retained from October [2]. The trough which previously had been along the west coast progressed rapidly into the Great Plains, where it was accompanied by vigorous cyclonic activity. Cold maritime air flooded the West under cyclonic flow and below normal heights at 700 mb. As a result the Southwest had the coldest average weekly temperatures (anomaly-wise) for the United States during the entire month (fig. 7.) This contrasted sharply with warm weather in the Northeast, as shown by an extreme difference of 30° F. in weekly temperature anomaly between Arizona and Michigan.

Precipitation which fell along the west coast (see fig. 8) was associated with cyclonic 700-mb. flow with a stronger than normal component against the mountains. Heavy rains, snowstorms, and blizzards were reported in areas of the Central Plains which were near the upper mean trough. In this region cyclonic flow aloft and strong DN flow from the Gulf of Mexico combined to produce

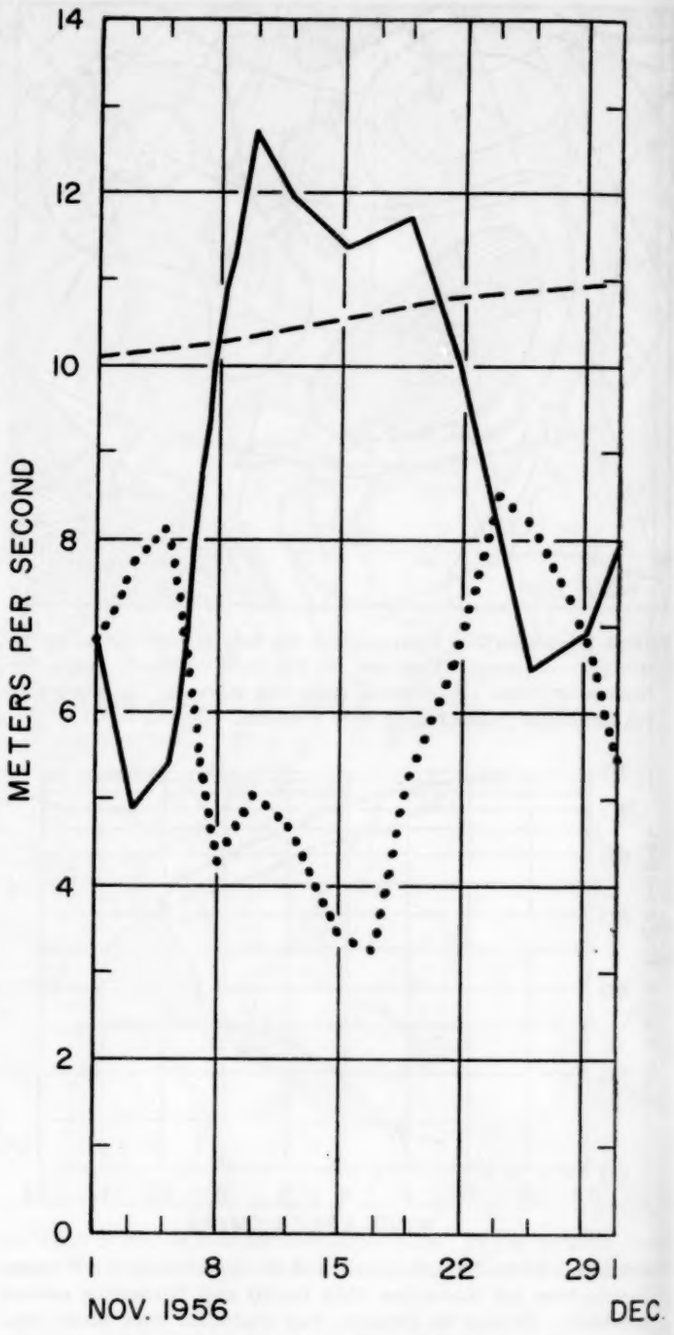

FIGURE 5.—Time variation of temperate-latitude zonal index (average strength in meters per second of 700-mb. zonal westerlies between 35° N. and 55° N. and from 5° W. westward to 175° E.) for November 1956. The solid line connects 5-day mean zonal index values (plotted at middle of the period). Dashed line shows variation of normal zonal index values. Dotted line is the time variation of the 5-day mean perturbation index (measure of the departure from normal meridional flow or the average of 10° longitude intervals of DN flow at 45° N. from 5° W. westward to 175° W.). Interesting out-of-phase relation existed between zonal and perturbation indices.

sizable amounts of precipitation (up to 4 inches in Texas). Along the eastern seaboard strong easterly DN flow was associated with heavy rainfall. In fact, as the wavelength shortened over the States and the ridge in the

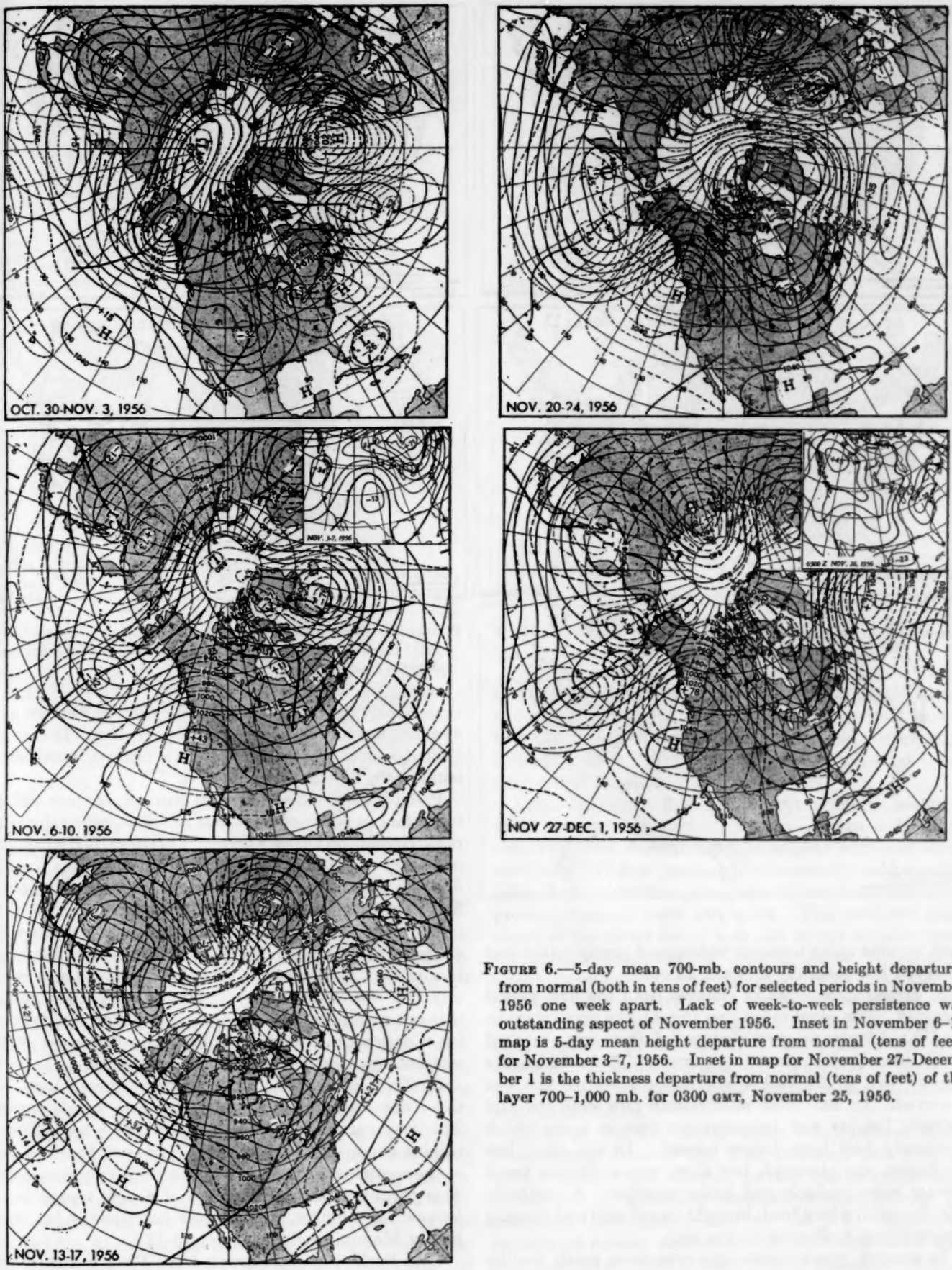

FIGURE 6.—5-day mean 700-mb. contours and height departures from normal (both in tens of feet) for selected periods in November 1956 one week apart. Lack of week-to-week persistence was outstanding aspect of November 1956. Inset in November 6–10 map is 5-day mean height departure from normal (tens of feet) for November 3–7, 1956. Inset in map for November 27–December 1 is the thickness departure from normal (tens of feet) of the layer 700–1,000 mb. for 0300 GMT, November 25, 1956.

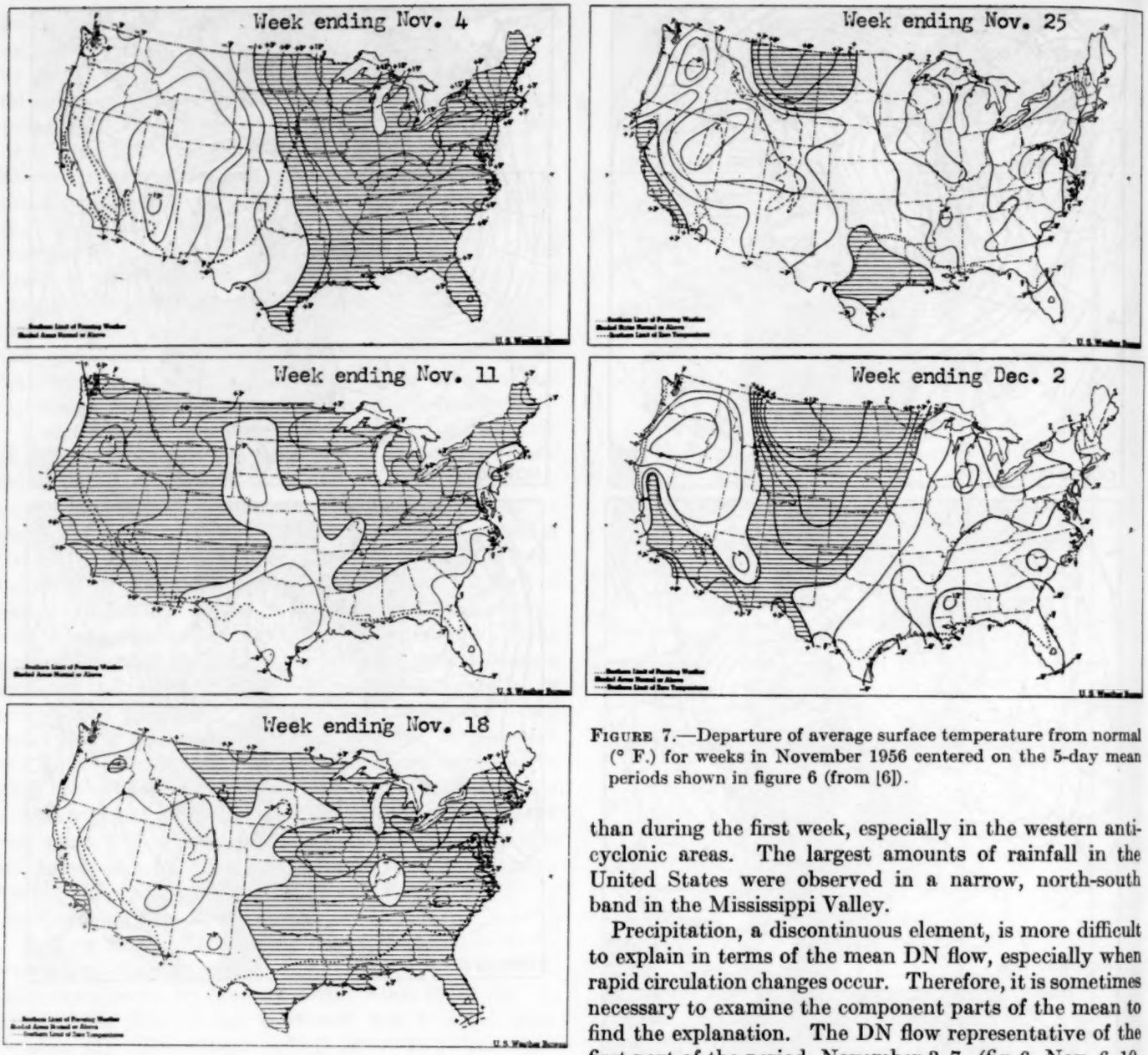

FIGURE 7.—Departure of average surface temperature from normal (° F.) for weeks in November 1956 centered on the 5-day mean periods shown in figure 6 (from [6]).

East became quite tenuous, widespread precipitation was observed but generally in small amounts.

B. Second week.—Major changes from the first period occurred. The zonal index rose (fig. 5), the mean wave in the United States progressed eastward, there was a marked oscillation about the monthly normal of 700-mb. heights (fig. 6, Nov. 6–10), and a new temperature pattern was observed. In the West anticyclonic flow emerged and 700-mb. heights and temperatures rose in areas which previously had been below normal. In the East less oscillation was observed, but there was a definite trend toward more cyclonic and cooler weather. A northerly DN flow with a long fetch brought record cold and freezing temperatures to Florida on the 10th.

In general, precipitation amounts were much smaller than during the first week, especially in the western anticyclonic areas. The largest amounts of rainfall in the United States were observed in a narrow, north-south band in the Mississippi Valley.

Precipitation, a discontinuous element, is more difficult to explain in terms of the mean DN flow, especially when rapid circulation changes occur. Therefore, it is sometimes necessary to examine the component parts of the mean to find the explanation. The DN flow representative of the first part of the period, November 3–7, (fig. 6, Nov. 6–10, inset) when the precipitation occurred, was southerly and advected moist air from the Gulf of Mexico into the heavy rain areas. As the week's circulation evolved and northerly DN was introduced over almost the entire country, it is not surprising that the early wet period was followed by a desiccating trend, with less than 6 percent of the stations reporting precipitation by the 10th.

C. Third week.—The zonal index remained high, but there was a significant return to the first week's pattern. This was particularly true in the West, where 700-mb. heights averaged below normal. The east Pacific trough of the second week filled, creating a very long wavelength. This permitted the introduction of a new trough in the favored area (under fast westerly flow) to the lee of the Rocky Mountains (fig. 6, Nov. 13–17).

Cold Pacific air again invaded the West, reducing tem-

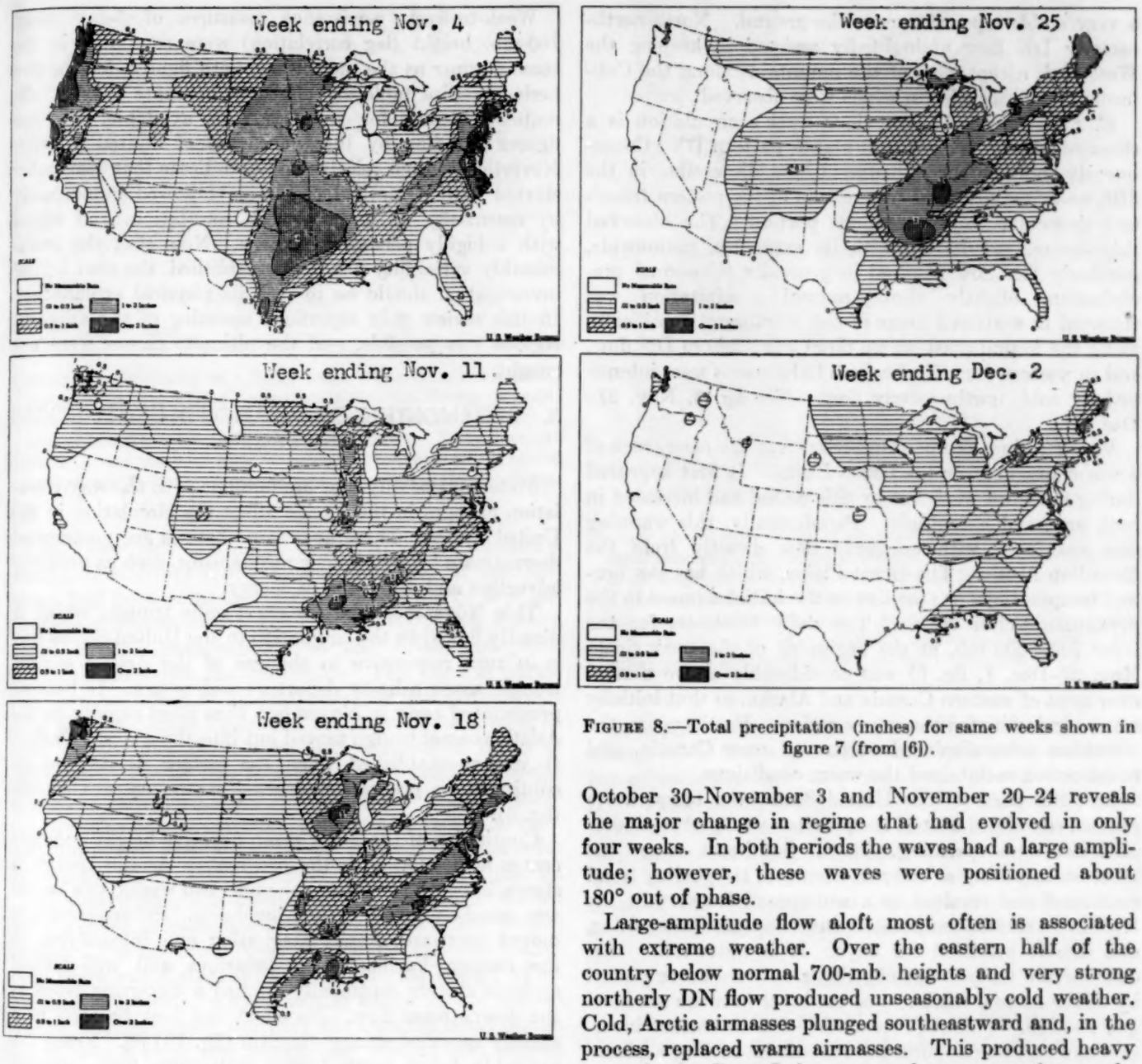

FIGURE 8.—Total precipitation (inches) for same weeks shown in figure 7 (from [6]).

peratures to subnormal values. In the East southerly wind components were associated with a general warming trend.

Sizable amounts of precipitation fell from the Central Plains eastward to the Atlantic Seaboard, associated with cyclonic winds aloft and southerly DN flow. On the Washington coast faster than normal westerly winds intensified the usual orographic precipitation.

D. Fourth week.—The return of a deep trough to the eastern Pacific effected another rapid readjustment of the circulation over the United States. The resulting pattern resembled the second week. The mean waves had a large amplitude, which is to be expected with a high perturbation index. Although this index was also high during the first week, only a superficial comparison of the maps for October 30–November 3 and November 20–24 reveals the major change in regime that had evolved in only four weeks. In both periods the waves had a large amplitude; however, these waves were positioned about 180° out of phase.

Large-amplitude flow aloft most often is associated with extreme weather. Over the eastern half of the country below normal 700-mb. heights and very strong northerly DN flow produced unseasonably cold weather. Cold, Arctic airmasses plunged southeastward and, in the process, replaced warm airmasses. This produced heavy snows in the Great Lakes area and severe weather reaching tornadic proportions in New England. Much of the week's precipitation was associated with one vigorous storm which originated in the Southern Plains on the 19th and subsequently moved northeastward through the Great Lakes. In the Southwest there was a continued absence of precipitation and fog. This was of particular interest since a serious forest fire problem continued to exist in California.

Although 700-mb. 5-day mean temperatures in the mountainous areas of the West increased and averaged above normal (not shown), surface temperatures failed to respond to the rising constant-pressure heights and increasing anticyclonic flow at 700 mb. Apparently, radiational cooling associated with the Great Basin High continued to cool the initially cold airmass and produced

a very stable lapse rate near the ground. North-northeasterly DN flow undoubtedly assisted in keeping the West cool, except west of the mountains along the California coast where foehn winds were observed.

E. Fifth week.—The previous week's circulation is a climatologically favored and stable pattern [7]. Consequently, only minor adjustment was discernible in the fifth week, mainly some progression of the eastern trough and deepening in its southern portion. The observed ridge-trough orientation with its extensive, nationwide, northerly DN flow resulted in generally subnormal precipitation. Slightly above normal precipitation was reported in scattered areas of the Northeast, specifically along the Maine coast where there was onshore DN flow, and in western New York where Lake snows were intensified by cold, northwesterly flow. (See fig. 6, Nov. 27–Dec. 1.)

Very striking (temperature-wise) was the emergence of a warm tongue over the Great Plains. It first appeared during the third week but by this period had increased in both area and magnitude. Paradoxically, this warming was associated with northerly flow directly from the Canadian Arctic. The Great Plains, which has low normal temperatures, is sensitive to the initial airmass in the proximate source region. The daily thickness for the layer 700–1000 mb. at the beginning of the week (inset Nov. 27–Dec. 1, fig. 6) was considerably above normal over most of western Canada and Alaska, so that initially warm air dominated the source region. Furthermore, the westerlies were displaced northward over Canada, and foehn action maintained the warm conditions.

In other parts of the United States the temperature pattern resembled that of the previous week, when similar processes were operating. In the Southeast, where the greatest deepening at 700 mb. occurred, the cooling trend continued and resulted in a widespread freeze. In the Northwest surface temperature inversions, radiational fog, and drizzle persisted for days. It is noteworthy that cold surface temperatures in this area were accompanied by above normal thickness of the layer between sea level and 700 mb. This requires a very shallow surface inversion and further supports the radiational cooling explanation for subnormal temperatures in the northern Great Basin.

F. Summary.—This rather brief examination of the five weekly periods substantiates the a priori opinion that major circulation changes were prevalent in November. Additional analysis of a statistical nature produced significant and interesting results.

TABLE 2.—*Lag correlations for 5-day mean 700-mb. height anomalies in the United States area*

Periods (1956)	Correlation coefficient
Oct. 30–Nov. 3 to Nov. 6–10	−0.57
Nov. 6–10 to Nov. 13–17	−0.14
Nov. 13–17 to Nov. 20–24	−0.10
Nov. 20–24 to Nov. 27–Dec. 1	+0.77

Week-to-week persistence measures of 5-day mean 700-mb. height (lag correlation) were computed in the same manner as the month-to-month figures, for the five periods. (See table 2.) It is unfortunate that no climatological data for comparison are available, for these figures standing by themselves are of limited interest. Nevertheless their relative values indicate that November started with a marked oscillation followed immediately by essentially no week-to-week correlation, and ended with a highly persistent pattern. Now that the intramonthly variability has been established, the next logical investigation should be to seek its physical explanation. In this review only superficial scanning of the adjacent regions was possible, and the ultimate causes were not sought.

5. INTRAMONTHLY CIRCULATION IN UNITED STATES AND PACIFIC

Meteorologists by now are familiar with the way circulation changes in the Pacific affect the circulation in the United States. These upstream changes are propagated downstream by well-known mechanisms, such as vorticity advection and dispersion of energy.

This November, the eastern Pacific trough, which is directly linked to the circulation in the United States and is in turn responsive to changes of the Asiatic coastal trough, made a hasty departure and return. It became pronounced early in November, then filled rapidly as the Asiatic coastal trough moved out into the western Pacific. It was re-established when the former Asiatic trough continued to progress and reached the eastern Pacific (fig. 6).

Continuity of the 5-day mean negative height anomaly center associated with the progressive Asiatic trough is shown in figure 9. During the first two weeks, this center was quasi-stationary over Manchuria. Subsequently, it moved eastward, finally stagnating and intensifying in the eastern Pacific. This tenacious and well-defined cyclonic system continually applied a distorting force to the downstream flow. Its effect can best be seen in a slightly modified energy diagram (fig. 10) [8]. From the available 5-day mean height departures from normal, differences were computed for 10° longitude intervals at 45° N. in the Western Hemisphere. These differences in height anomaly are proportional to the meridional DN flow. (The average of these values from 5° W. to 175° W. was used to get the perturbation index referred to previously.)

On November 12 (mid-day of 5-day mean period) the meridional flow, except for a southerly band in the Atlantic, was neither strong nor well organized. There were many weak filaments of northerly and southerly flow. Three days later, November 15, the southerly flow in the western Pacific associated with the 340-foot negative anomaly center (fig. 9) began to intensify, and two previous filaments joined (fig. 10). Southerly flow then existed from 157° W. westward to Asia. This same band

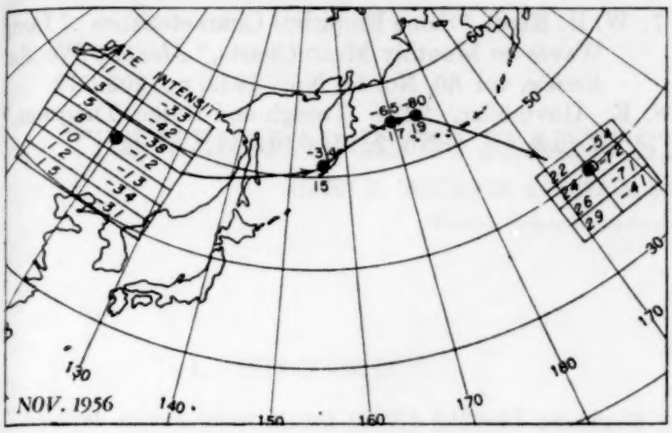

FIGURE 9.—Continuity of a 5-day mean 700-mb. height anomaly center (negative) during November 1956. Middle day of period plotted below circle or left side of box and central intensity in tens of feet above the circle or right side of box. Early in month anomaly was stagnant over Manchuria. Subsequently it moved into central Pacific and acted as an anchor point of the circulation.

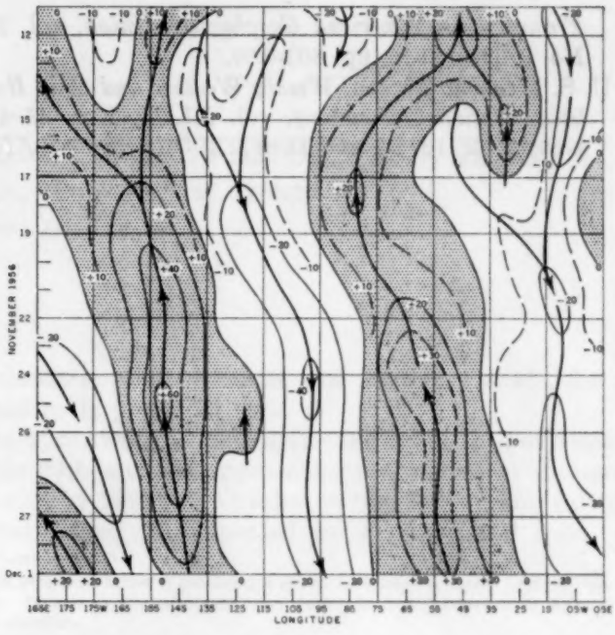

FIGURE 10.—Energy diagram or time cross-section of the 5-day mean anomalous meridional flow (tens of feet per 10° of longitude) at 10° longitude intervals at 45° N. from 5° E. westward to 165° E. Values are plotted at middle of periods. Wind components from the south considered positive. Southerly flow was established in the Pacific (147° W. to 165° E.) on November 15 and 17 and subsequently molded the flow over the United States.

of southerly flow continued to intensify and reached a maximum intensity about the 26th. As early as the 15th, there had been some increase in the northerly flow immediately downstream (147° W.–96° W.), and a definite trend toward amalgamation of the earlier and weak northerly filaments was discernible. This band of northerly flow continued to intensify, and the flow downstream over eastern United States and the Atlantic responded, so that by the 22d there were four pronounced rivers of meridional flow or two complete waves sympathetically spaced in climatologically favored areas. This arrangement, with a little progression, persisted the rest of November and is well exemplified by the 5-day mean charts for November 20–24, and November 27–December 1 (fig. 6).

In summation, the circulation of November started with a ridge in eastern and a trough in western United States. Far upstream, over Manchuria and the Yellow Sea, there was a stagnant and intensifying trough which favored and yielded a sympathetic trough in the eastern Pacific. Subsequently, vorticity flux from the latter trough introduced a ridge and trough into western and eastern United States respectively, and an oscillation in the States had occurred. Then the Asiatic trough, subjected to seasonal alterations, left the Asiatic mainland and continued to progress across the Pacific. This progression, due mainly to wavelength considerations, no longer favored a trough in the eastern Pacific but instead farther downstream. Heights at 700 mb. rose in the eastern Pacific and fell over western United States from the second to third week, and cyclonic flow returned to western portions of the United States. Later, the former Asiatic perturbation progressed to the eastern Pacific, where it stagnated. This trough favored the reappearance of the ridge in western United States and the trough downstream. The stable pattern of the end of the month had been established.

It appears that as winter approached and the seasonal change in the heat sources and sinks occurred, accompanying adjustments were necessary in the general circulation [1]. These seasonal alterations, in the United States at least, did not take place in a smooth, uniform fashion, but rather through marked fluctuations in the week-to-week circulation. Consequently, this November most areas of the United States experienced periods of both late summer and precursory winter weather.

REFERENCES

1. J. Namias, "The Annual Course of Month-to-Month Persistence in Climatic Anomalies," *Bulletin of the American Meteorological Society*, vol. 33, No. 7, Sept. 1952, pp. 279–285.
2. H. F. Hawkins, Jr., "The Weather and Circulation of October 1956—Including a Discussion of the Relationship of Mean 700-mb. Height Anomalies to Sea Level Flow," *Monthly Weather Review*, vol. 84, No. 10, Oct. 1956, pp. 363–370.
3. U. S. Weather Bureau, "Normal Charts for the Northern Hemisphere," *Technical Paper* No. 21, Washington, D. C., Oct. 1952, 74 pp.
4. Canada, Climate Services, Meteorological Division, Dept. of Transport, *Monthly Means and Departures from Normal Temperature and Precipitation*, Nov. 1956.
5. H. Willett, "Patterns of World Weather Changes,"

Transactions, American Geophysical Union, vol, 29, No. 6, Dec. 1948, pp. 803–809.
6. U. S. Weather Bureau, *Weekly Weather and Crop Bulletin, National Summary*, vol. XLIII, Nos. 45–49, Nov. 5, 12, 19, 26, and Dec. 3, 1956.
7. W. H. Klein, "Some Empirical Characteristics of Long Waves on Monthly Mean Charts," *Monthly Weather Review*, vol. 80, No. 11, Nov. 1952, pp. 203–219.
8. E. Hovmöller, "The Trough-and-Ridge Diagram," *Tellus*, vol. 1, No. 2, May 1949, pp. 62–66.

Water Supply Forecast for the Western United States

Published monthly from January to May, inclusive. Contains text, map, and tabulations of water supply forecasts for the 11 Western States, by the Weather Bureau and the California State Division of Water Resources. For copies of the 1957 forecasts apply to River Forecast Center, Weather Bureau Office, 712 Federal Office Building, Kansas City 6, Mo.

THE CENTRAL HIGH PLAINS STORM OF NOVEMBER 1-3, 1956

HENRY L. JACOBSON, ROBERT A. SANDERS, AND DONALD M. HANSON

Weather Bureau District Forecast Center, Kansas City, Mo.

1. INTRODUCTION

The first severe snow storm of the 1956–57 season in the High Plains began on November 1, and continued through November 3, 1956.

The storm left up to 20 inches of snow in northwestern Nebraska, and driven by winds of 50 to 70 m. p. h., huge drifts were formed, paralyzing traffic and disrupting communications. Several deaths were attributed to the storm. The storm reached blizzard proportions on November 2. It met all qualifications of the "severe blizzard" except that temperatures were not low enough.

Hardest hit was the area of the Nebraska Panhandle, extreme northwestern Kansas, northeastern Colorado, eastern Wyoming, and extreme western South Dakota. The storm snowfall pattern shown in figure 1 is based on snow depths reported at 0630 CST, November 4, from stations reporting regularly by teletypewriter, plus a special report from Harrison in the northwestern corner of Nebraska. Also shown is the path and central pressure of the sea level low pressure center.

The development of the storm was rather typical of the High Plains blizzard type or Colorado Low, but the path was unusual in that the storm moved northwestward out of the Nebraska area, filling rapidly as it passed through western South Dakota.

The purpose of this paper is to review some of the synoptic aspects of the storm, and to present practical approaches to the forecasting of its development and the associated precipitation.

2. EARLY STAGES

An important prelude to both the development and the peculiar path of the storm was the persistent warm ridge centered over the eastern third of North America. The strength of this ridge was reflected in positive departures from normal of the 5-day mean 700-mb. heights of more than 600 feet near the St. Lawrence Valley. This positive anomaly had its origin over the Ohio Valley the second week in October, moved rather quickly to the St. Lawrence Valley, and intensified in that position. The strength of this ridge was also reflected in abnormally cold stratospheric air (−65° C. at 200 mb. over James Bay at 1500 GMT, October 30, fig. 2) which persisted over northeastern United States and eastern Canada for a considerable period of time.

An upper trough began deepening in the Gulf of Alaska on the 29th, and was approaching the west coast of North America by 1500 GMT, October 30 (fig. 3).[1] As this trough moved inland, accompanied by a strong mP front, a

[1] The general evolution of the storm is shown in figures 3-6, copied from facsimile charts. Being general in nature, they may disagree in details of exact storm positions given elsewhere.

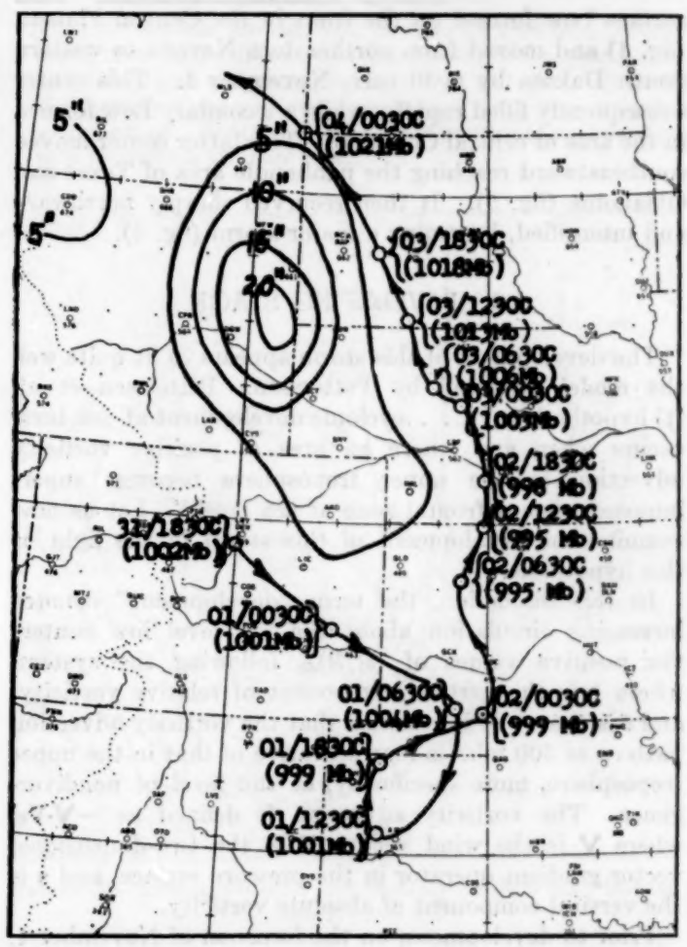

FIGURE 1.—Isopleths of storm snowfall (inches) for November 1–3, 1956, together with successive positions and central pressure of the sea level Low center.

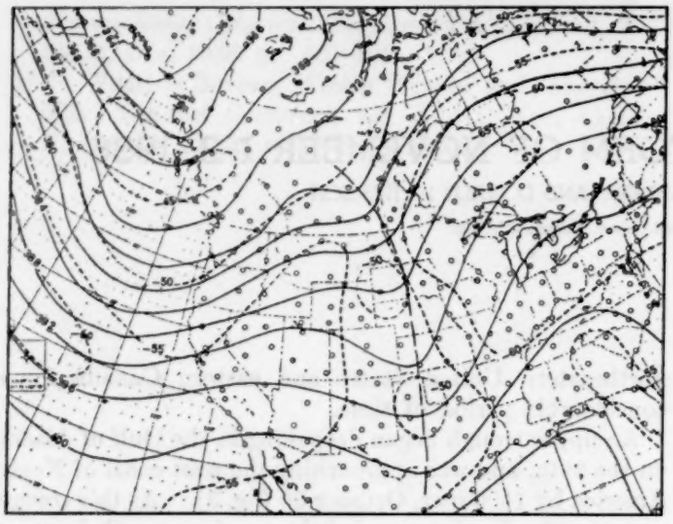

FIGURE 2.—200-mb. chart for 1500 GMT, October 30, 1956. Solid lines are contours labeled in hundreds of feet, and dashed lines are isotherms labeled in degrees Celsius.

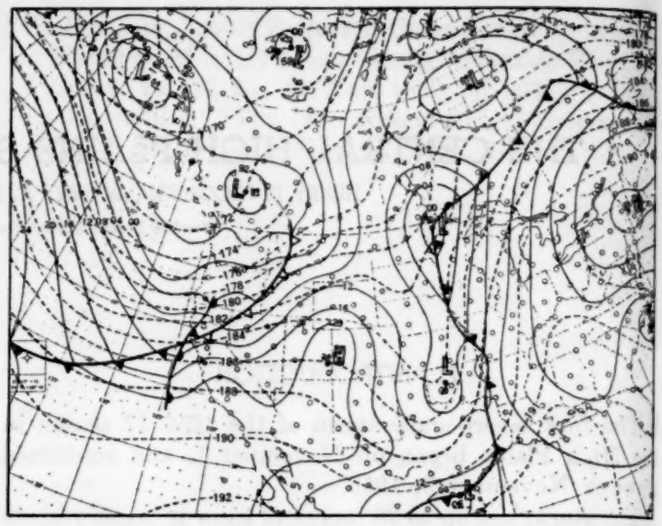

FIGURE 3.—Composite sea level chart (solid lines, 1230 GMT) and 500-mb. chart (dashed lines, 1500 GMT) for October 30, 1956. Surface fronts are indicated with standard symbols. The system near the west coast later developed and became the important storm.

surface Low formed on the front in the Central Plateau (fig. 4) and moved from northeastern Nevada to western South Dakota by 0030 GMT, November 1. This center subsequently filled rapidly, while a secondary Low formed in the area of central Colorado. This latter center moved southeastward reaching the panhandle area of Texas and Oklahoma (fig. 5). It then recurved sharply northward and intensified, becoming a major storm (fig. 6).

3. DEVELOPING STAGE

The development of this storm appears to fit quite well the model proposed by Petterssen. Petterssen et al. [1] hypothesize, " . . . cyclonic development at sea level occurs when and where an area of positive vorticity advection in the upper troposphere becomes superimposed upon a frontal zone at sea level." Let us now examine the development of this storm in the light of this hypothesis.

In this discussion, the term "development" denotes increasing circulation about the sea level low center; viz: positive values of $(\delta\zeta/\delta t)_{SL}$ following the system, where ζ is the vertical component of relative vorticity, and t is time. It is assumed that the vorticity advection pattern at 500 mb.[2] is representative of that in the upper troposphere, more specifically, at the level of nondivergence. The vorticity advection is defined as $-\mathbf{V}\cdot\nabla\eta$, where $\mathbf{V}$ is the wind vector, ∇ is the two-dimensional vector gradient operator in the pressure surface, and η is the vertical component of absolute vorticity.

Prior to development, on the forenoon of November 1, the vorticity advection pattern was relatively weak, and centered near a weak surface Low in the vicinity of

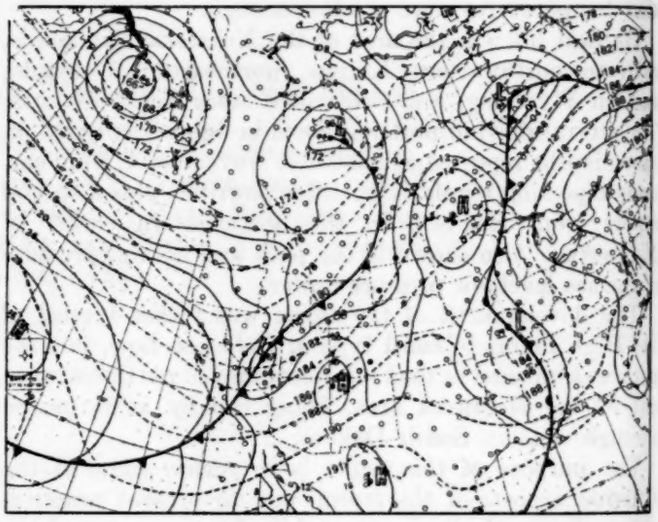

FIGURE 4.—Composite sea level and 500-mb. chart for October 31, 1956.

Albuquerque, N. Mex. (fig. 7). This is climatologically an unfavorable area for development. At the same time there was a weak sea level low center in the Texas Panhandle, statistically a much more favorable area for development.

By the evening of November 1 (fig. 8) a weak vorticity advection pattern still existed in the southeastern New Mexico area, but a stronger pattern had appeared in the area of western Kansas. Whether this latter pattern was associated with a trough which had moved from New Mexico during the day while a new one formed in New Mexico, or whether the trough over the Oklahoma Panhandle at 02/0300 GMT was a new development is not

[2] Hereafter referred to merely as "vorticity advection."

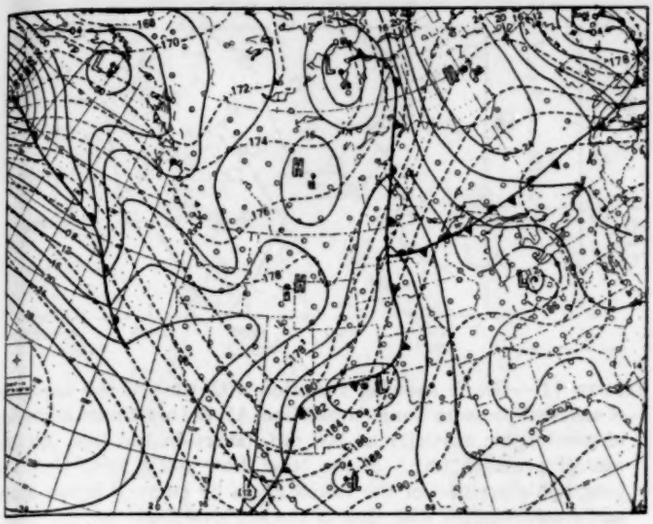

FIGURE 5.—Composite sea level and 500-mb. chart for November 1, 1956.

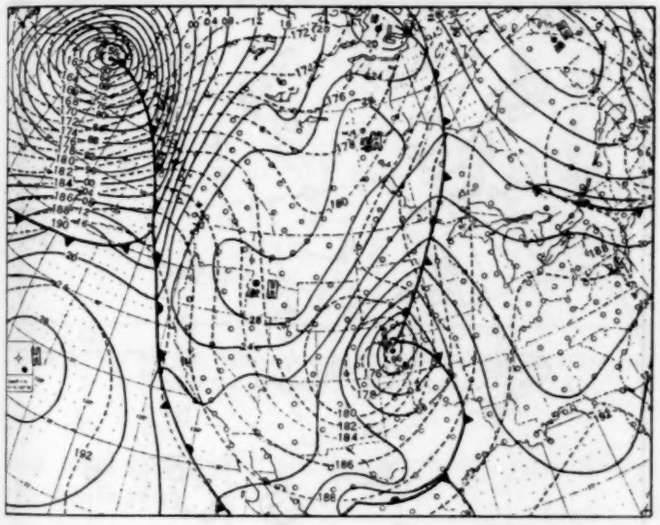

FIGURE 6.—Composite sea level and 500-mb. chart for November 2, 1956.

known. At any rate, by that time the Panhandle Low had already begun to develop while the Low near Albuquerque disappeared. The development of the Panhandle Low was probably at least partly a result of the development of this vorticity advection pattern. This pattern subsequently retained its identity, strengthened, and moved northward and northwestward.

Figures 7–10 suggest that the area of maximum vorticity advection "leads" the sea level low center. In fact, the 12-hour mean vector movement of the Low for the period t_0 to t_{0+12} appears to be in the general direction of the maximum of vorticity advection at t_0. In this particular instance, it appears to be a good clue to the unusual northwesterly motion of the storm.

In figure 11 the development and deepening of the sea

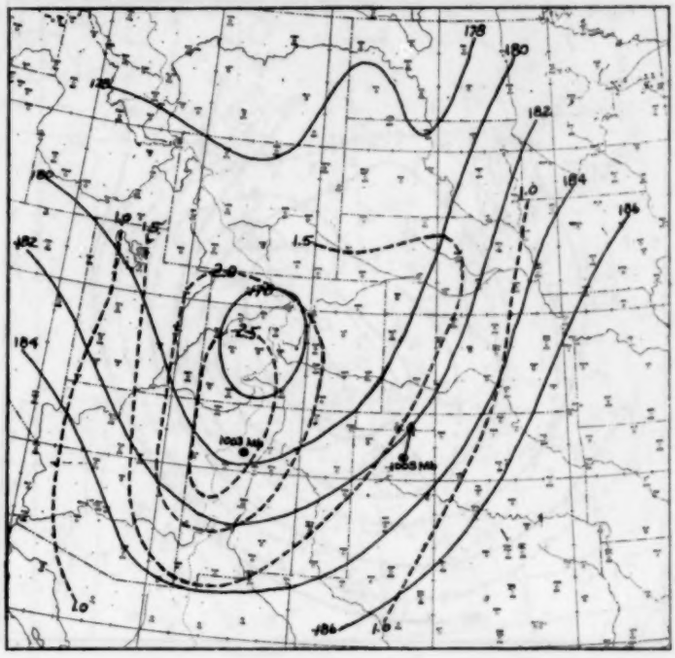

FIGURE 7.—500-mb. contours and vorticity for 1500 GMT, November 1, 1956. Solid lines are contours labeled in hundreds of feet, and dashed lines are geostrophic vorticity $\times 10^{-4}$ sec^{-1}. $\oplus$ marks the position of the sea level Low one-half hour after upper air synoptic time. Arrow connects current position of sea level Low with its position 12 hours later.

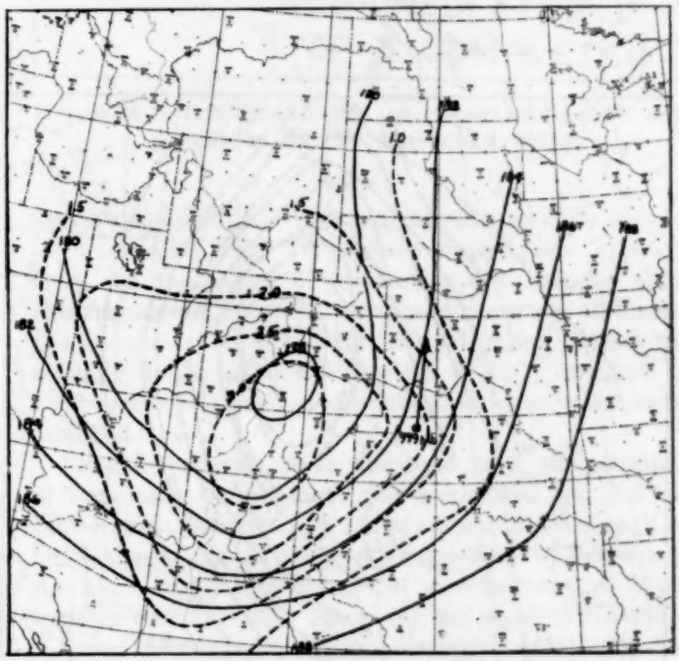

FIGURE 8.—500-mb. contours and vorticity for 0300 GMT, November 2, 1956.

level Low are compared with the associated maximum vorticity advection. Curve A, the Laplacian of the sea level pressure (a quantity that is proportional to the

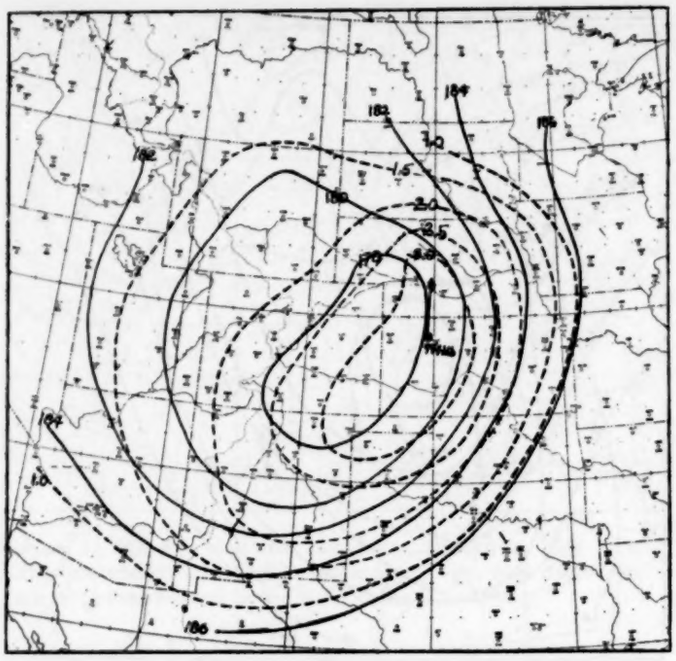

FIGURE 9.—500-mb. contours and vorticity for 1500 GMT, November 2, 1956.

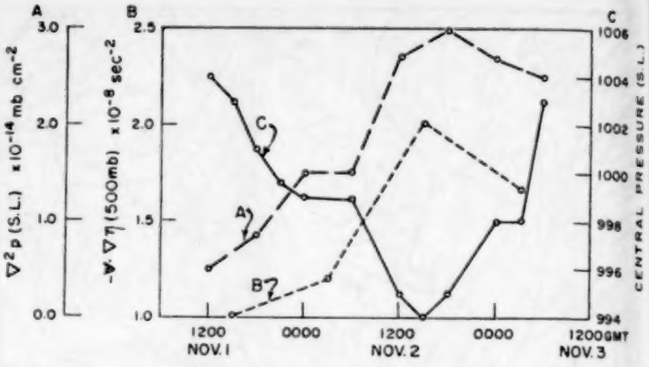

FIGURE 11.—Graph showing variation with time of the Laplacian of sea level pressure (long-dashed line, A), the maximum advection of geostrophic vorticity at 500 mb. (short-dashed line, B), and central pressure (mb.) of sea level Low (solid line, C). The geographic position of the values given by curve B is not necessarily coincidental with that of the sea level Low.

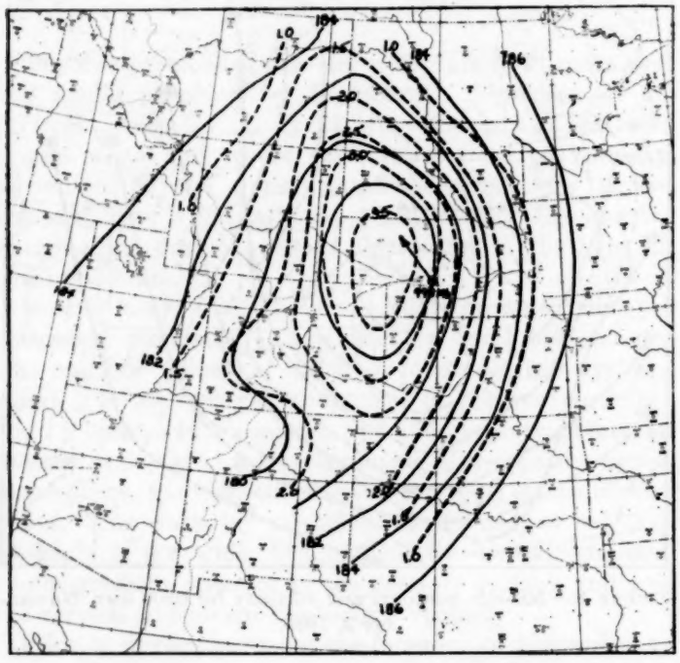

FIGURE 10.—500-mb. contours and vorticity for 0300 GMT, November 3, 1956.

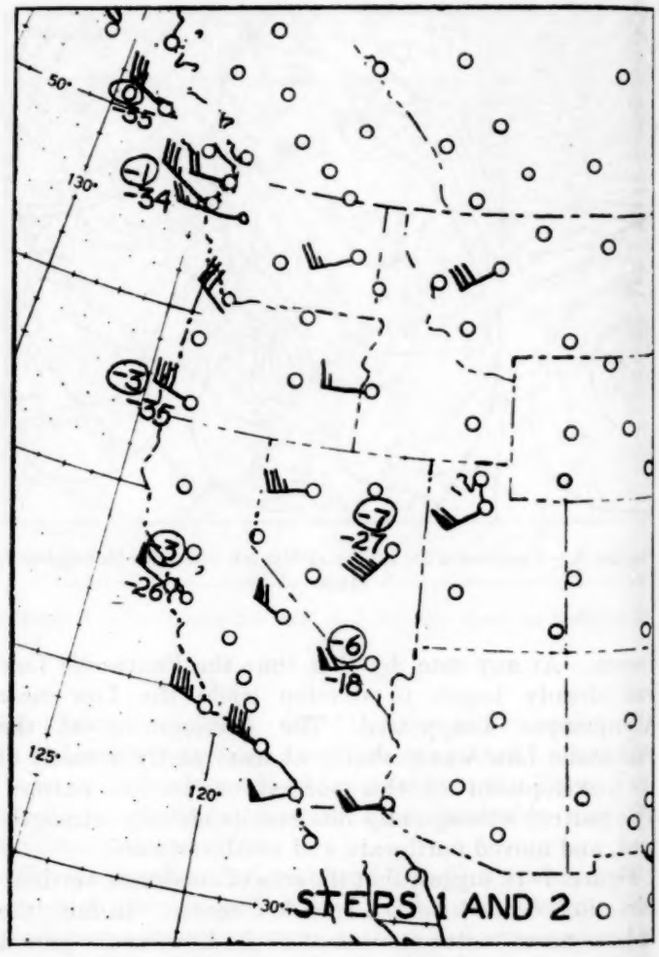

FIGURE 12.—Chart at 500 mb. for 1500 GMT, October 31, 1956, showing winds, selected temperatures (° C.), and temperature changes (° C.) for the preceding 12-hour period (numbers encircled).

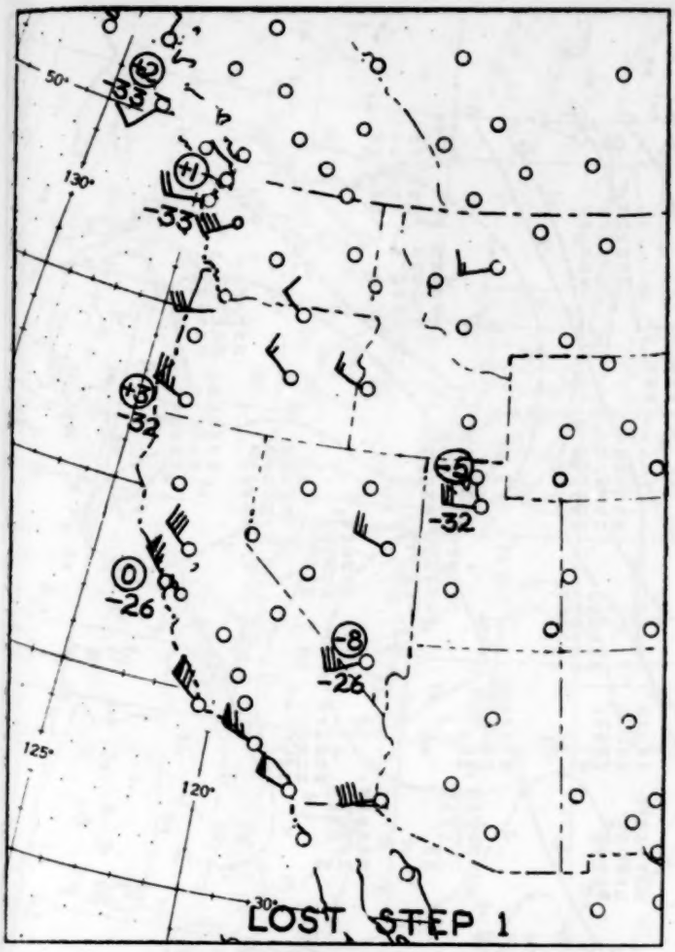

FIGURE 13.—Wind, temperature, and 12-hour temperature change chart for 0300 GMT, November 1, 1956.

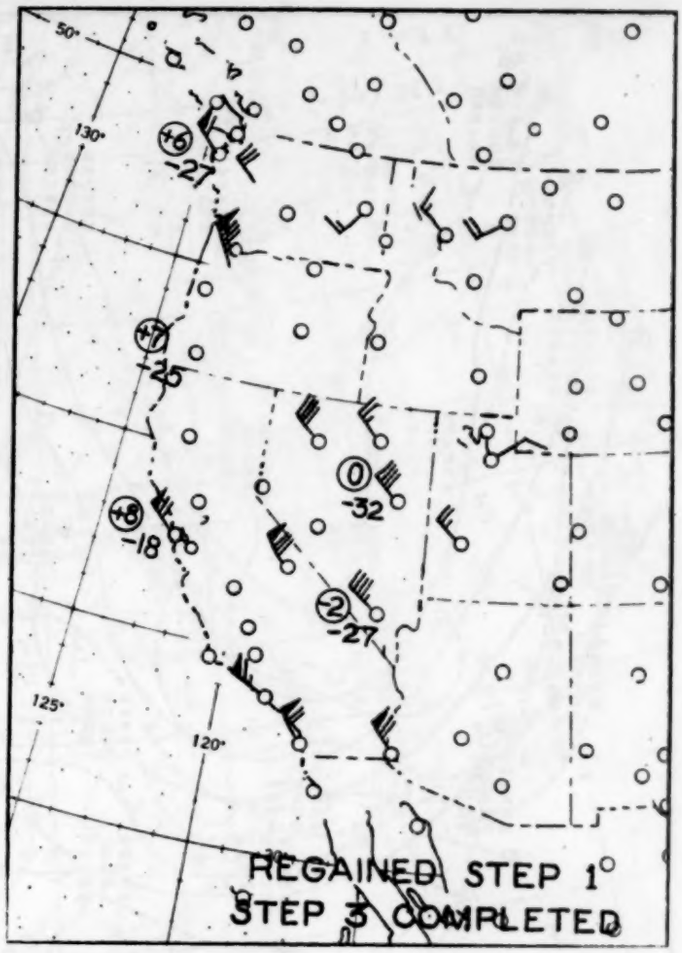

FIGURE 14.—Wind, temperature, and 12-hour temperature change chart for 1500 GMT, November 1, 1956.

sea level geostrophic relative vorticity), was computed by the formula

$$\nabla^2 p = \frac{p_1 + p_2 + p_3 + p_4 - 4p_0}{D^2}$$

where p_0=central pressure of the sea level Low.

p_1, p_2, p_3, p_4=sea level pressure at points 4° latitude distance at each of four cardinal directions from the low center.

D=4° latitude.

Vorticity advection, curve B in figure 11, was taken as the maximum value of positive advection at the 500-mb. surface computed from the geostrophic wind field.

The intensification of vorticity advection appears to have occurred roughly simultaneously with the development at sea level (fig. 11), although precise timing of vorticity advection intensification is difficult since the interval between maps is 12 hours. Thus, from the diagnostic standpoint, development appears to have occurred in accordance with Petterssen's hypothesis. However, from the standpoint of forecasting development within this framework, it would have been necessary to forecast the intensification of the vorticity advection pattern that actually occurred mainly between 01/1500 GMT and 02/1500 GMT. That this could have been done is somewhat doubtful.

For other reasons, to be discussed later, the possibility of important development was mentioned by the forecast staff at the Weather Bureau District Forecast Center, Kansas City, as early as the forenoon of October 31. An alert to the possibility of development of severe weather over the High Plains for the night of November 1–2 was included in the FP–1 discussion of 01/0339 GMT. Formal warnings for heavy snow and strong winds were issued at 02/0339 GMT, and increased to blizzard warnings at 02/0939 GMT.

4. THE FORECASTING OF DEVELOPMENT

The "Colorado" type development is considered one

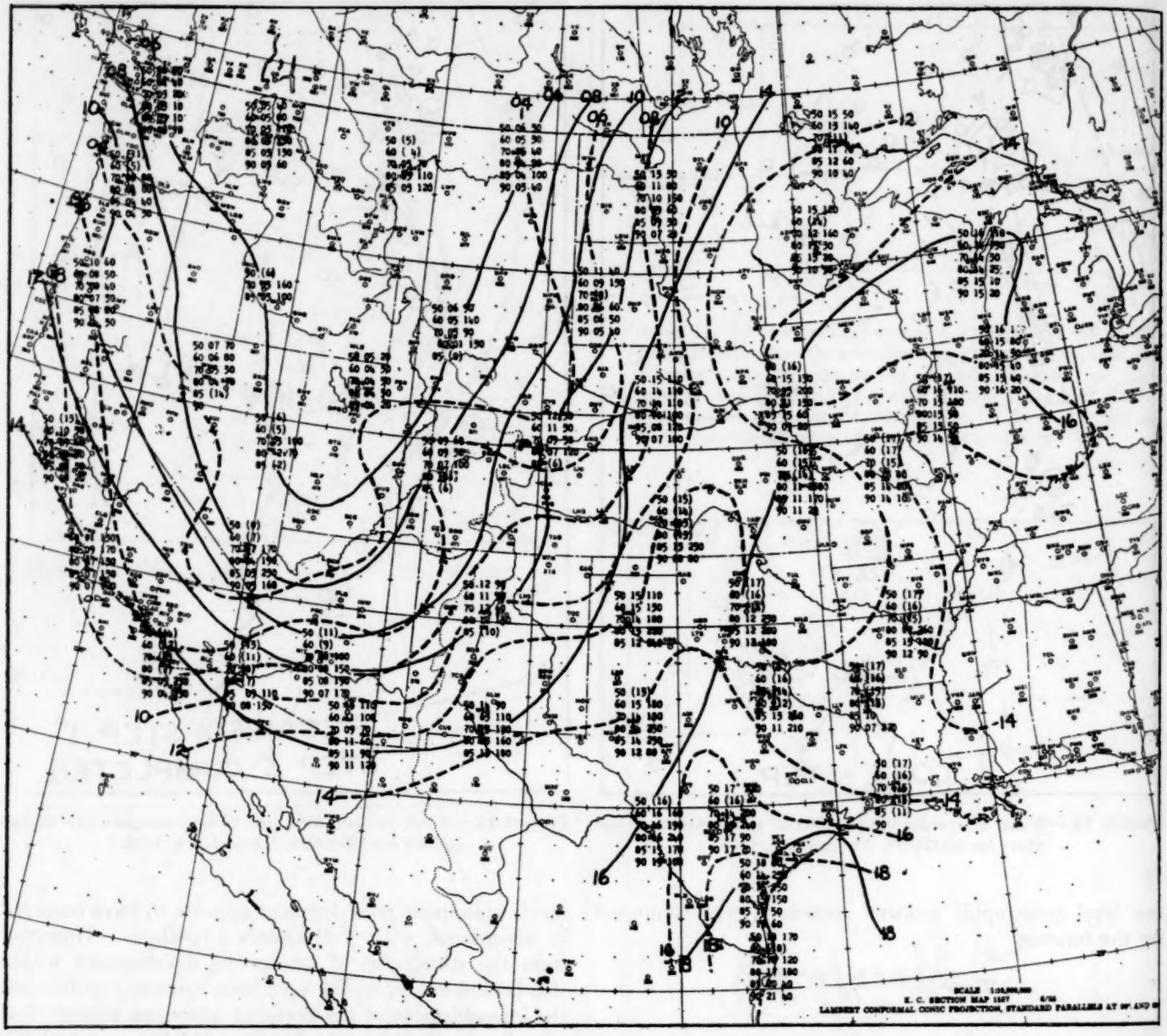

FIGURE 15.—Theta prime chart for 1500 GMT, November 1, 1956. First column of plotted figures is the pressure level indicator; i. e., 90 for 900 mb., 85 for 850 mb., etc. Second column is wet-bulb potential temperature in ° C. Third column (where shown) is the lift in millibars required to reach saturation. Also shown are isotherms of θ' at 500 mb. (solid lines), and at 850 mb. (dashed lines).

of the most acute forecast problems of the Great Plains region. To meet this challenge, the Kansas City Forecast Center has, for the past several years, utilized a system involving several antecedent steps that comprise direct clues to area of development, time, and intensity. The steps must by necessity be reduced to their simplest form with the absolute minimum of exceptions and must apply to the 500-mb. level.

Step 1: A shift in wind flow to a northerly component at Seattle and/or Tatoosh at the 500-mb. level.

It is important to note that this northerly component must be retained through the entire period of development. It may also be noted here that losing the criterion of Step 1 may involve the approach of another wave or foreshadow the formation of a cutoff cold vortex over the Plateau.

Step 2: A fall in 500-mb. temperature at Medford, reaching a value of −25° C. or lower.

This is an essential step (although in many cases it may appear to occur simultaneously with Step 1) and is necessary as an indicator of intensification of the approaching or developing trough in that region.

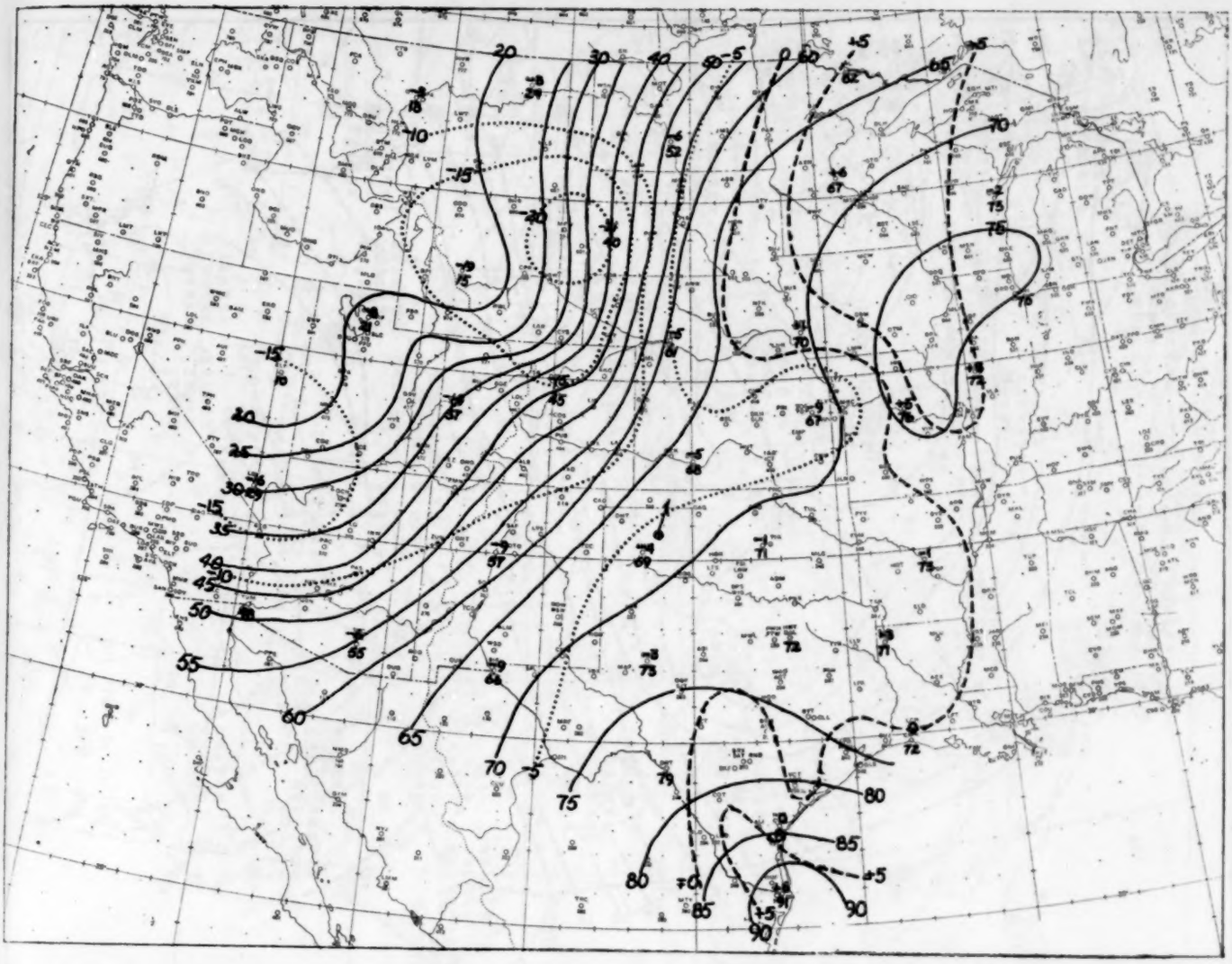

FIGURE 16.—Chart for 1500 GMT, November 1, 1956, showing isopleths of the summation of θ' from 850 mb. upward through 500 mb. (solid lines), and changes in these values during the preceding 12-hour period (dashed and dotted lines). Location of sea level Low indicated by ⊕, future 12-hour movement shown by arrow.

Step 3: A fall in temperature to a value of −25° C. or lower at Ely and/or Las Vegas attended or shortly followed by a distinct temperature rise at Medford.

This will then assure necessary amplitude and southward extension, and sufficient eastward motion of the trough to effect and promote a distinctly favorable area of cyclogenesis in the region of southeastern Colorado. It is again emphasized that Step 1 must be held through Step 3 to preserve the sequence of necessary developments.

This forecast procedure was utilized and is well illustrated in the November 1–3 case of development. In light of the above discussion of the three steps, consideration of conditions preceding the development of November 1–3 shows that Step 1 was first apparent on the 500-mb. chart at 1500 GMT, October 31 (fig. 12), making possible issuance of our first alerts at that time.

Step 2 was almost simultaneous and was already assured due to prevailing conditions at the time.

Step 1 was lost by 0300 GMT November 1 (fig. 13) due to the approach of another short wave, thus delaying development 12 to 18 hours. However, it will be noted that Step 3 became a very distinct feature by 1500 GMT, November 1 (fig. 14), making possible the issuance of bulletins and warnings during the late afternoon and evening of that day.

5. FILLING STAGE

The trough at 500 mb. closed off in its southern portion before development occurred, but retained enough asymmetry to maintain a significant vorticity advection pattern. As has already been shown (fig. 10), by 03/0300 GMT the vorticity advection area had shifted to the north-

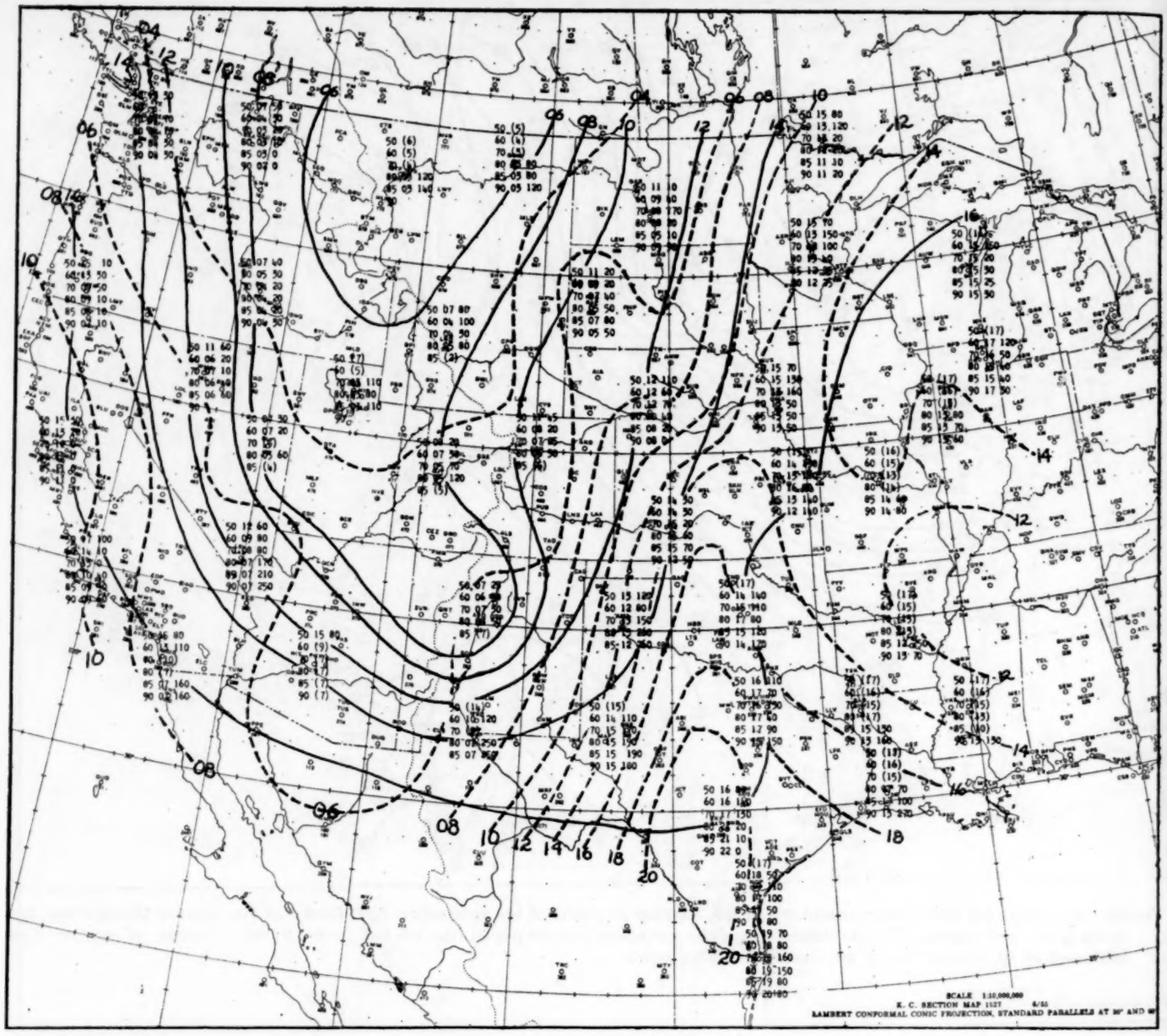

FIGURE 17.—Theta prime chart for 0300 GMT, November 2, 1956.

west quadrant of the 500-mb. Low. Subsequently, the upper Low drifted in a northwesterly direction. At the same time it became somewhat more circular and consequently the strength of the vorticity advection pattern diminished. As this occurred the surface Low moved northwestward and filled rapidly.

6. APPLICATION OF THE THREE-DIMENSIONAL POTENTIAL WET-BULB TEMPERATURE (θ')

DESCRIPTION OF θ' CHART

The theta prime chart consists of a plot of potential pseudo-wet-bulb temperatures (θ') in the vertical at standard levels 900, 850, 800, 700, 600, and 500 mb. In addition, the amount of lift in millibars required for saturation is plotted for each level. Where humidity values are "motorboating," the value of θ' is placed in parenthesis with the dew point taken as the maximum "motorboat" value for the observed temperature.

The chief value of a chart of this kind is that it facilitates a grasp of temperature-humidity relations and stability in a three-dimensional field.

DEVELOPMENT

Petterssen's [2] development equation may be written in the form

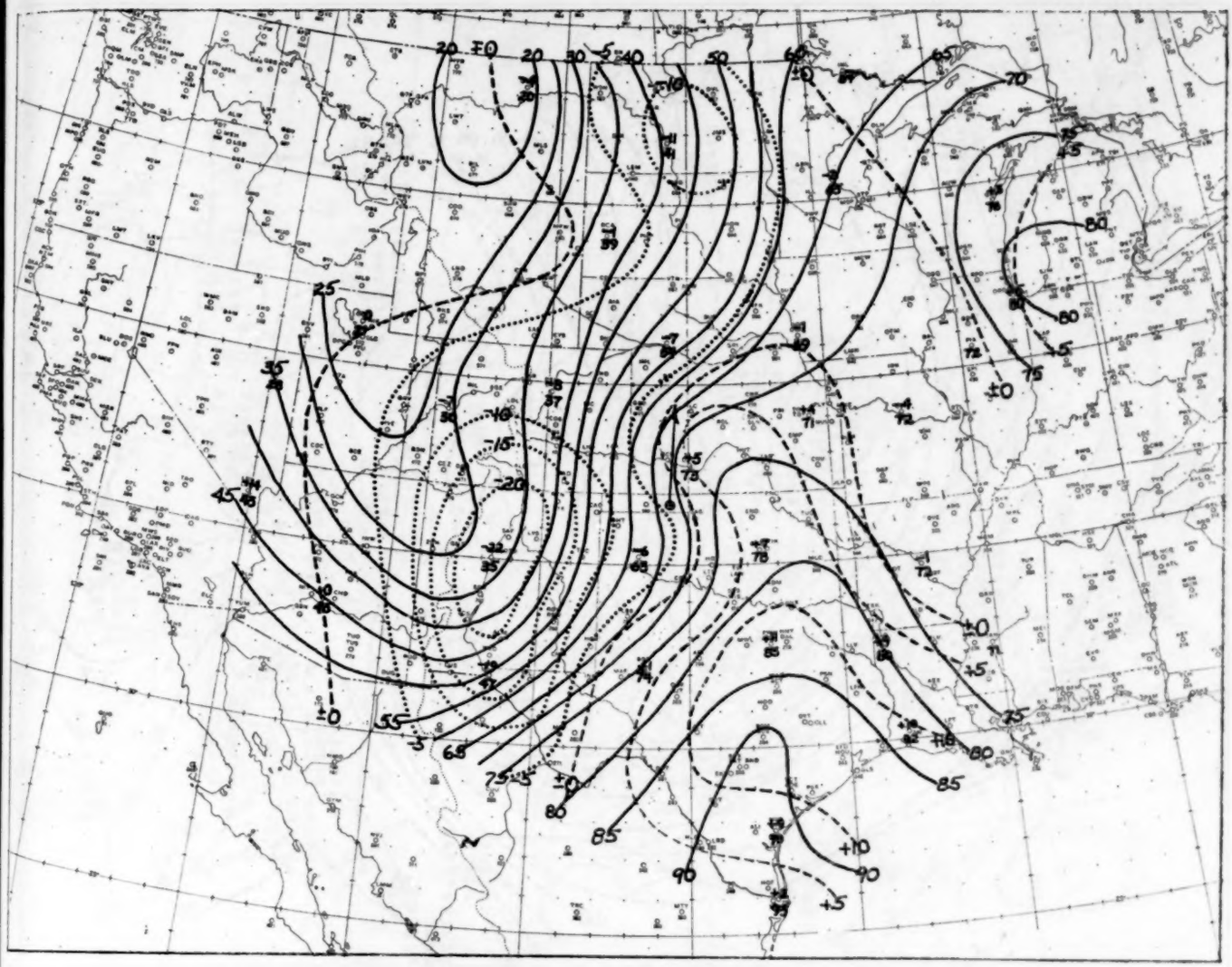

FIGURE 18.—Summation of θ' and its 12-hour change, 0300 GMT, November 2, 1956.

(1) $$\frac{d\eta_0}{dt}=-\mathbf{V}\cdot\nabla\eta-\frac{\partial\zeta_s}{\partial t}$$

where subscript 0 refers to a low-level surface of pressure p_0 and subscript s refers to shear through the layer from p_0 to the level of nondivergence at pressure p. Thus the first term on the right side of equation (1) is the advection of vorticity at the level of nondivergence; this term was evaluated at the 500-mb. level in the foregoing discussion. The second term can be shown by use of the thermal wind equation to be essentially

(2) $$-\frac{\partial\zeta_s}{\partial t}\simeq-\frac{R}{f}\ln\frac{p_0}{p}\nabla^2\frac{\partial\overline{T}}{\partial t}$$

where R is the gas constant, f the Coriolis parameter, and $\overline{T}$ is the mean virtual temperature of the layer between p_0 and p. Because our primary interest is in the mean temperature field after the layer becomes saturated (in which case $\overline{T}$ is proportional to $\overline{\theta}'$), it is proposed to change (2) to the following:

(3) $$-\frac{\partial\zeta_s}{\partial t}\simeq-\frac{kR}{f}\ln\frac{850}{500}\nabla^2\frac{\partial\overline{\theta}'}{\partial t}$$

where k is the constant of proportionality between $\overline{T}$ and $\overline{\theta}'$ for the saturated layer. For qualitative use, $\Sigma\theta'$ can be substituted for $\overline{\theta}'$, and $\partial\overline{\theta}'/\partial t$ expressed as the change per 12 hours, $\Delta\Sigma\,\theta'/12$. This principal variable, $\Delta\Sigma\theta'/12$, is evaluated in the following manner. Sum the θ' values for each sounding from 850 mb. through 500 mb. and place on an auxiliary chart. Twelve-hour changes ($\Delta\Sigma\theta'/12$) are made from these values and the change field is analyzed. Although according to equation (3) it is the Laplacian of this change field that is important, attention here is restricted to an inspection of the centers of change, centers of warm and cold advection, and the gradients about these centers.

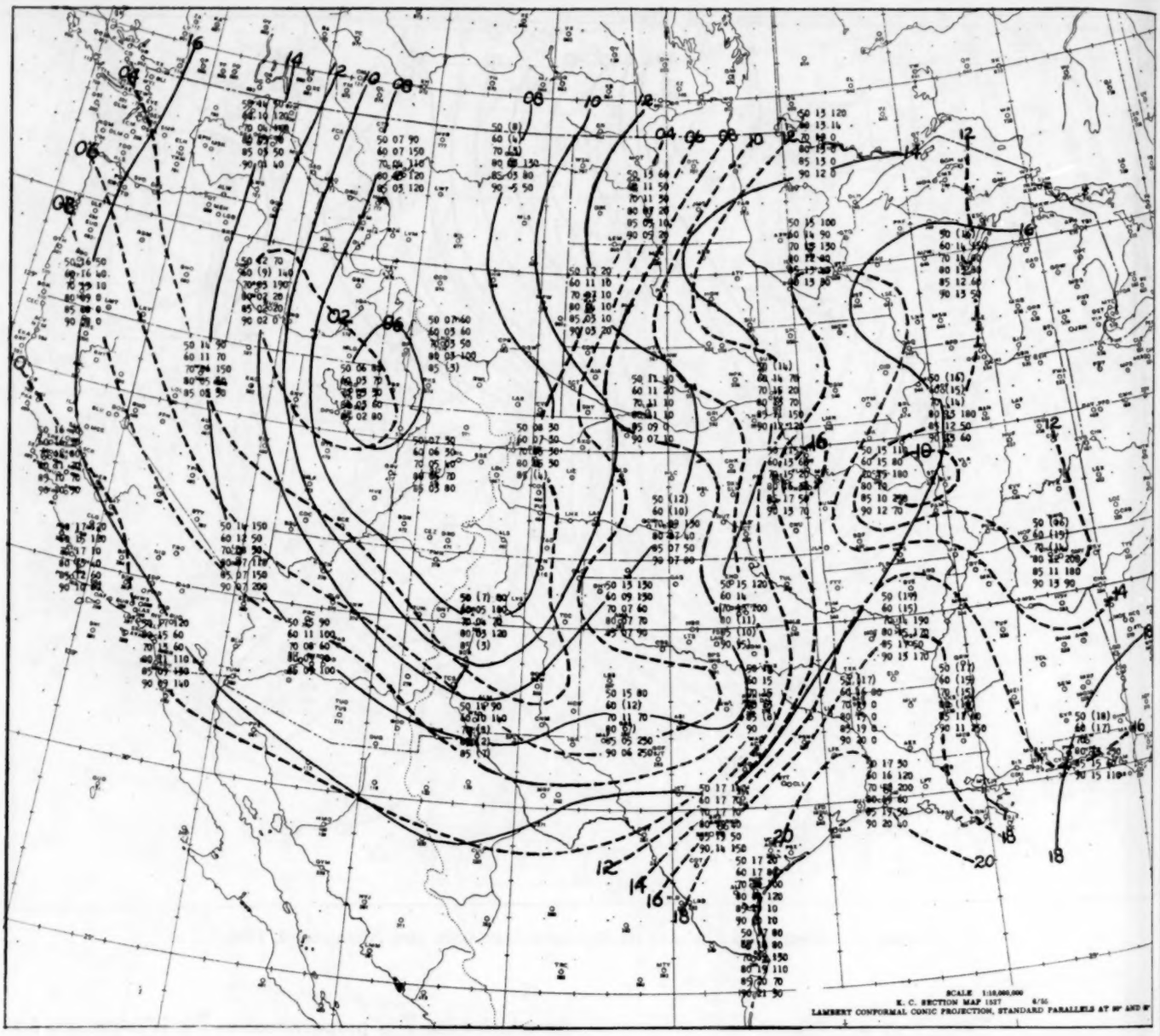

FIGURE 19.—Theta prime chart for 1500 GMT, November 2, 1956.

The first wave to move around the cold trough moved north-northeastward through the Dakotas, filled, and was centered in North Dakota on the 1230 GMT November 1 surface chart (fig. 5). This wave had the effect of shifting low-level winds to northerly in the High Plains and dropping temperatures into the range where later precipitation would be snow. This is shown as maximum of cooling over Wyoming and western South Dakota with warm advection over Iowa and Minnesota in figures 15 and 16. The same charts show that another maximum of cooling was approaching in Arizona with the beginning of a warm tongue from western Texas north to Dodge City.

By 0300 GMT, November 2 (figs. 17 and 18) the cold advection, centered over Albuquerque, was quite strong and warm advection had developed further, extending from southern Texas northward into south-central Kansas. The easterly component of the thermal wind was increasing north of the cold advection center and for the following 24 hours the actual low-level winds turned to easterly north of the low center.

Twelve hours later (figs. 19 and 20) cold advection had reached the Plains of Kansas and had begun to cut off the southerly winds east of the low center. However, moisture values were high in Minnesota and Iowa, partly residual from the first wave of the series. This moisture was beginning to move westward and precipitation continued north and west of the low center.

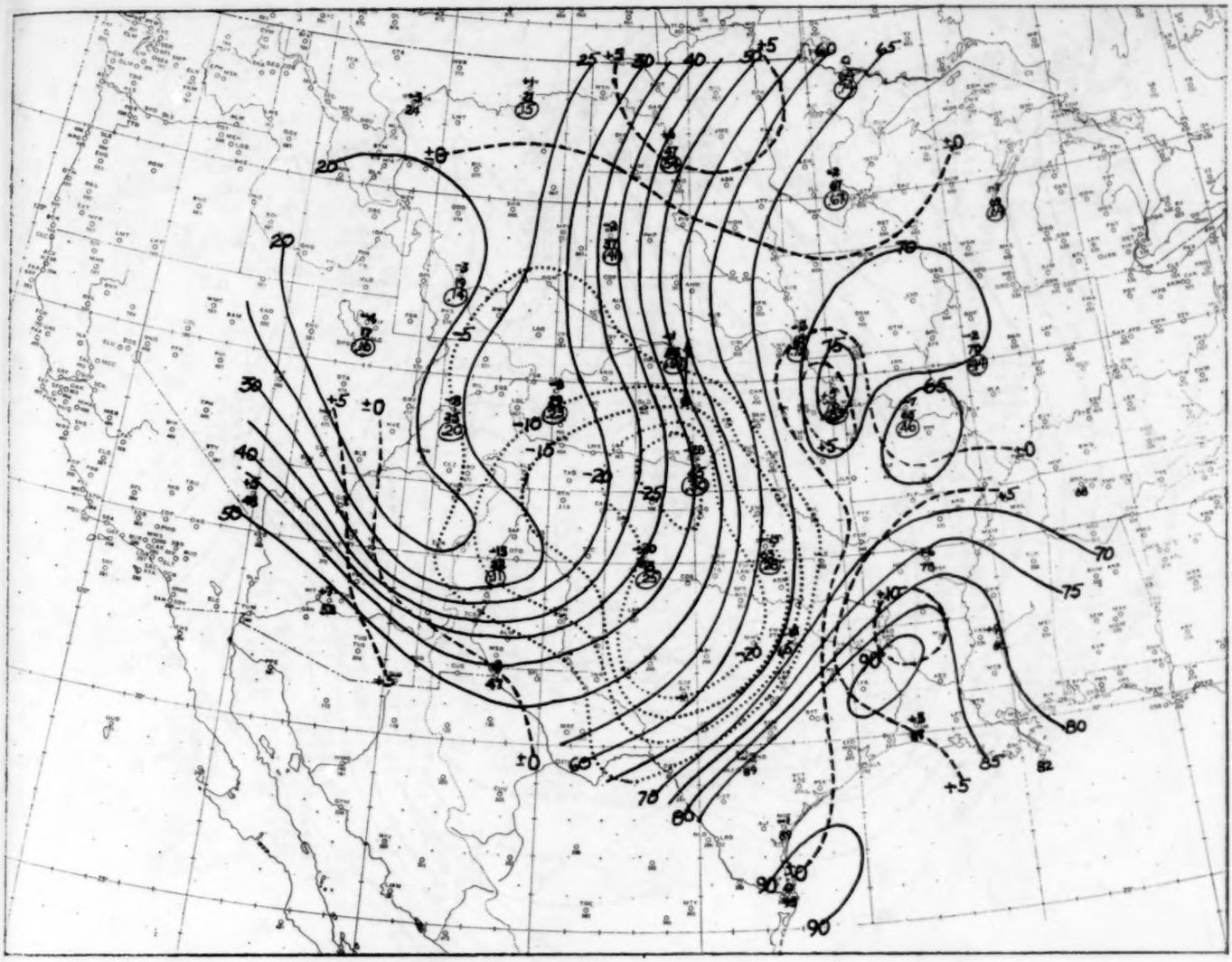

FIGURE 20.—Summation of θ' and its 12-hour change, 1500 GMT, November 2, 1956. Encircled figures are computed precipitable water.

PRECIPITATION AMOUNTS

Hewsen [3] has shown a method of forecasting precipitation amounts and has given a statistical relation between a decrease in θ' with height and the amount of precipitation in a following 12-hour period. Some modification of Hewson's idea can be used here.

An examination of the soundings for 1500 GMT, November 2 (fig. 19), at the time cold advection had covered Kansas, shows upslope conditions existed from east to west at all levels from Minnesota and Iowa westward to the mountains. The maximum in this slope as shown by the strong horizontal gradients of $\Sigma\,\theta'$ in figure 20 extended from central North Dakota southward into western Nebraska. While the low-level winds were easterly, winds at 500 mb. were advecting cold air from the south causing convective instability along the east side of the $\Sigma\,\theta'$ gradient. North Platte had a condition of neutral instability for the saturated state at the 800-mb. level and above.

The amount of precipitable water was computed for 1500 GMT, November 2, by the method of Solot [4] and entered as the third number in the station model of figure 20. There existed a moisture differential of some 0.55 inch between the air mass in Iowa and Minnesota and the two soundings in Colorado. It is our experience that in a developing storm the soundings in the cold air take on a saturated lapse rate through the 500-mb. wet-bulb temperature. As represented by the Denver and Grand Junction soundings, absorption of some 0.20 inch of water was indicated, while the soundings to the east in the source region showed an average of about 0.75 inch available. This excess could be realized as precipitation along the maximum gradient of slope and in a time interval determined by the winds.

412896—57——3

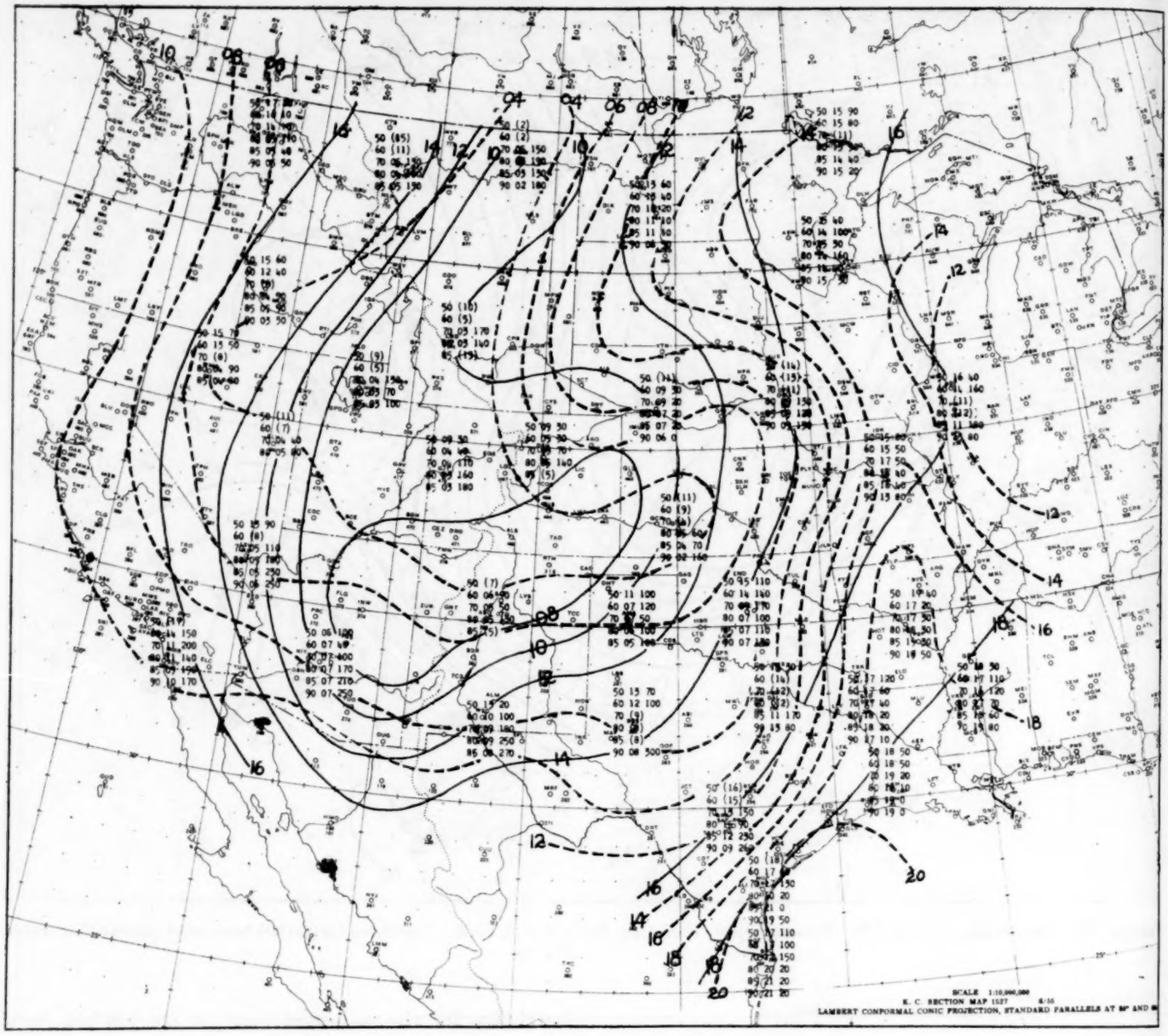

FIGURE 21.—Theta prime chart for 0300 GMT, November 3, 1956.

There were few observations of the wind north of the low center, but with 25 kt. taken as a mean value of the easterly component for the soundings from the surface to 500 mb., 0.55 to 1.10 inches of precipitation would be expected in the 12-hour period following the 1500 GMT, November 2, soundings. This precipitation would be confined principally to the zone of convective instability and the maximum slope. The 24-hour amounts of precipitation ending 1230 GMT, November 3, are shown in figure 23.

Figures 21 and 22 show the continuing occluding process with the thermal advection centers, suggesting the more northwest direction for the surface Low.

Such a detailed analysis is hardly feasible on a routine basis at present in the District Forecast Center. However, soundings between the Mississippi River and the Rocky Mountains are usually plotted and processed on a θ' chart to give a measure of slope, the available moisture, and in a qualitative way the changes in warm and cold advection centers that would exist should saturation occur.

7. CONCLUSIONS

(1) From the diagnostic standpoint, the development of this storm appears qualitatively to have occurred in accordance with Petterssen's development hypothesis; but

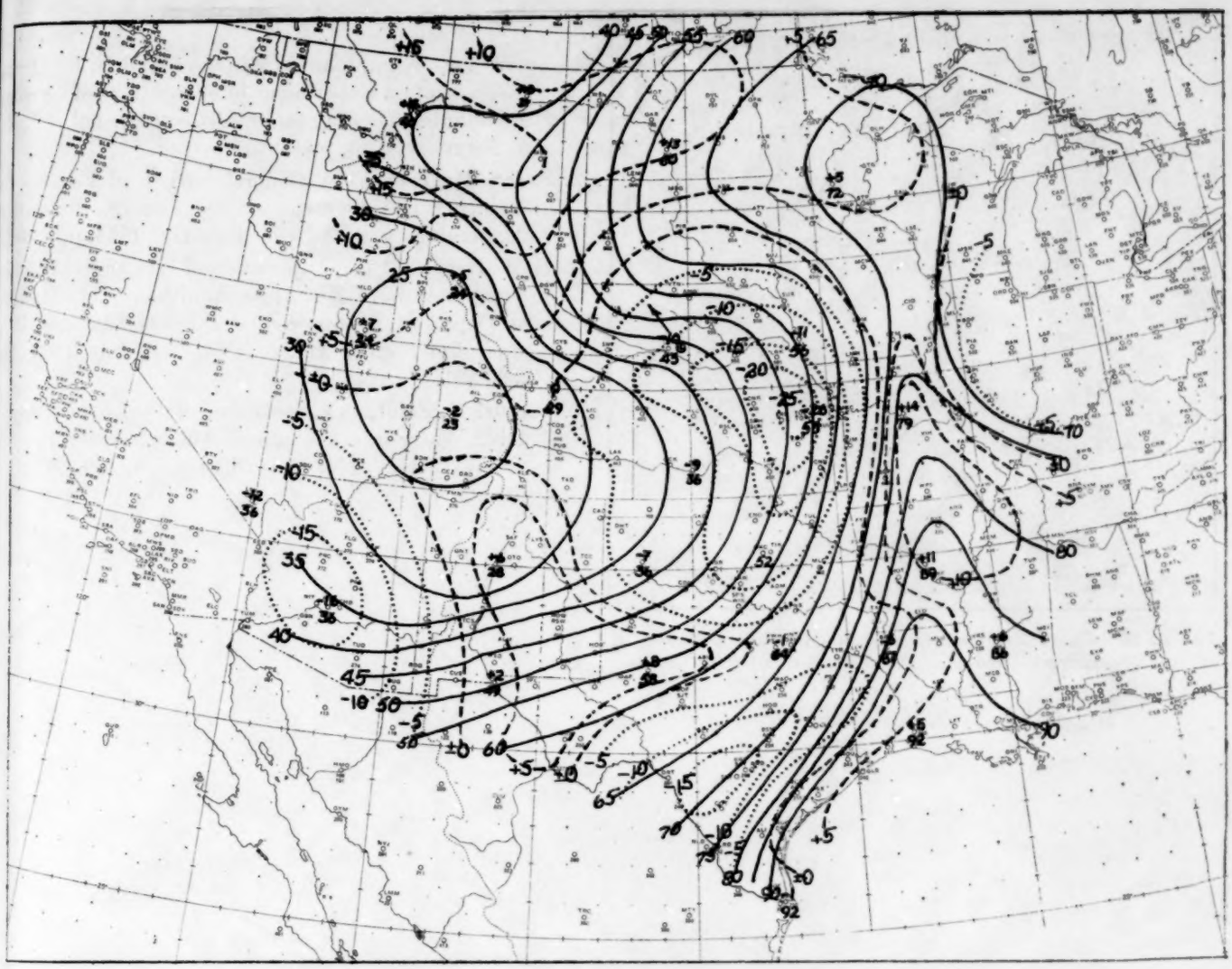

FIGURE 22.—Summation of θ' and its 12-hour change, 0300 GMT, November 3, 1956.

the degree of development, which is related instantaneously in Petterssen's development equation to the degree of vorticity advection, likely would not have been forecast from these considerations alone because of the necessity to forecast independently the movement and development of the upper trough.

(2) This case contains the suggestion that the sea level Low tended to follow the area of maximum vorticity advection at 500 mb. Although this result is not entirely unexpected, the relation should be investigated further to determine circumstances under which it may or may not hold.

(3) A useful tool in forecasting development in this case (as in many others) was the progression through the three "steps" at the 500-mb. level.

(4) A useful tool in forecasting precipitation is the vertical theta prime chart. At or near saturation, it suggests the slope of isentropic surfaces. It also suggests the degree of vertical stability and changes therein.

ACKNOWLEDGMENTS

The authors wish to express sincere thanks to Mr. Benjamin L. Brown, Research Assistant at the District Forecast Center in Kansas City, for his painstaking effort in preparing the illustrations.

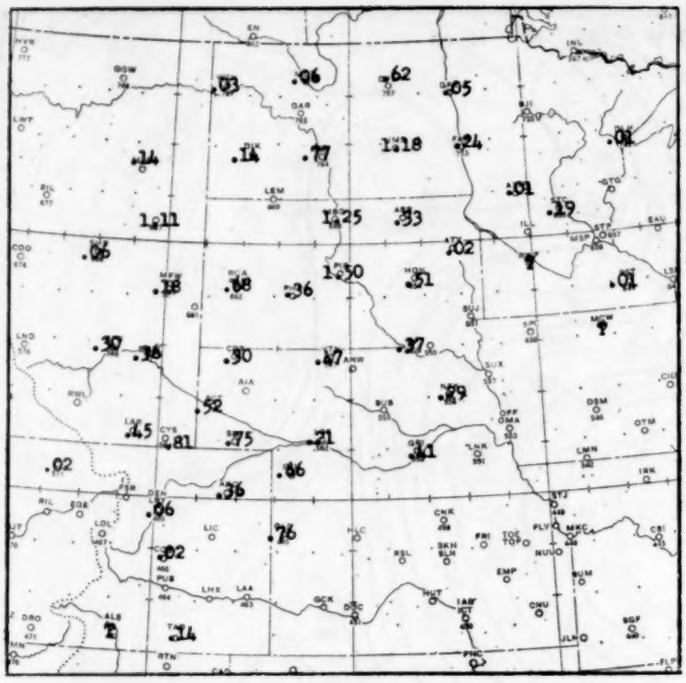

FIGURE 23.—Chart showing reported precipitation amounts for the 24-hour period ending at 1230 GMT, November 3, 1956.

REFERENCES

1. Sverre Petterssen, Gordon E. Dunn, and L. L. Means, "Report of an Experiment in Forecasting of Cyclonic Development," *Journal of Meteorology*, vol. 12, No. 1, February 1955, pp. 58–67.
2. Sverre Petterssen, "A General Survey of Factors Influencing Development at Sea Level," *Journal of Meteorology*, vol. 12, No. 1, February 1955, pp. 36–42.
3. E. W. Hewson, "The Application of Wet Bulb Potential Temperature to Air Mass Analysis. III. Rainfall in Depressions," *Quarterly Journal of the Royal Meteorological Society*, vol. 63, No. 271, July 1937, pp. 323–331.
4. Samuel B. Solot, "Computation of Depth of Precipitable Water in a Column of Air," *Monthly Weather Review*, vol. 67, No. 4, April 1939, pp. 100–103.

ANALYSIS OF FRONTAL BOUNDARIES BY MEANS OF THICKNESS ANOMALIES, NOVEMBER 12–16, 1956

HAROLD M. JORDAN AND JOHN R. CLARK

National Weather Analysis Center, U. S. Weather Bureau, Washington, D. C.

1. INTRODUCTION

The National Weather Analysis Center (NAWAC) for the last four years has used the gradient discontinuity on the 1000–500-mb. thickness chart as a criterion for the existence and intensity of a front. However, when a frontal discontinuity lies in an area of strong normal thickness gradient, the magnitude of the normal gradient can obscure the thermal gradient caused by the presence of the front. Or inversely, the strong normal thickness gradient frequently can suggest the existence of a front when none is present. Thus, it seems logical to subtract the normal thickness gradient from the synoptic thickness gradient to obtain the frontal thickness gradients. This subtraction is made on a routine basis at NAWAC to obtain the 1000–500-mb. thickness anomaly analysis for other uses.[1] The gradient discontinuities of these thickness anomaly contours also can be used to aid in establishing a position and intensity of the frontal zones [1].

The above concepts can be expressed as follows [2]:

$$\nabla Z=\nabla Z'+\nabla Z_i, \text{ and}$$

$$\frac{\partial}{\partial y}(\nabla Z)=\frac{\partial}{\partial y}(\nabla Z')+\frac{\partial}{\partial y}(\nabla Z_i)$$

where Z=1000–500-mb. thickness

Z'=normal 1000–500-mb. thickness

Z_i=departure from normal 1000–500-mb. thickness

∇=horizontal gradient operator.

When the gradient of the normal is uniform, then

$$\frac{\partial}{\partial y}(\nabla Z')=0, \text{ and } \frac{\partial}{\partial y}(\nabla Z)=\frac{\partial}{\partial y}(\nabla Z_i)$$

that is, the component change of thickness gradient is equal to the component change of thickness anomaly gradient, and any discontinuity of one gradient is equal to the discontinuity of the other. Since the strongest 1000–500-mb. thickness gradient discontinuity lies along the front, the strongest anomaly gradient discontinuity will also lie along the front. When $\partial(\nabla Z')/\partial y$ is not zero, i. e., when the gradient of the normal is not uniform, the front can lie along the discontinuity in the normal gradient without showing an anomaly gradient discontinuity.

The southwestern part of North America and the adjoining Pacific Ocean is an area in which there is a strong climatological thickness gradient. The synoptic situation of November 12–16, 1956, is used in this article to illustrate how the thickness anomaly gradient aids frontal analysis in this area.

2. THE COLD FRONT AND THE THICKNESS ANOMALY

Preceding this situation unseasonably high temperatures were recorded in the southwestern United States. Los Angeles reached 95° F. on November 9; Winnemucca 74° F. on the 10th; Prescott 75° F. on the 11th; all were near or above record for the date. Subsequent to the passage of the cold front under discussion, Prescott measured a record minimum of 15° F. for the date on November 15.

On November 12 at 0630 GMT (fig. 1A) there was a front lying from western Lake Erie through Oklahoma and the Texas Panhandle into Wyoming, then westward through northern Oregon off the coast to 46° N., 130° W. and then southwestward. The portion of the front from 46° N., 130° W. southwestward is the subject of this discussion. At this time the 1,000–500-mb. anomalies (fig. 1B, solid lines) showed above normal thickness over the western United States. This was associated with the abnormally warm surface temperatures throughout the area of the Plateau High.

Behind the cold front in the Pacific there was a strong thickness gradient and a parallel strong thickness anomaly gradient. There was also a moderate thickness gradient through New Mexico, Arizona, southern Nevada and central California suggesting a front somewhere near the southern edge of this gradient. However, the reverse anomaly gradient indicates that the thickness gradient there was less than normal.

At 0630 GMT of November 13 (fig. 2A), the cold front under discussion had moved to a position through north-

[1] The routine at NAWAC for deriving the thickness anomaly analysis utilizes graphic subtraction techniques. The monthly normal contours are traced with grease pencil upon a sheet of clear acetate. Then this acetate is overlaid upon the synoptic thickness analysis acetate and graphic subtraction is performed onto a third acetate.

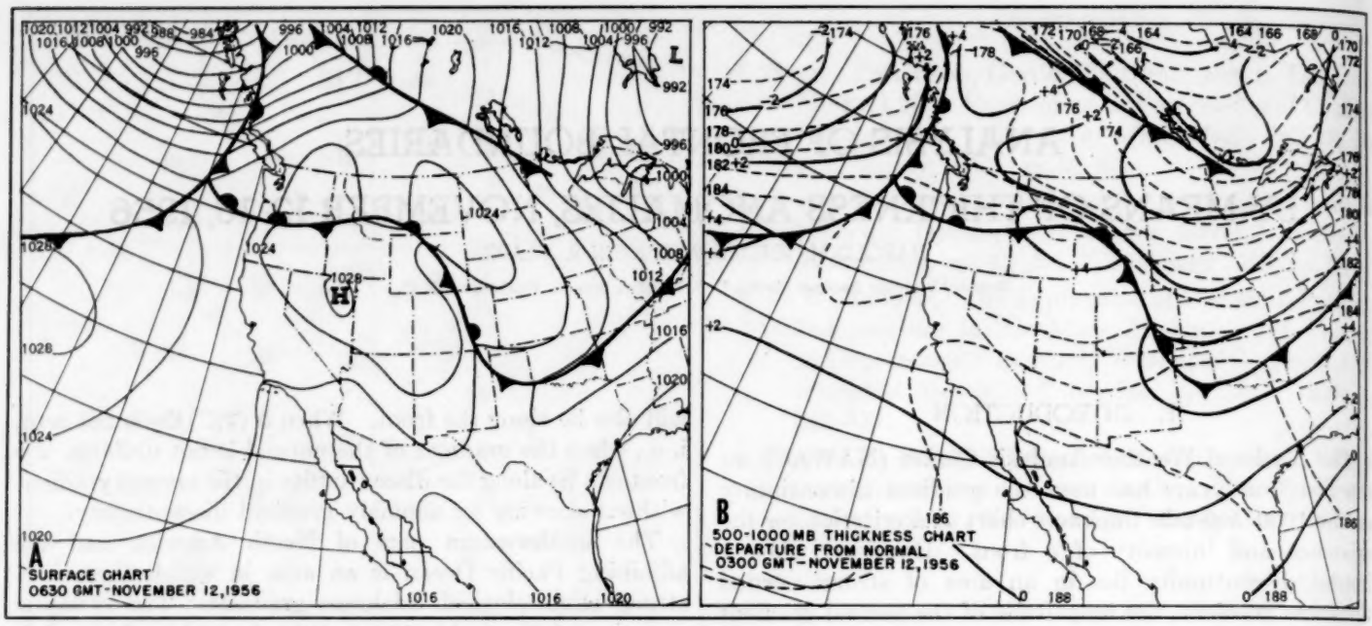

FIGURE 1.—November 12, 1956. (A) Surface fronts and isobars, 0630 GMT. (B) 1000–500-mb. thickness contours (dashed lines) and their departure (solid lines) from November thickness normals, 0300 GMT.

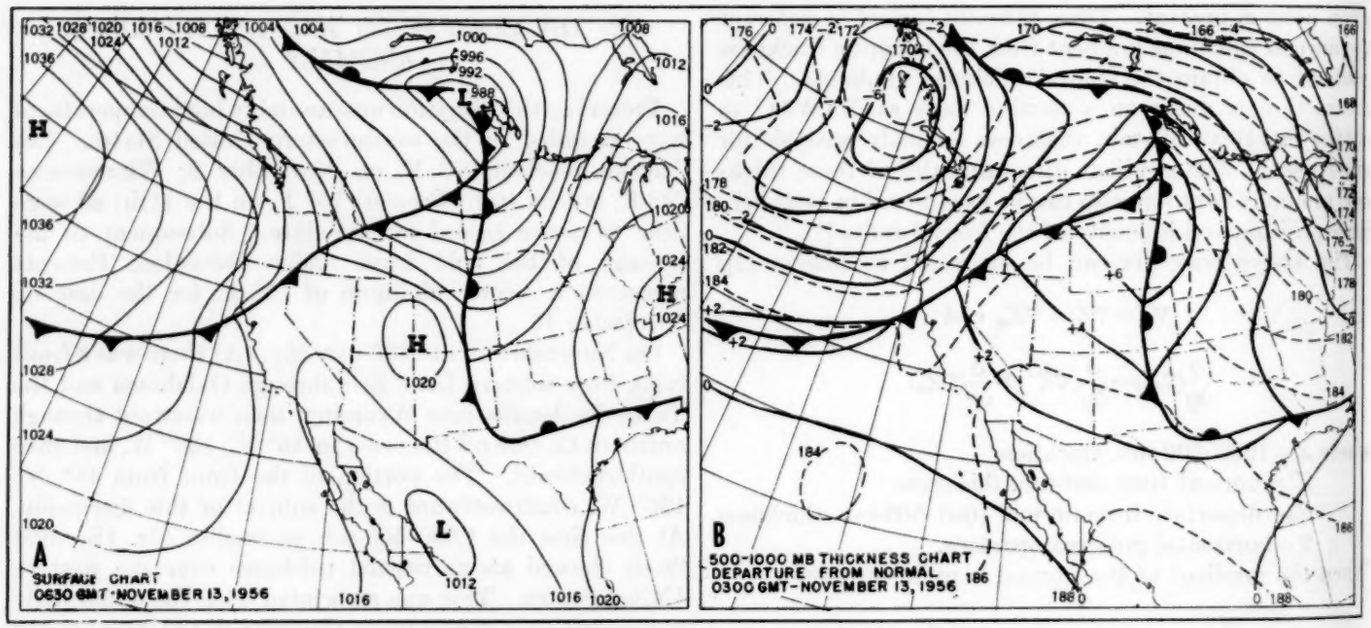

FIGURE 2.—November 13, 1956. (A) Surface fronts and isobars, 0630 GMT. (B) 1000–500-mb. thickness contours (dashed lines) and their departure (solid lines) from November thickness normals, 0300 GMT.

western North Dakota, Montana, central Idaho, southeastern Oregon, northern California, and southwestward to 35° N., 130° W. The thickness gradient discontinuity (fig. 2B, dashed lines) across this front leaves no doubt as to its existence or intensity. The components of the anomaly gradients parallel to the thickness lines also show a sharp discontinuity.[2] Also, any other considerations leave little or no area of doubt in the position of the front at this time; pressure tendencies, cloud forms, precipitation, wind shifts, temperature changes, radiosonde, rawin changes, etc., all confirm the position. An examination of the departure from normal 1000–500-mb. thickness chart shows that it is not the scalar magnitude of the

[2] To investigate the components of the gradients parallel to a portion of a front, the following graphic technique can be used: (1) Using two copies of the 1000–500-mb. anomaly contours (analyzed in 200-ft. intervals), displace one from the other by a distance equal to the geostrophic spacing for 25 knots and in the direction perpendicular to the front. (2) Subtract graphically. The resulting contours are isotachs of the geostrophic spacing of the component of 1000–500-mb. anomaly parallel to the front in 25-knot intervals.

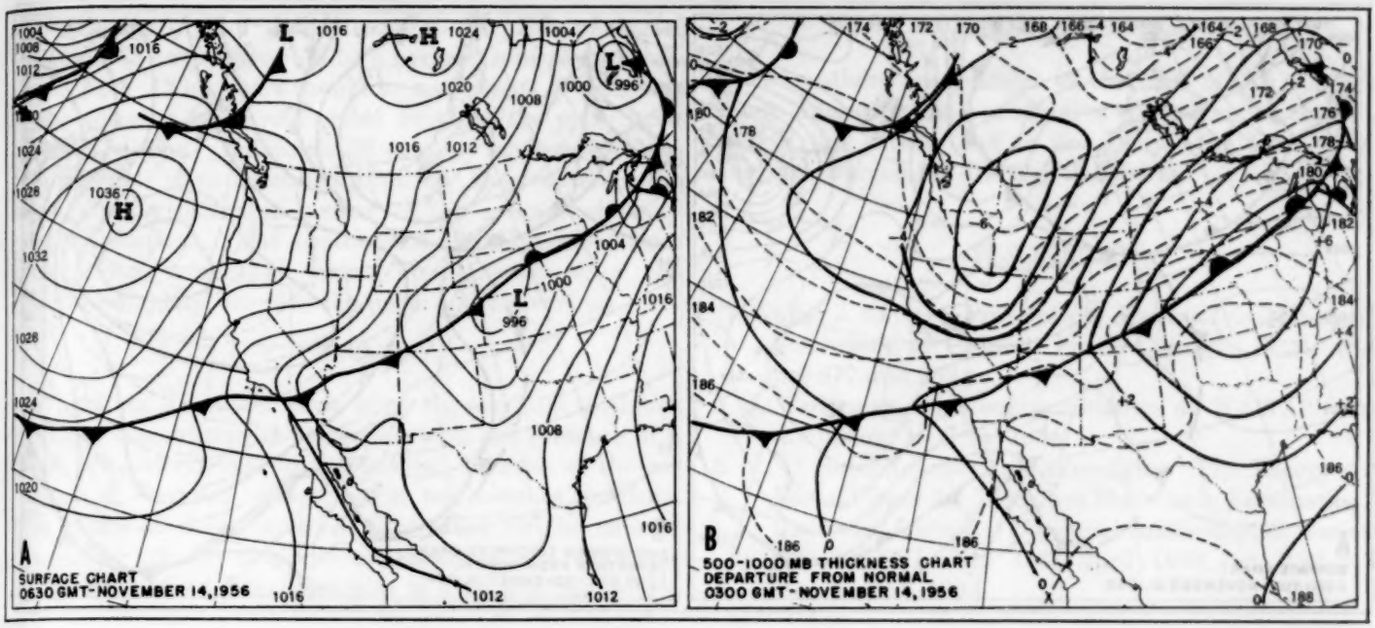

FIGURE 3.—November 14, 1956. (A) Surface fronts and isobars, 0630 GMT. (B) 1000–500-mb. thickness contours (dashed lines) and their departure (solid lines) from November thickness normals, 0300 GMT.

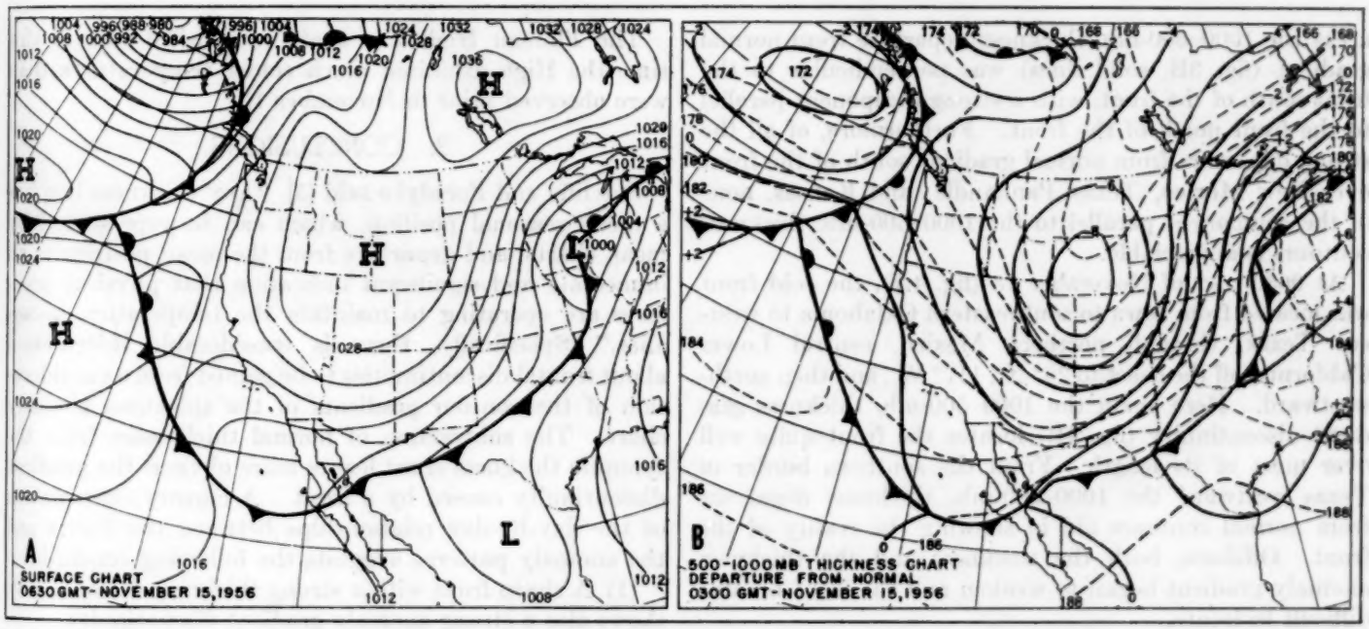

FIGURE 4.—November 15, 1956. (A) Surface fronts and isobars, 0630 GMT. (B) 1000–500-mb. thickness contours (dashed lines) and their departure (solid lines) from November thickness normals, 0300 GMT.

anomaly field which is important to delineate the frontal boundary, but rather the vector difference of the components of the gradients parallel to the front which is important. For example, in figure 2B through Nevada, southern Idaho, and Wyoming, the departure from normal contour gradient is perpendicular to the front, so that any component parallel to the front is zero. North of the front the component parallel to the front is large.

On November 14 at 0630 GMT (fig. 3A), the front lay from Lake Michigan through Nebraska, northern Arizona, and southern California, and west-southwestward off the coast. The 1000–500-mb. thickness gradient discontinuity clearly defines the front over most of the area (fig. 3B, dashed lines). The small cold protrusions ahead of the front in New Mexico and off the coast, might seem significantly contradictory. However, in both these

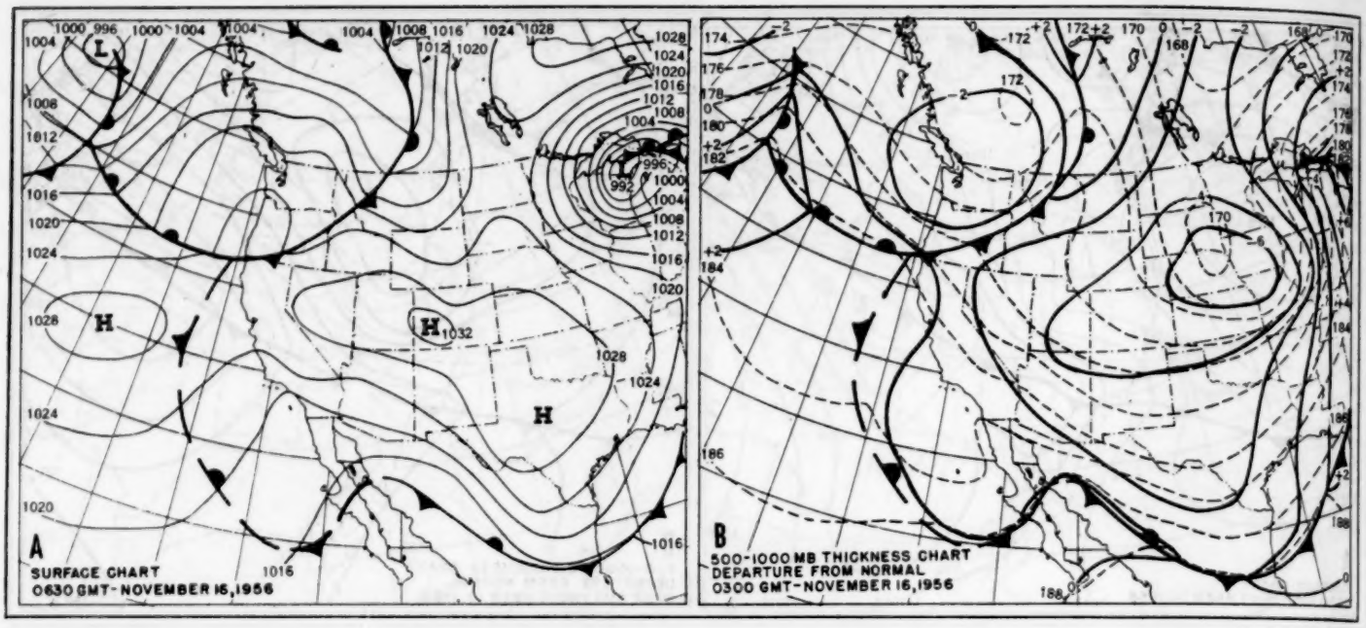

FIGURE 5.—November 16, 1956. (A) Surface fronts and isobars, 0630 GMT. (B) 1000–500-mb. thickness contours (dashed lines) and their departure (solid lines) from November thickness normals, 0300 GMT.

areas the 1000–500-mb. thickness departure from normal gradient (fig. 3B, solid lines) was perpendicular to the front south of the front, with a strong component parallel to the front north of the front. Furthermore, of all the strong departure from normal gradient south of the front over New Mexico, Texas Panhandle, and Kansas, none of the component parallel to the 1000–500-mb. thickness contours is appreciable.

At 0630 GMT of November 15 (fig. 4A), the cold front was located from Iowa to southeastern Oklahoma to western Texas, through northern Mexico, central Lower California, off the coast to 26° N., 117° W., and then northwestward. Here again the 1000–500-mb. thickness gradient discontinuity (fig. 4B) locates the front quite well over most of its length. From the southern border of Texas westward the 1000–500-mb. thickness departure from normal contours aid in showing the reality of the front. Offshore, both the thickness and the thickness anomaly gradient began to weaken and the front became difficult to locate.

The cold front reached its southernmost position on November 16. At 0630 GMT (fig. 5A), it lay from southeastern Mississippi and Louisiana southwestward through the western part of the Gulf of Mexico to the east coast of Mexico at 23° N., then northwestward to the northern Gulf of California. The 1000–500-mb. thickness and the 1000–500-mb. departure from normal thickness gradients (fig. 5B) still define this portion of the front quite well. However, the lack of anomaly gradient off the west coast demonstrates that any 1000–500-mb. thickness gradient in that area is purely climatological, so that the front can be frontolized.

The Plateau High was again established but at this time the High exhibited much colder temperatures than were observed prior to November 12.

3. CONCLUSIONS

Sutcliffe and Forsdyke said [3], "Any thickness line has a mean seasonal position, which can be represented by mean charts, and departure from the mean position is an immediate and significant indication that physical processes are operating to maintain the temperature anomalies." Specifically, there is considerable information about frontal discontinuities to be gained from a consideration of the contour gradients of the thickness anomaly chart. The subtraction of normal thicknesses from the synoptic thickness chart leaves more obvious the gradient discontinuity caused by a front. A cursory examination of the day-by-day relationships between the fronts and the anomaly patterns suggests the following conclusions:

(1) A sharp front with a strong thickness discontinuity shows also a strong anomaly gradient discontinuity.

(2) The scalar magnitude of the anomaly field is of no significance in delineating a front. The vector difference of the components of the gradients parallel to the front is the only important measurement.

(3) There are some areas of the normal thickness chart which contain contiguous gradient differences of sufficient magnitude to suggest the existence of a front. In these areas the anomaly gradient can be near zero when the front lies along this normal thickness gradient discontinuity. Thus, a thickness departure from normal gradient discontinuity can be said to be a sufficient but not necessary criterion to define a frontal discontinuity.

(4) A better tool than a normal thickness chart for deriving an anomaly would be a normal tropical-air thickness chart. This chart should be an average of thickness measurements made exclusively south of the polar front at each station. Sutcliffe's [3] extreme maximum charts approximate these normals except that they represent the one extreme maximum instead of the average of many warm situations. The contours of the departures from this normal tropical-air chart would better show the frontal boundary between the polar and tropical air.

4. SUMMARY

There are times and areas when the synoptic thickness gradient discontinuities associated with the presence of a front are not obvious to the analyst, because of the existence of a strong climatological temperature gradient. For many of these times, as illustrated by the case of November 12–16, 1956, consideration of the thickness anomaly gradient discontinuities is a helpful procedure.

ACKNOWLEDGMENTS

The authors are grateful to the staff of NAWAC for many interesting and productive discussions of the subject of this article, and to the Daily Map Unit of the Weather Bureau for drafting the charts.

REFERENCES

1. Walter J. Saucier, *Principles of Meteorological Analysis*, University of Chicago Press, Chicago, 1955. (See pp. 277 and 383.)
2. J. Vederman, oral communication at NAWAC map discussion, Dec. 14, 1956.
3. R. C. Sutcliffe, and A. G. Forsdyke, "The Theory and Use of Upper Air Thickness Patterns in Forecasting," *Quarterly Journal of the Royal Meteorological Society*, vol. LXXVI, No. 328, April 1950, pp. 189–217. (See pp. 198–199.)

U. S. GOVERNMENT PRINTING OFFICE: 1957

Chart I. A. Average Temperature (°F.) at Surface, November 1956.

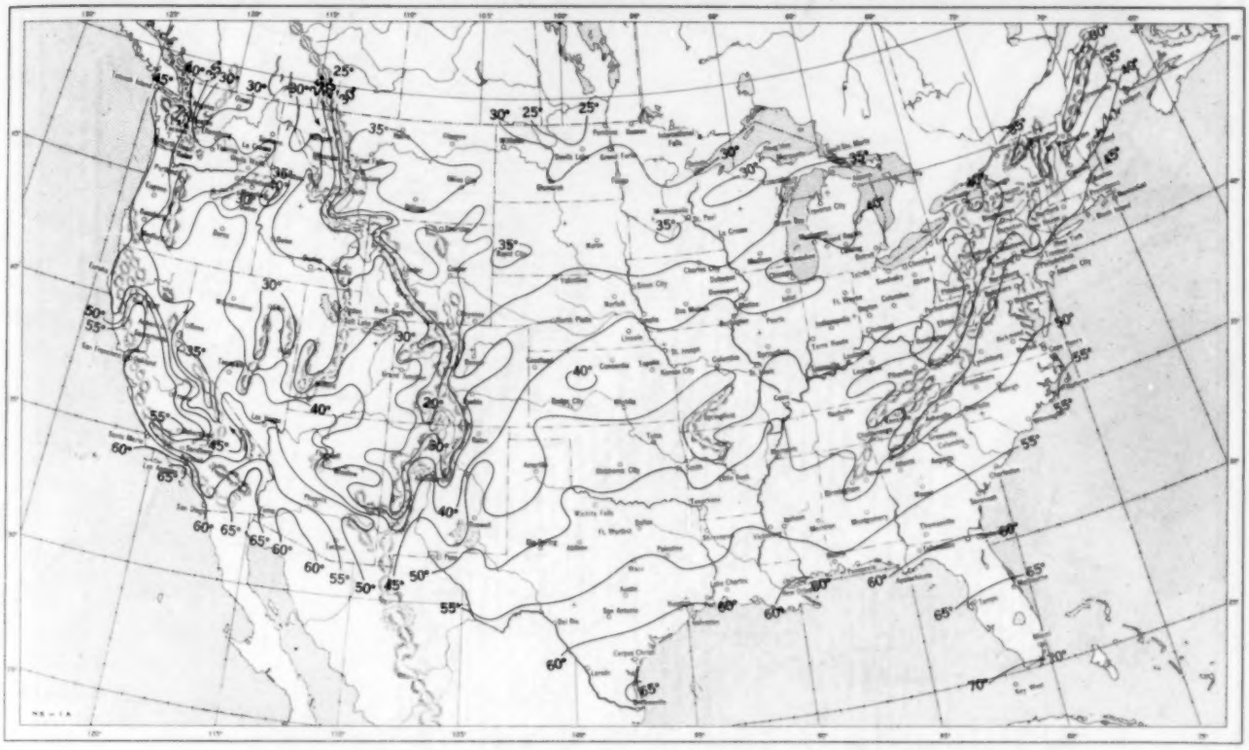

B. Departure of Average Temperature from Normal (°F.), November 1956.

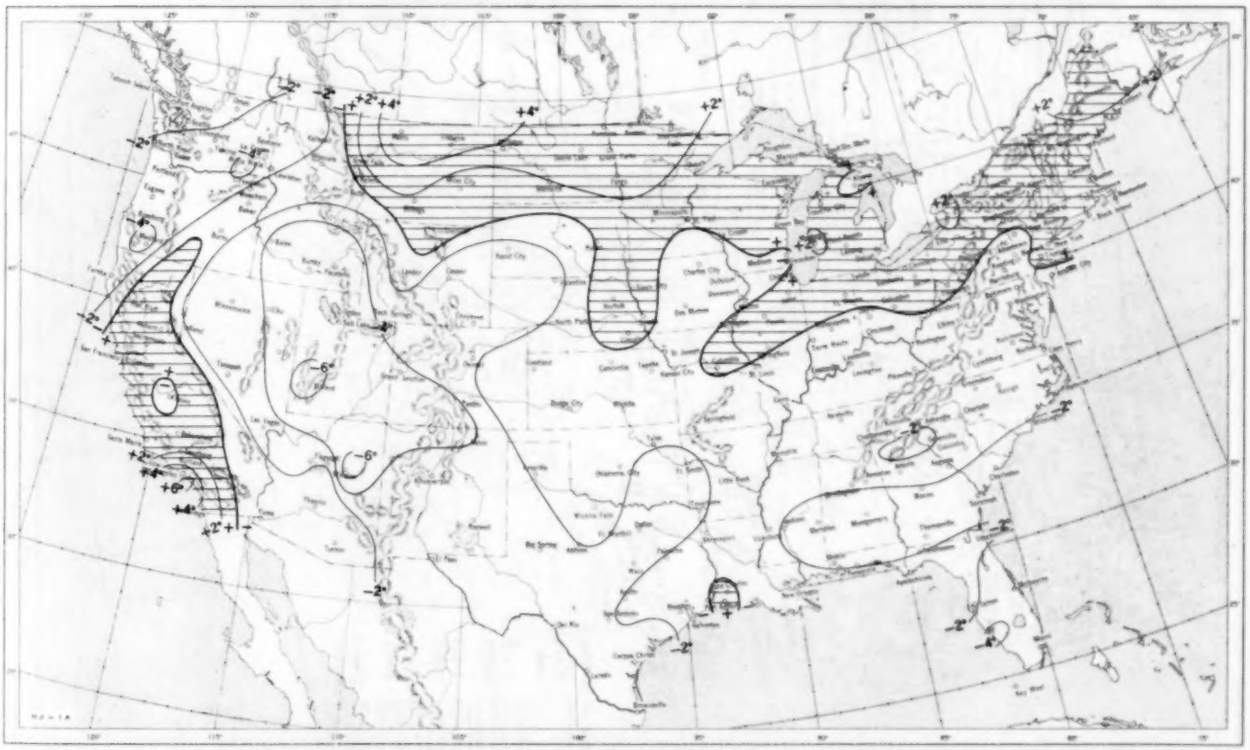

A. Based on reports from 800 Weather Bureau and cooperative stations. The monthly average is half the sum of the monthly average maximum and monthly average minimum, which are the average of the daily maxima and daily minima, respectively.
B. Normal average monthly temperatures are computed for Weather Bureau stations having at least 10 years of record.

Chart II. Total Precipitation (Inches), November 1956.

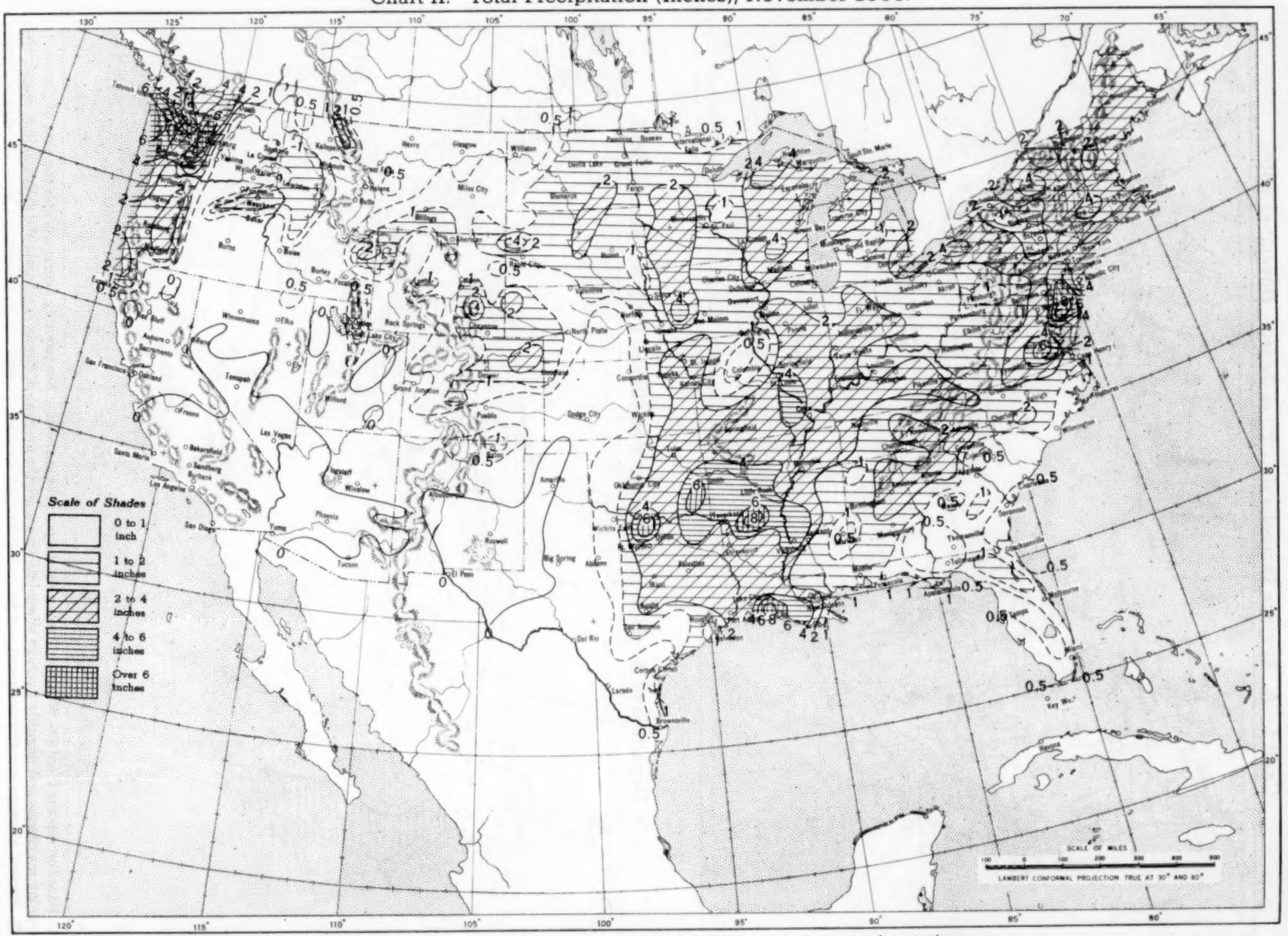

Based on daily precipitation records at 800 Weather Bureau and cooperative stations.

Chart III. A. Departure of Precipitation from Normal (Inches), November 1956.

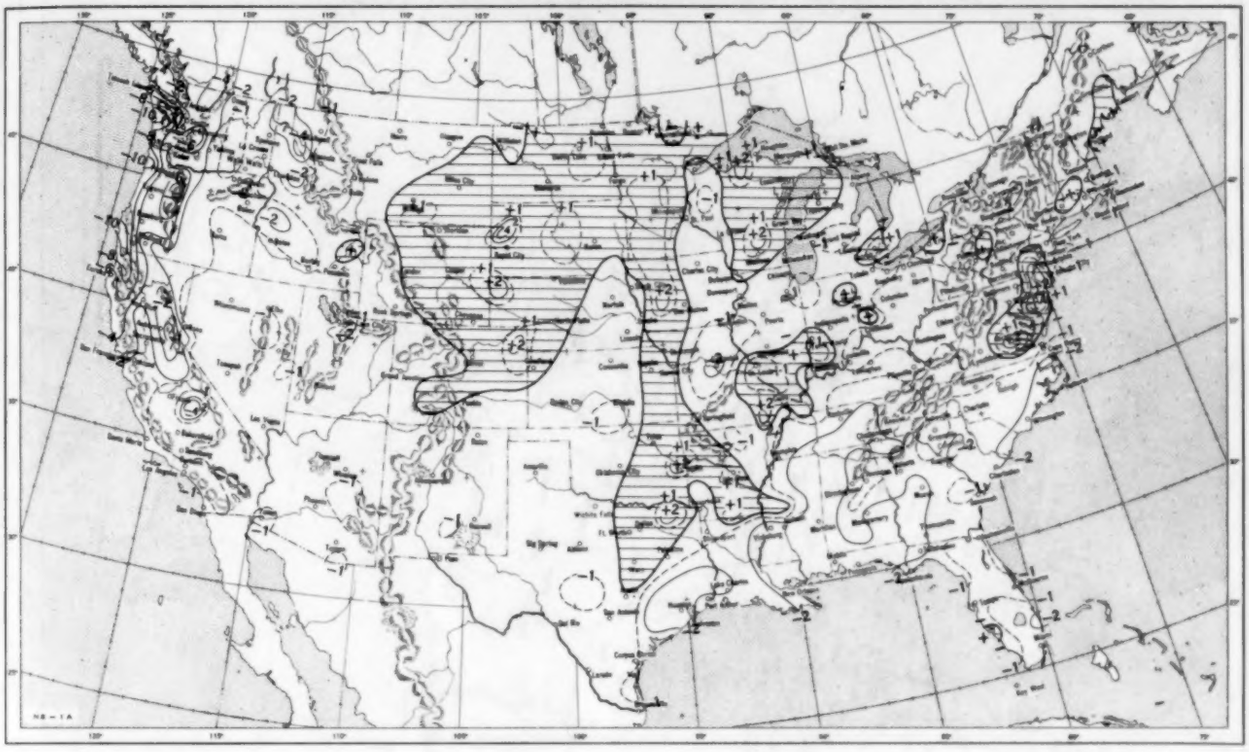

B. Percentage of Normal Precipitation, November 1956.

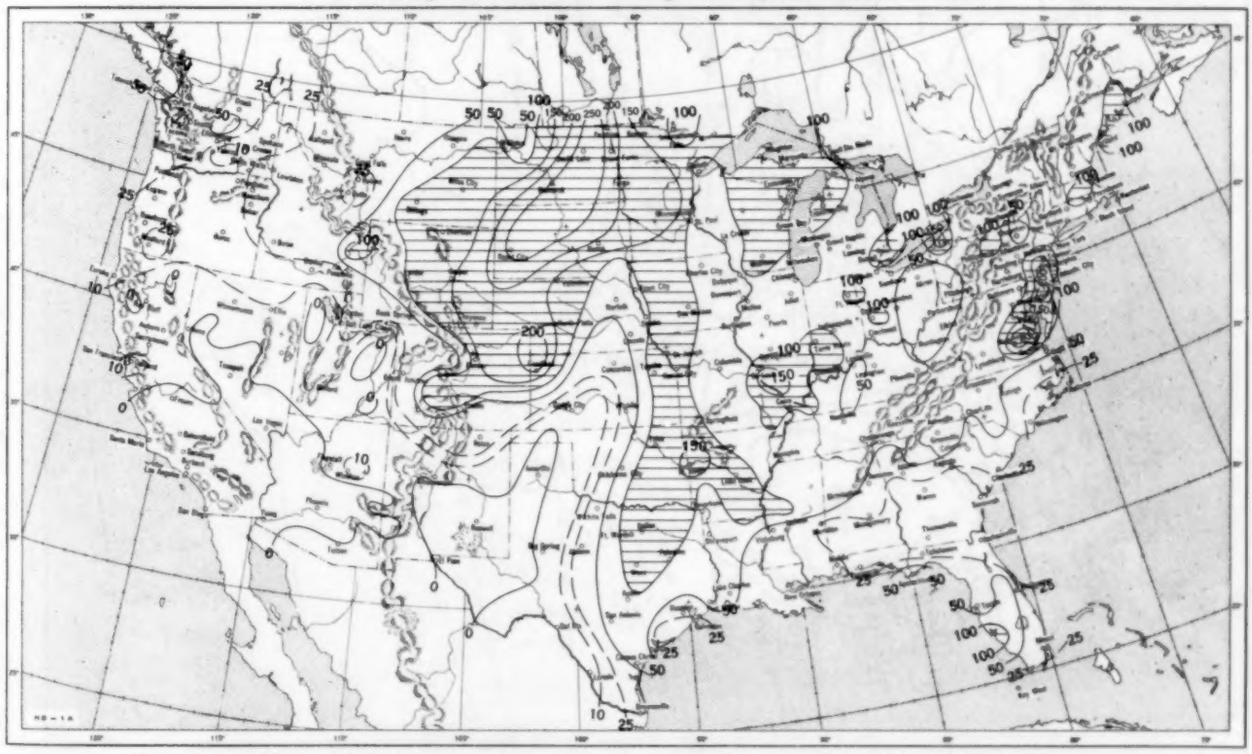

Normal monthly precipitation amounts are computed for stations having at least 10 years of record.

Chart IV. Total Snowfall (Inches), November 1956.

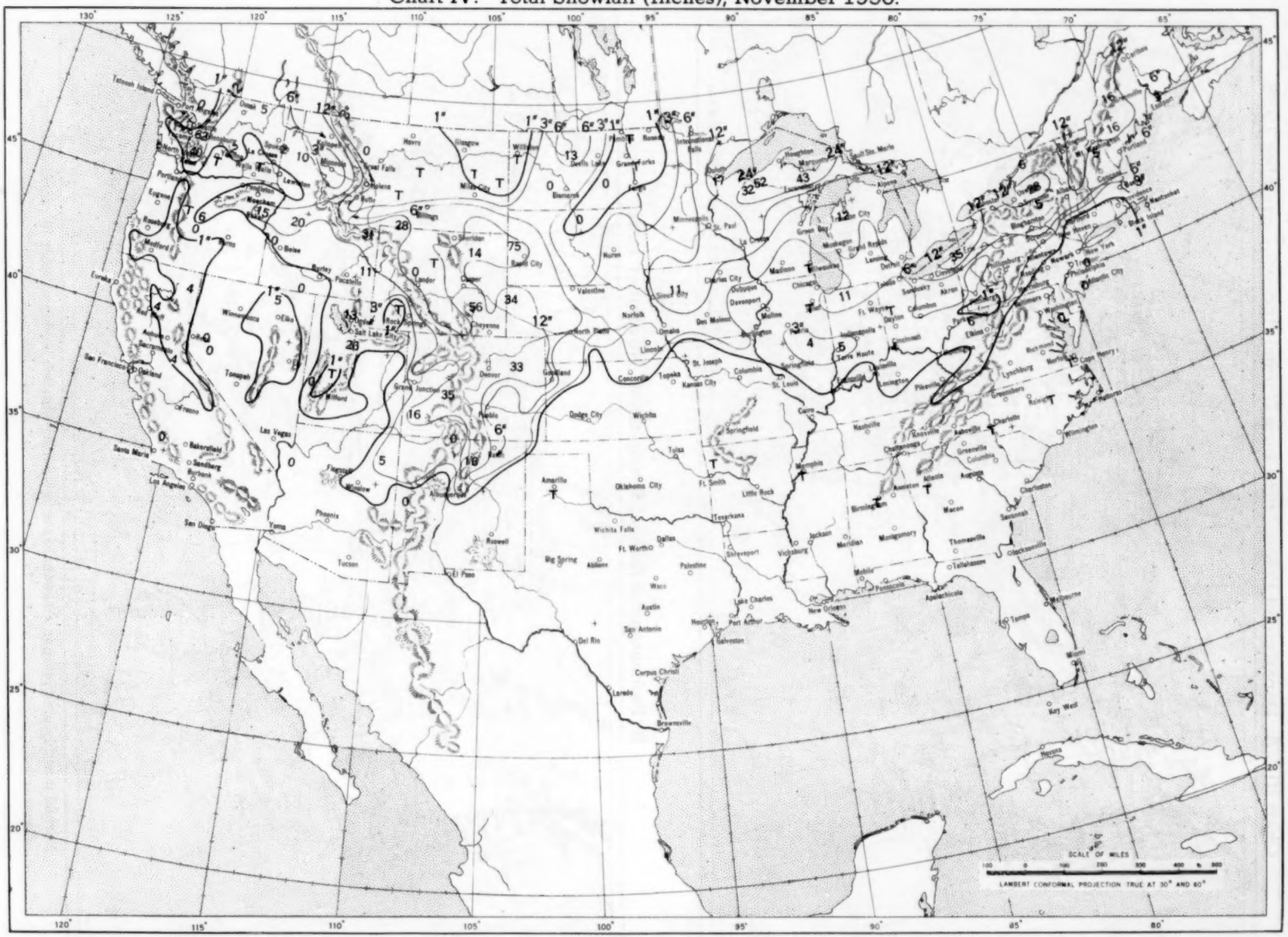

This is the total of unmelted snowfall recorded during the month at Weather Bureau and cooperative stations. This chart and Chart V are published only for the months of November through April although of course there is some snow at higher elevations, particularly in the far West, earlier and later in the year.

Chart V. A. Percentage of Normal Snowfall, November 1956.

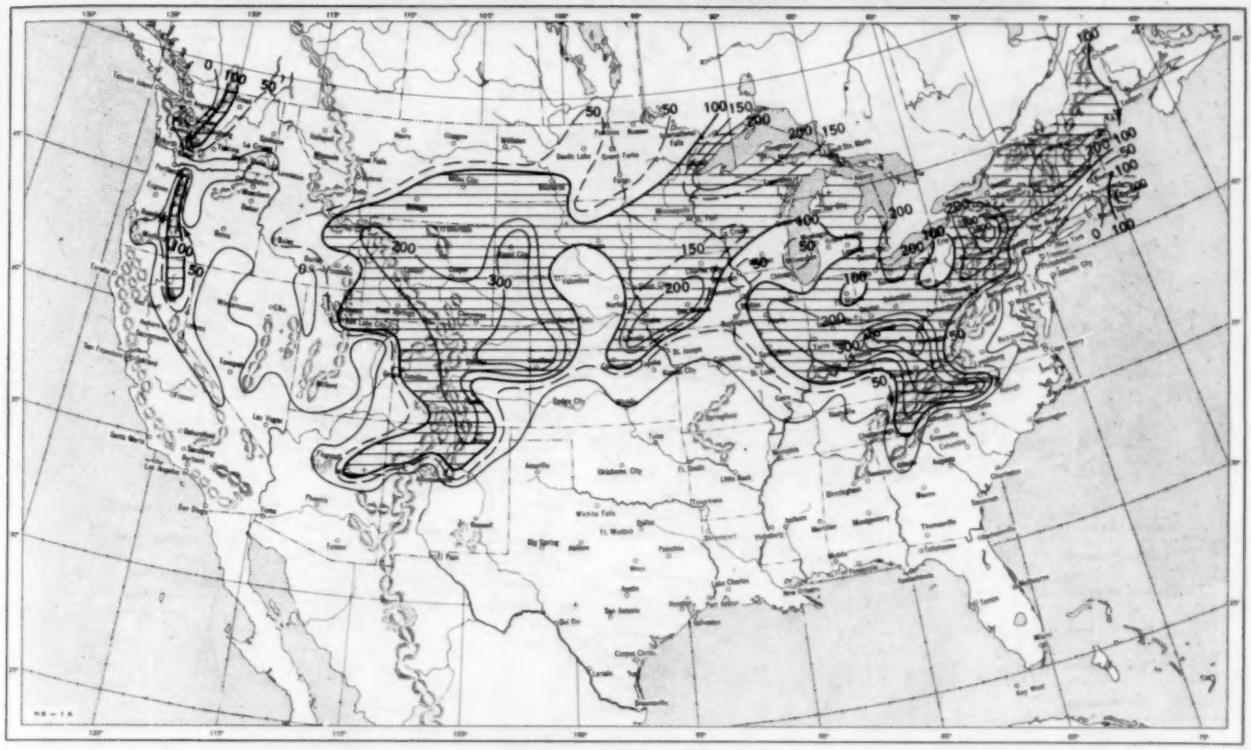

B. Depth of Snow on Ground (Inches).

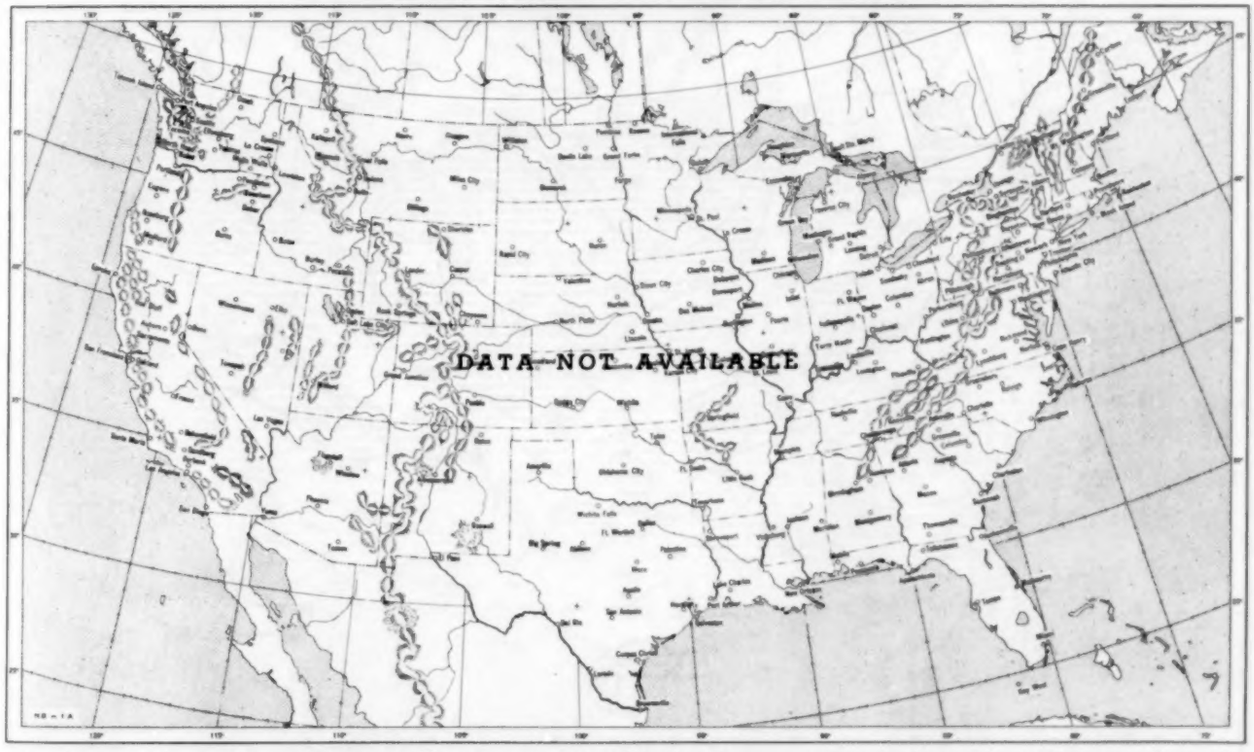

A. Amount of normal monthly snowfall is computed for Weather Bureau stations having at least 10 years of record.
B. Shows depth currently on ground at 7:30 a.m. E.S.T., of the Tuesday nearest the end of the month. It is based on reports from Weather Bureau and cooperative stations. Dashed line shows greatest southern extent of snowcover during month.

Chart VI. A. Percentage of Sky Cover Between Sunrise and Sunset, November 1956.

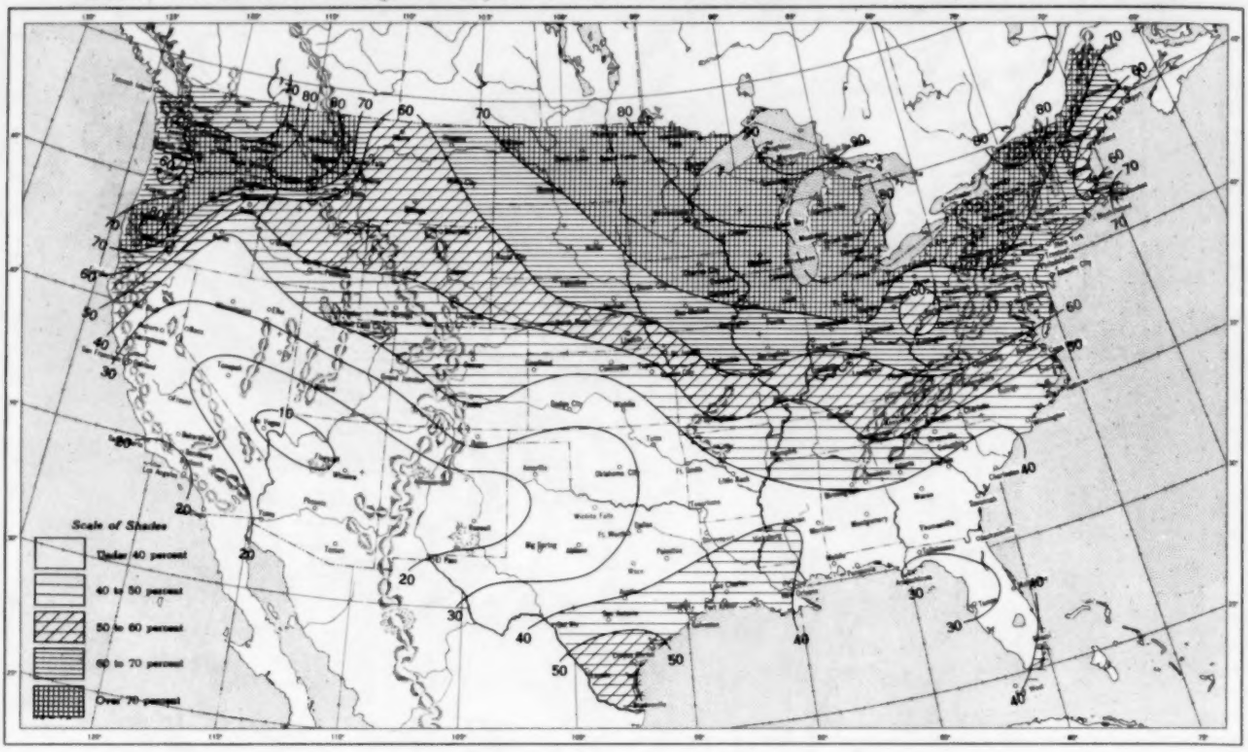

B. Percentage of Normal Sky Cover Between Sunrise and Sunset, November 1956.

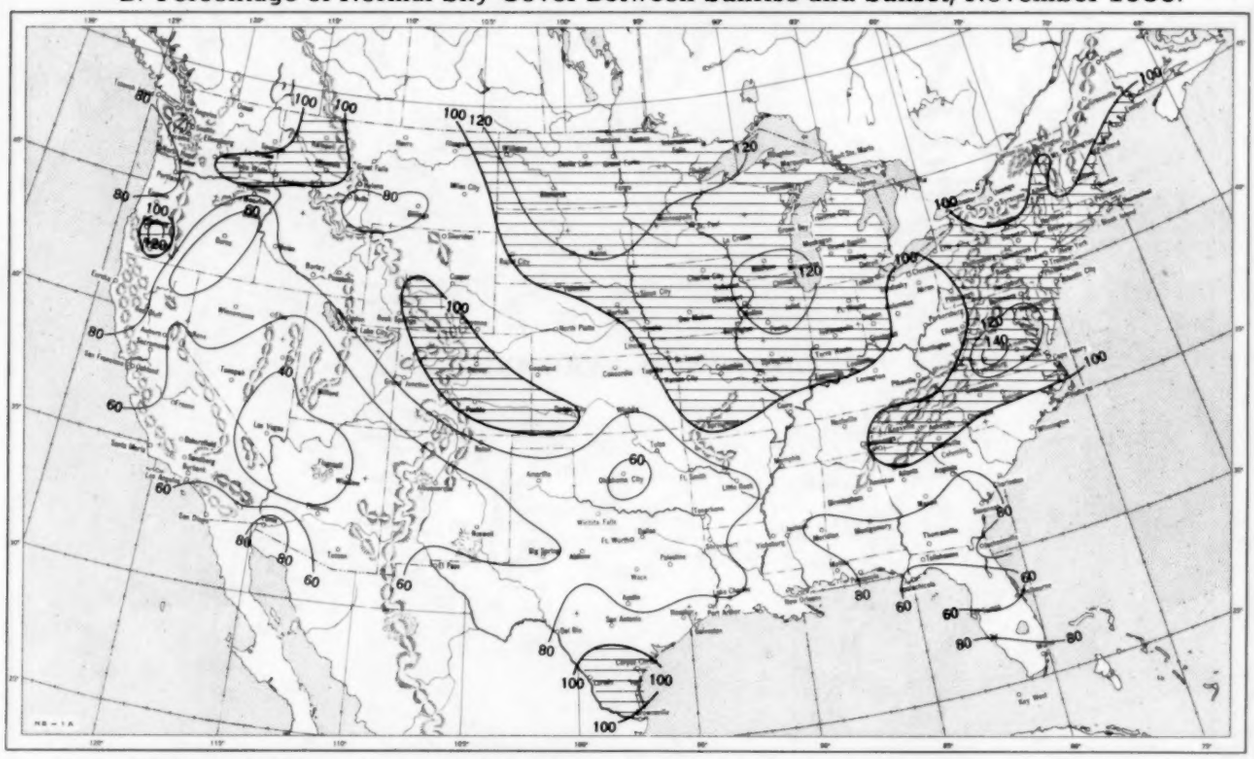

A. In addition to cloudiness, sky cover includes obscuration of the sky by fog, smoke, snow, etc. Chart based on visual observations made hourly at Weather Bureau stations and averaged over the month. B. Computations of normal amount of sky cover are made for stations having at least 10 years of record.

Chart VII. A. Percentage of Possible Sunshine, November 1956.

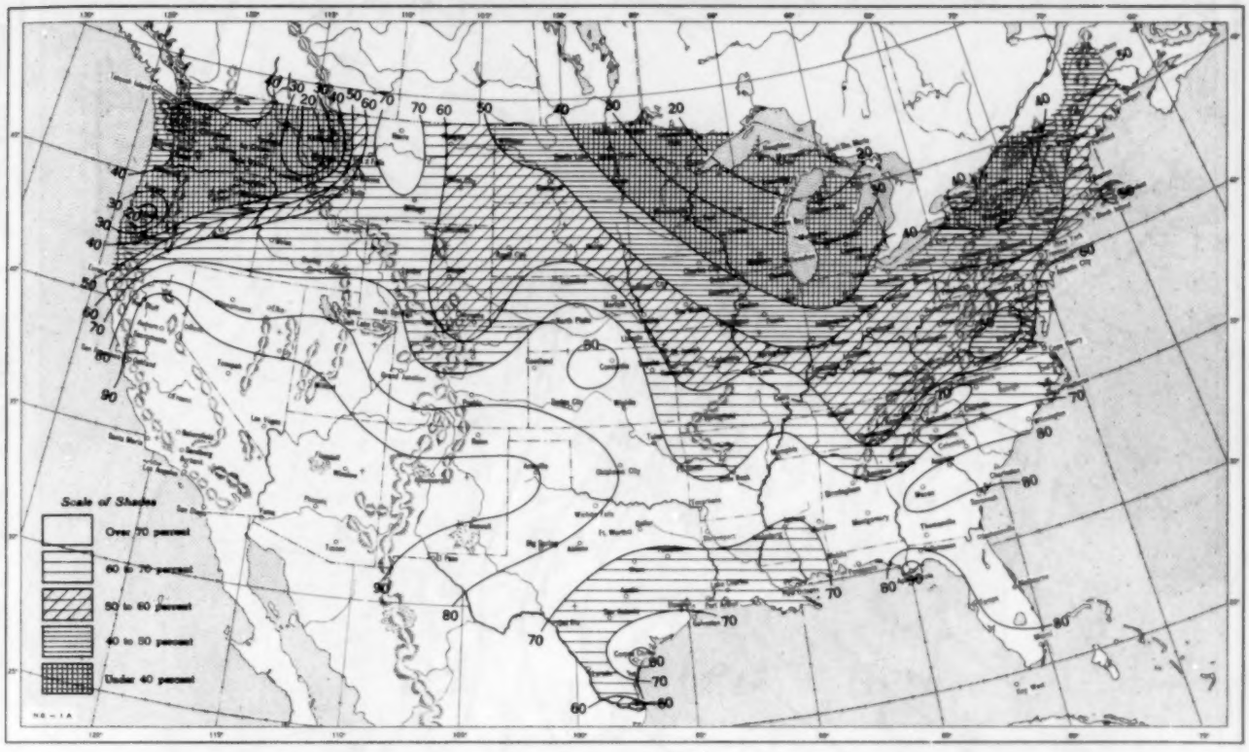

B. Percentage of Normal Sunshine, November 1956.

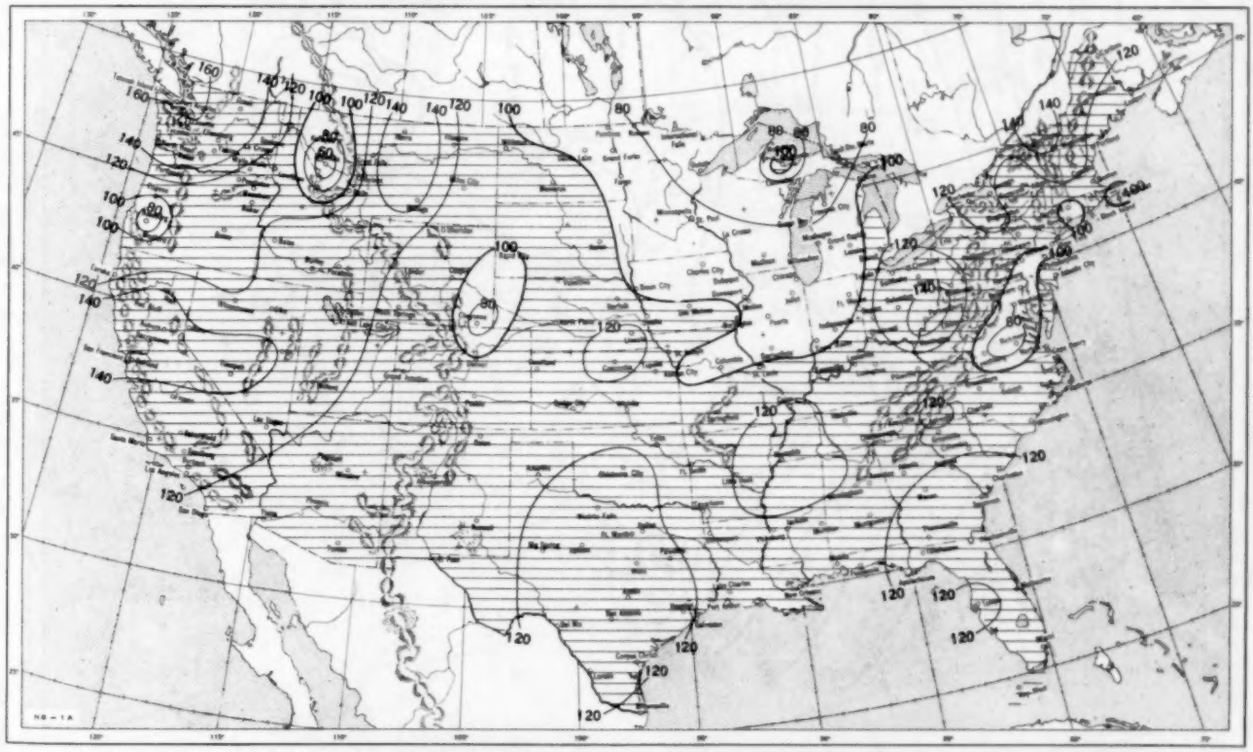

A. Computed from total number of hours of observed sunshine in relation to total number of possible hours of sunshine during month. B. Normals are computed for stations having at least 10 years of record.

Chart VIII. Average Daily Values of Solar Radiation, Direct + Diffuse, November 1956. Inset: Percentage of Mean Daily Solar Radiation, November 1956. (Mean based on period 1951-55.)

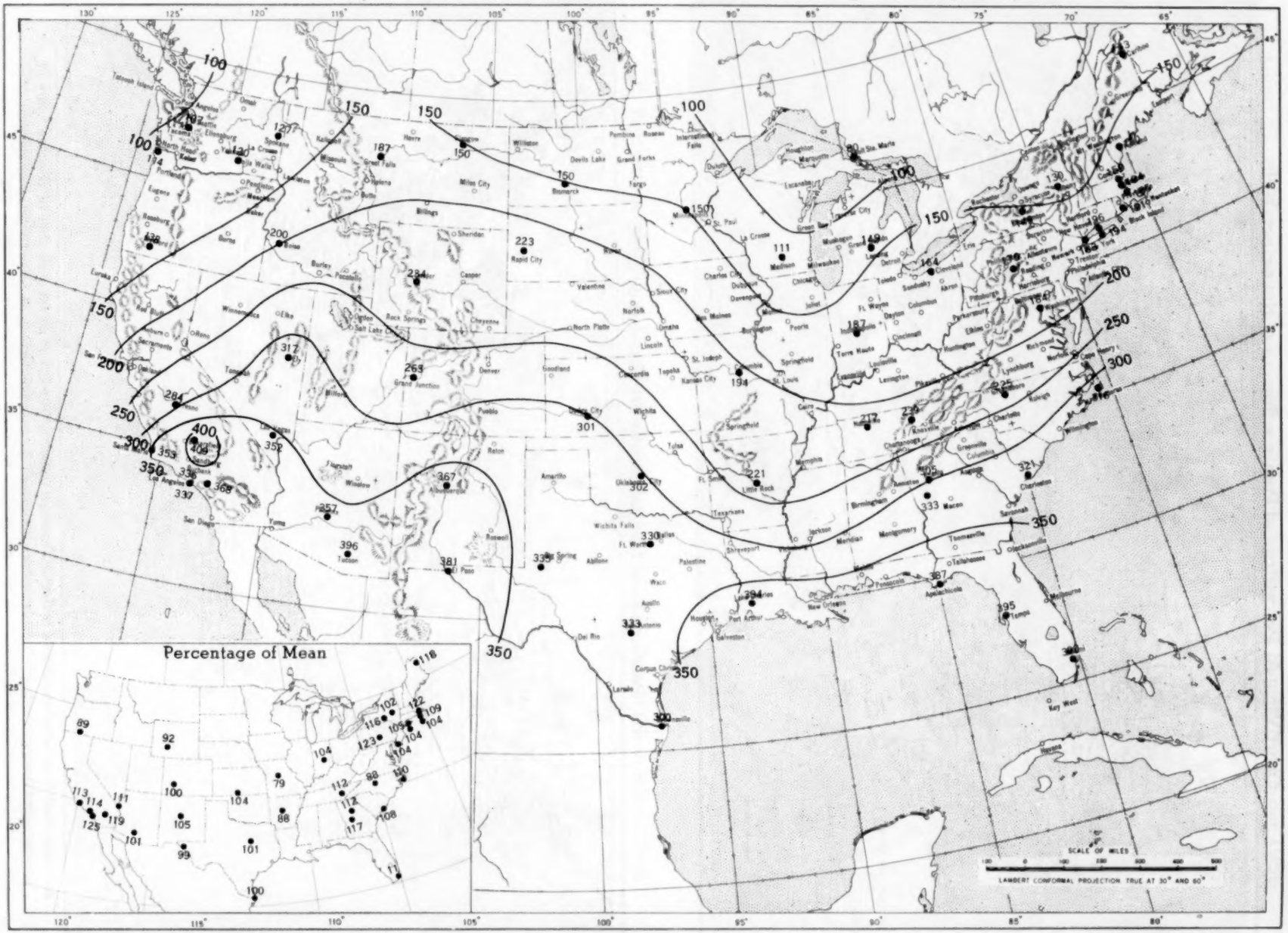

Chart shows mean daily solar radiation, direct + diffuse, received on a horizontal surface in langleys (1 langley = 1 gm. cal. cm. $^{-2}$). Basic data for isolines are shown on chart. Further estimates are obtained from supplementary data for which limits of accuracy are wider than for those data shown.

Chart IX. Tracks of Centers of Anticyclones at Sea Level, November 1956.

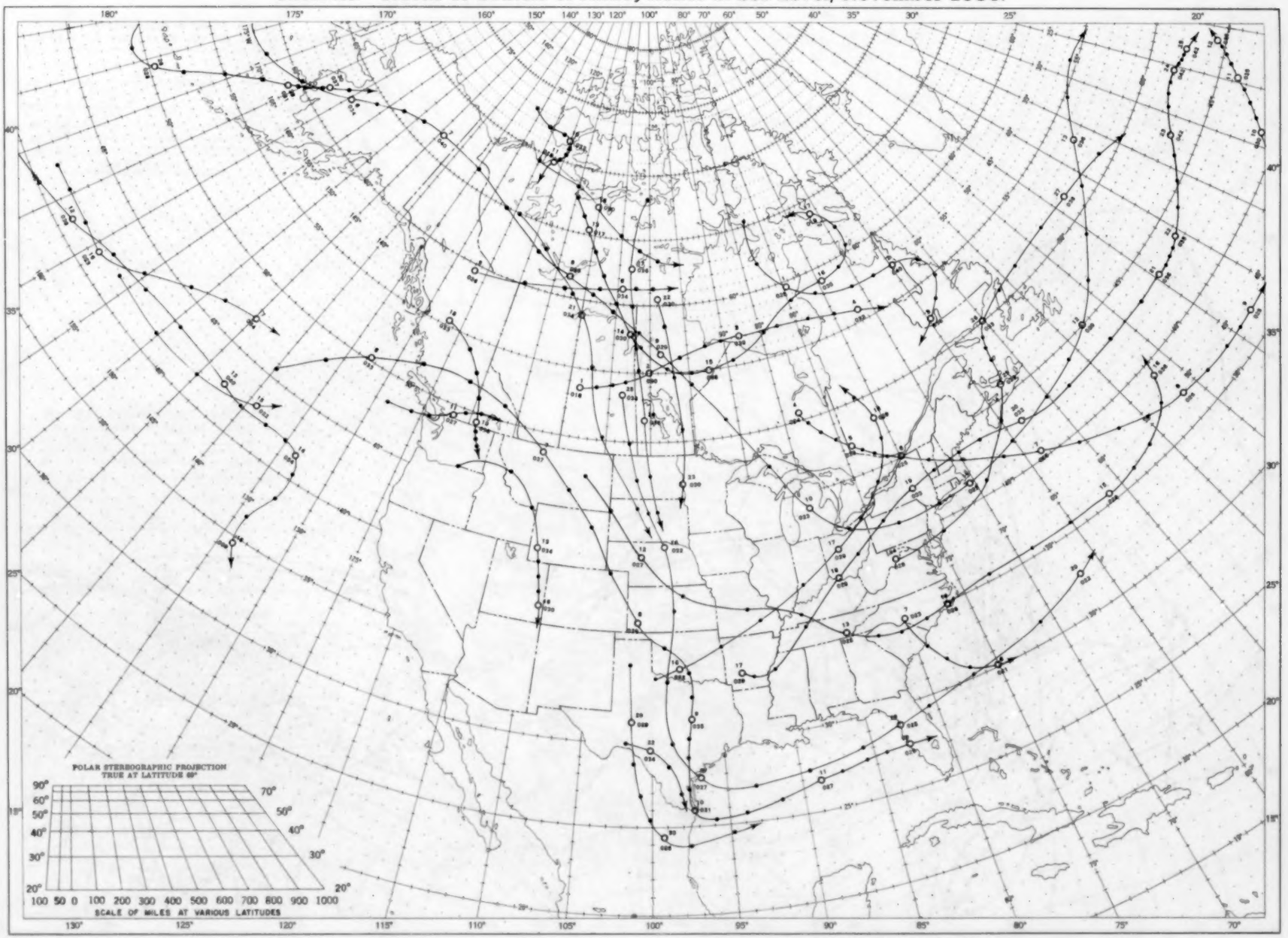

Circle indicates position of center at 7:30 a. m. E. S. T. Figure above circle indicates date, figure below, pressure to nearest millibar. Dots indicate intervening 6-hourly positions. Squares indicate position of stationary center for period shown. Dashed line in track indicates reformation at new position. Only those centers which could be identified for 24 hours or more are included.

Chart X. Tracks of Centers of Cyclones at Sea Level, November 1956.

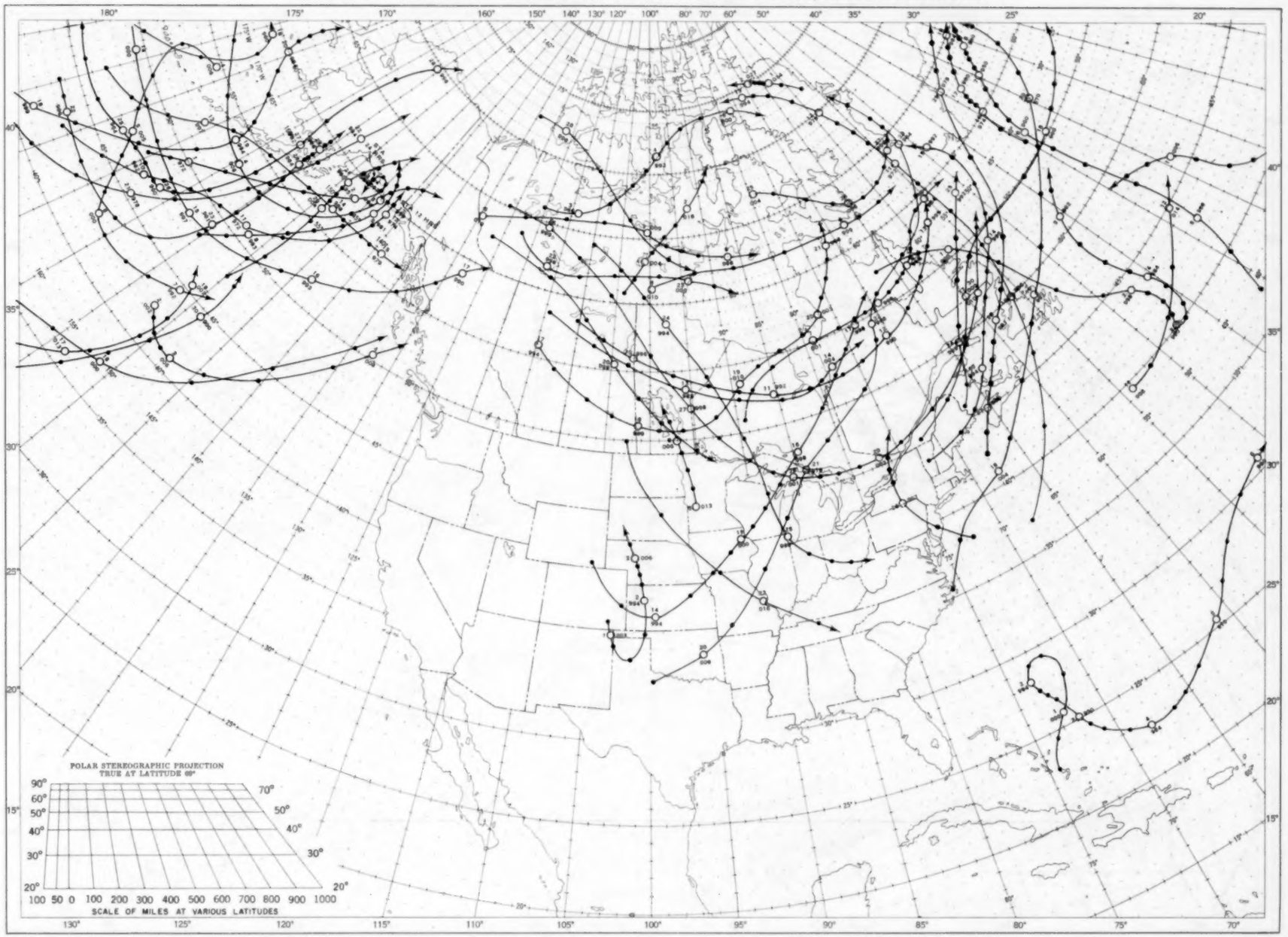

Circle indicates position of center at 7:30 a. m. E. S. T. See Chart IX for explanation of symbols.

Chart XI. Average Sea Level Pressure (mb.) and Surface Windroses, November 1956. Inset: Departure of Average Pressure (mb.) from Normal, November 1956.

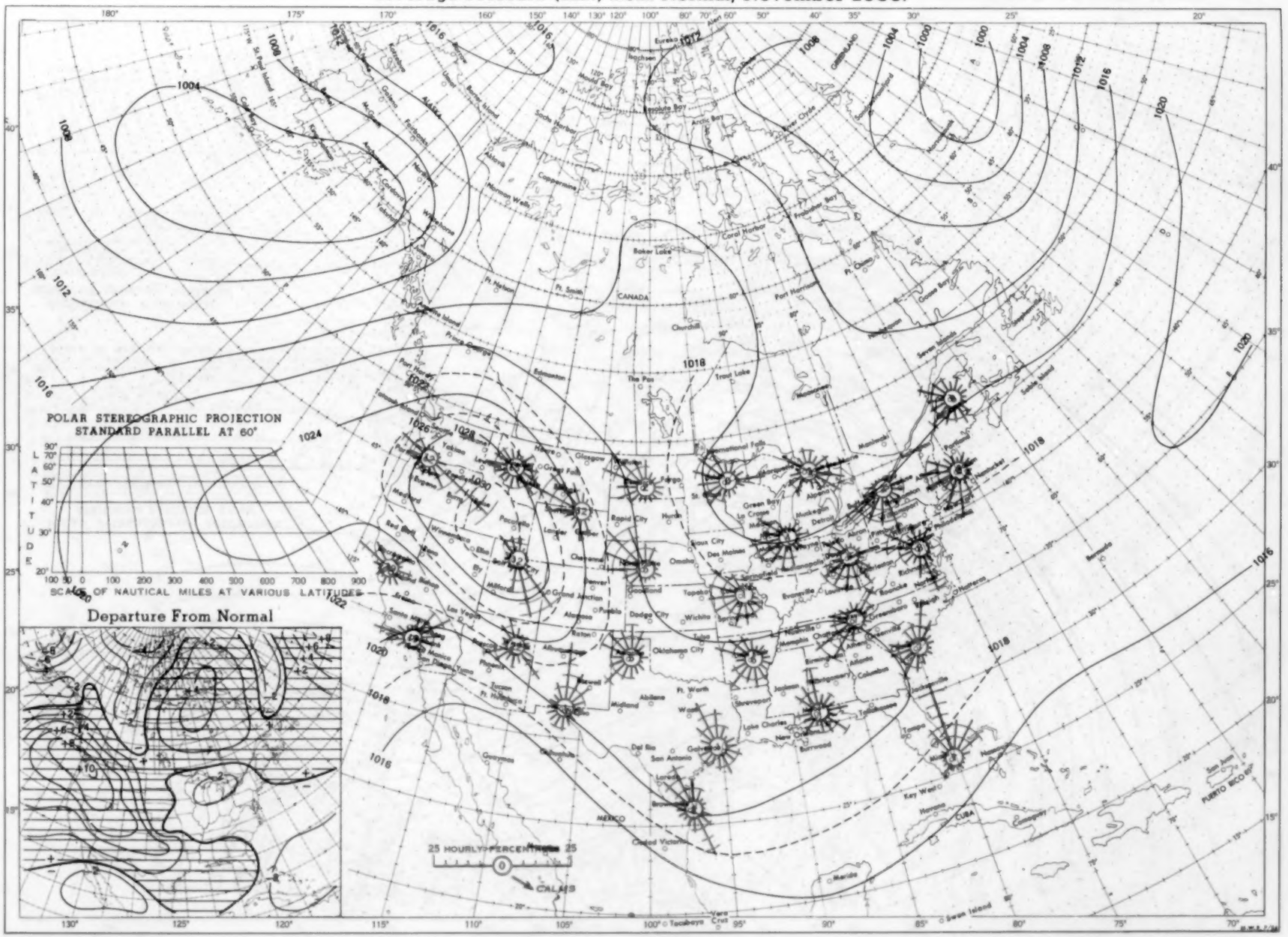

Average sea level pressures are obtained from the averages of the 7:30 a. m. and 7:30 p. m. E. S. T. readings. Windroses show percentage of time wind blew from 16 compass points or was calm during the month. Pressure normals are computed for stations having at least 10 years of record and for 10° intersections in a diamond grid based on readings from the Historical Weather Maps (1899-1939) for the 20 years of most complete data coverage prior to 1940.

Chart XII. 850-mb. Surface, 0300 GMT, November 1956. Average Height and Temperature, and Resultant Winds.

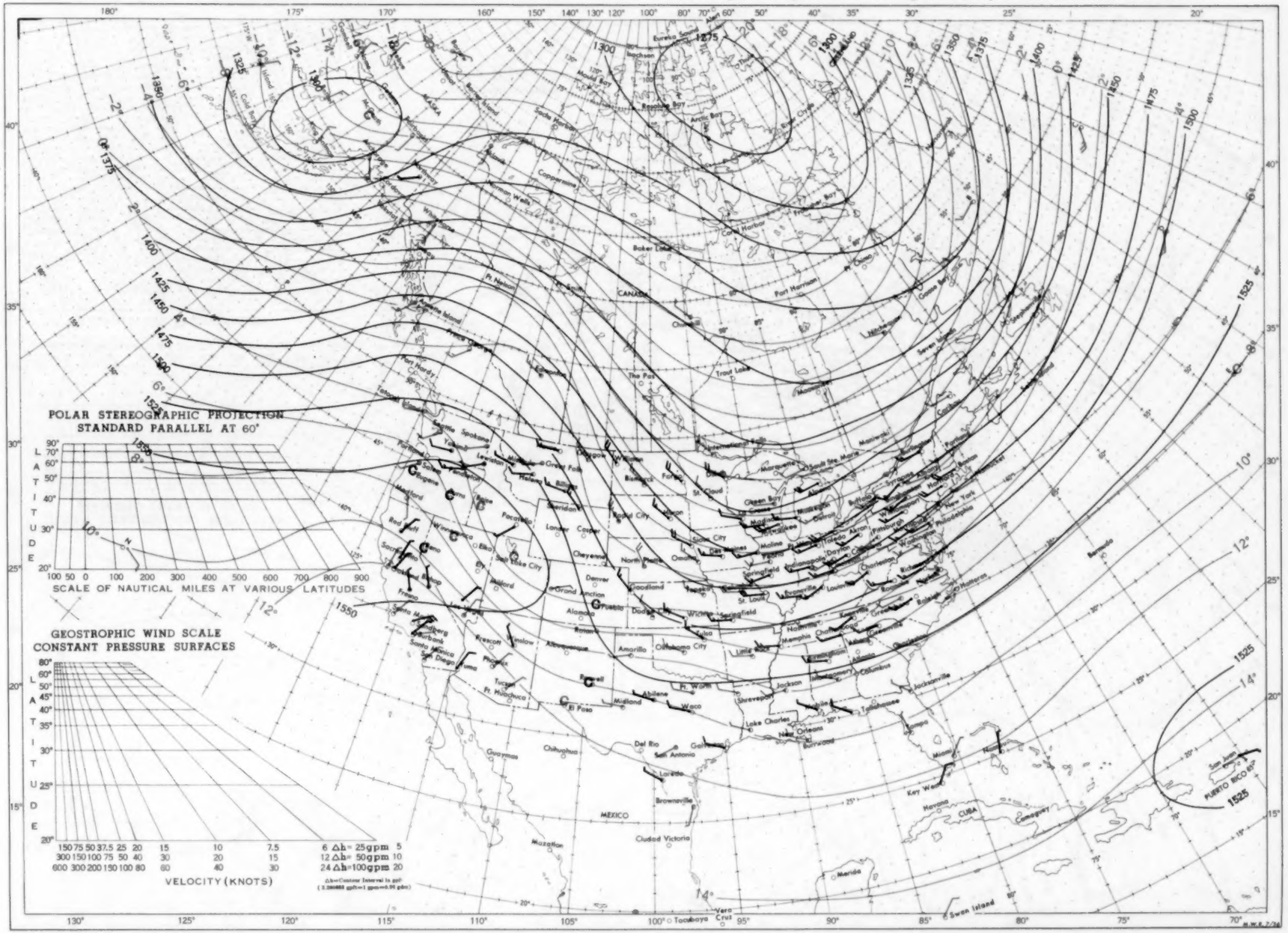

Height in geopotential meters (1 g.p.m. = 0.98 dynamic meters). Temperature in °C. Wind speed in knots; flag represents 50 knots, full feather 10 knots, and half feather 5 knots. Winds shown in red are based on rawins taken at the indicated pressure surface and time. Those in black are based on pibals taken at 2100 GMT and are for the nearest standard height level.

on pibals taken at 2100 GMT and are for the nearest standard height level.

Chart XIII. 700-mb. Surface, 0300 GMT, November 1956. Average Height and Temperature, and Resultant Winds.

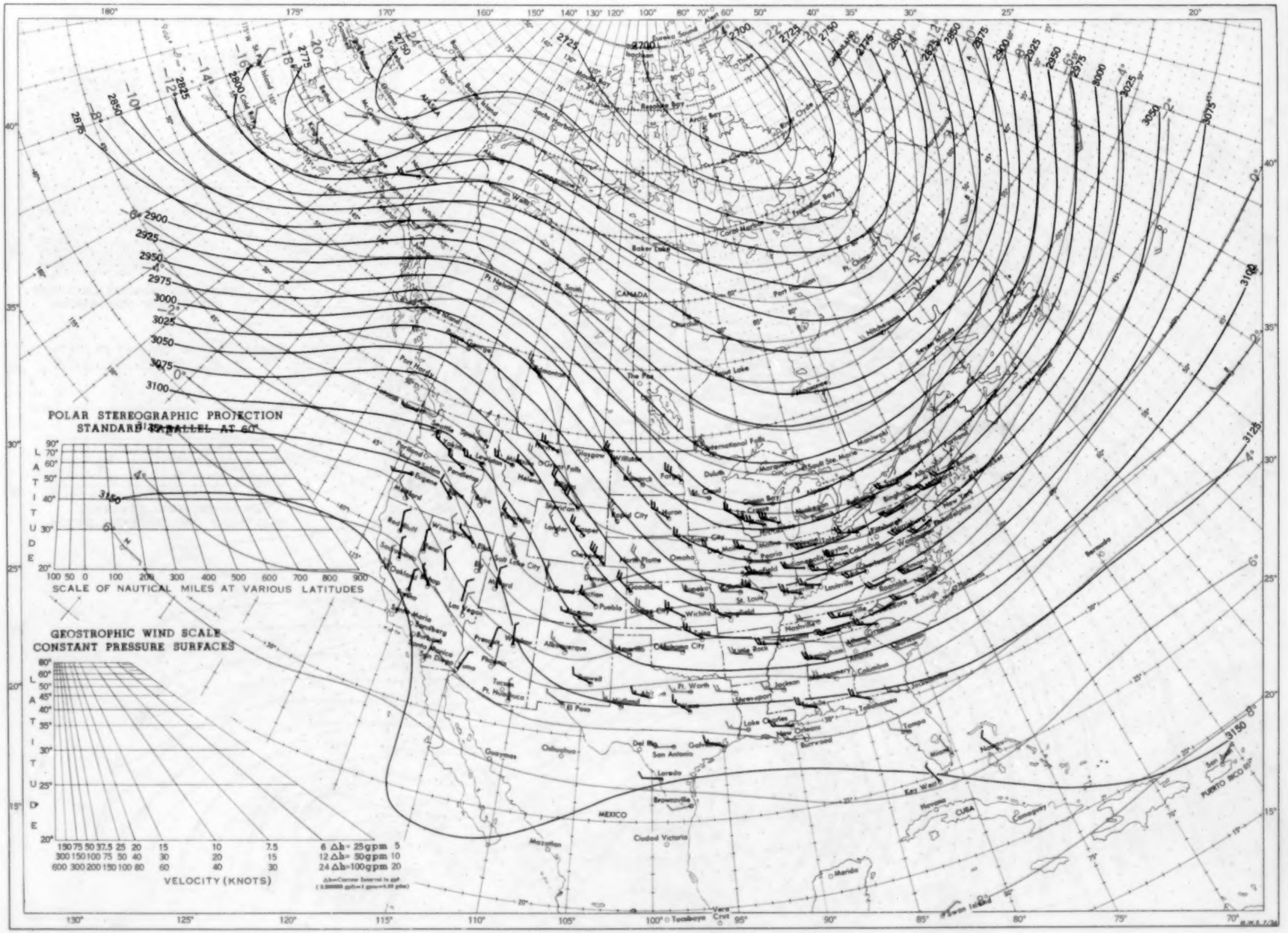

See Chart XII for explanation of map.

Chart XIV. 500-mb. Surface, 0300 GMT, November 1956. Average Height and Temperature, and Resultant Winds.

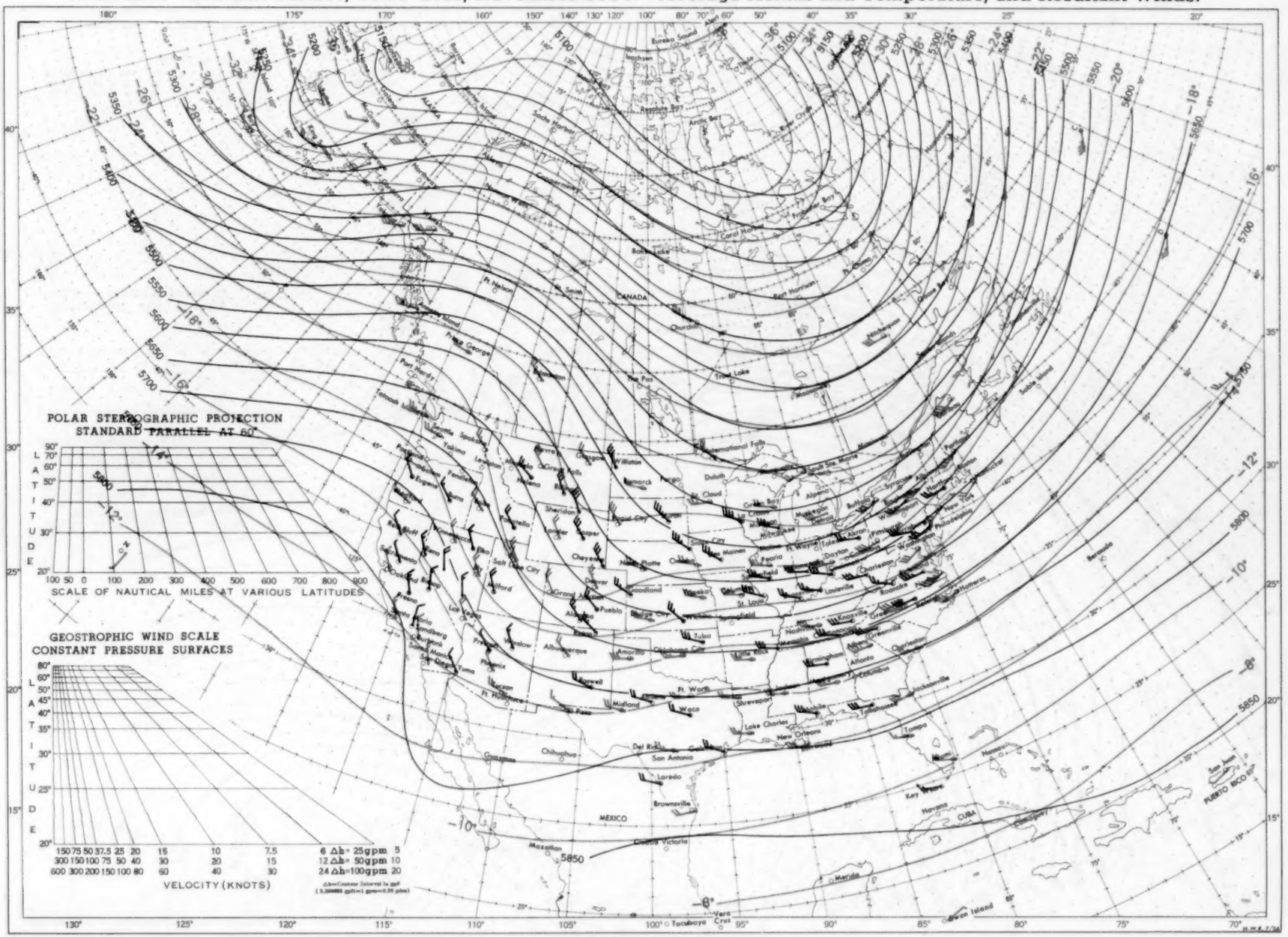

See Chart XII for explanation of map.

Chart XV. 300-mb. Surface, 0300 GMT, November 1956. Average Height and Temperature, and Resultant Winds.

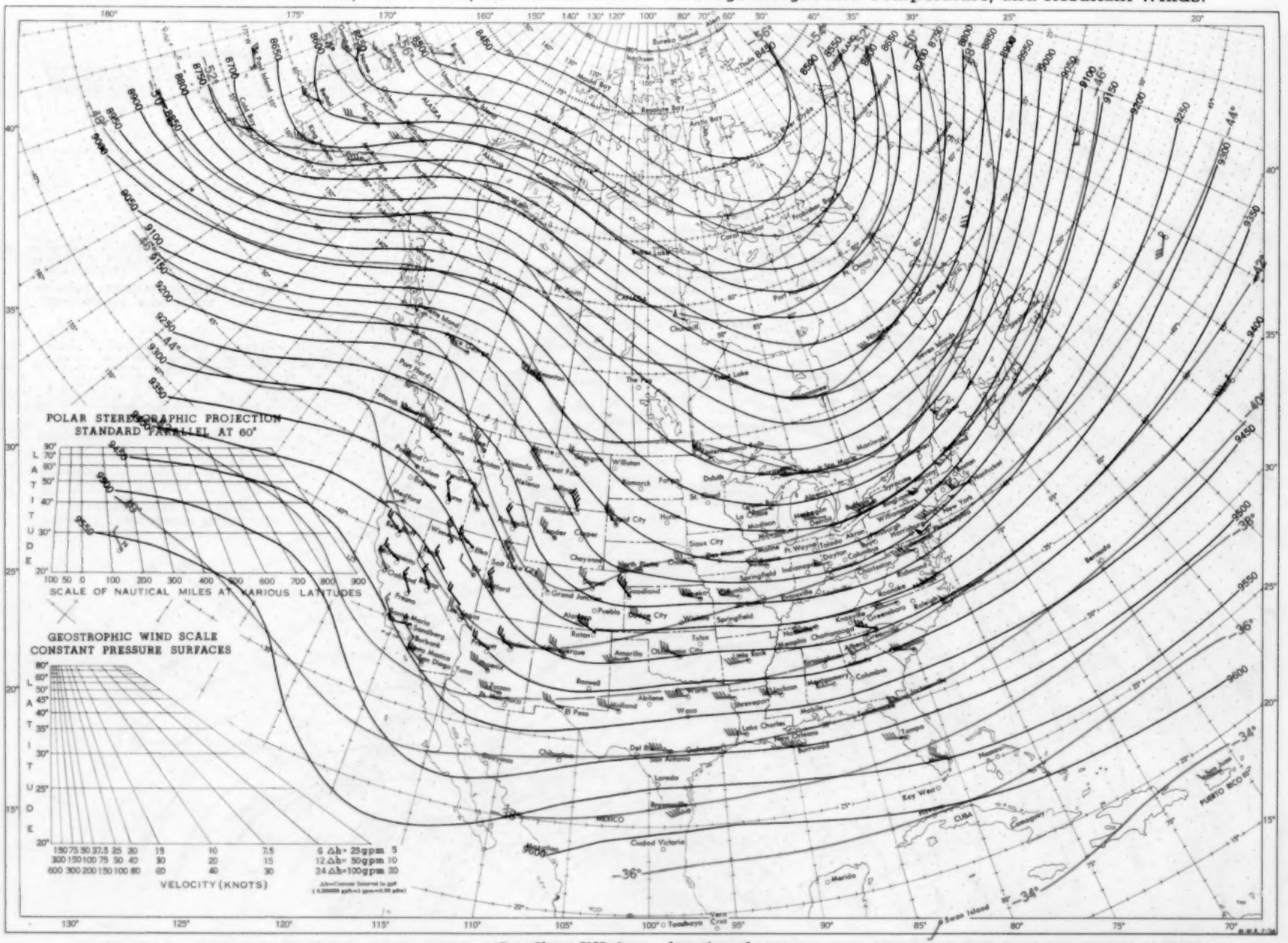

See Chart XII for explanation of map.

Chart XVI. 200-mb. Surface, 0300 GMT, November 1956. Average Height and Temperature, and Resultant Winds.

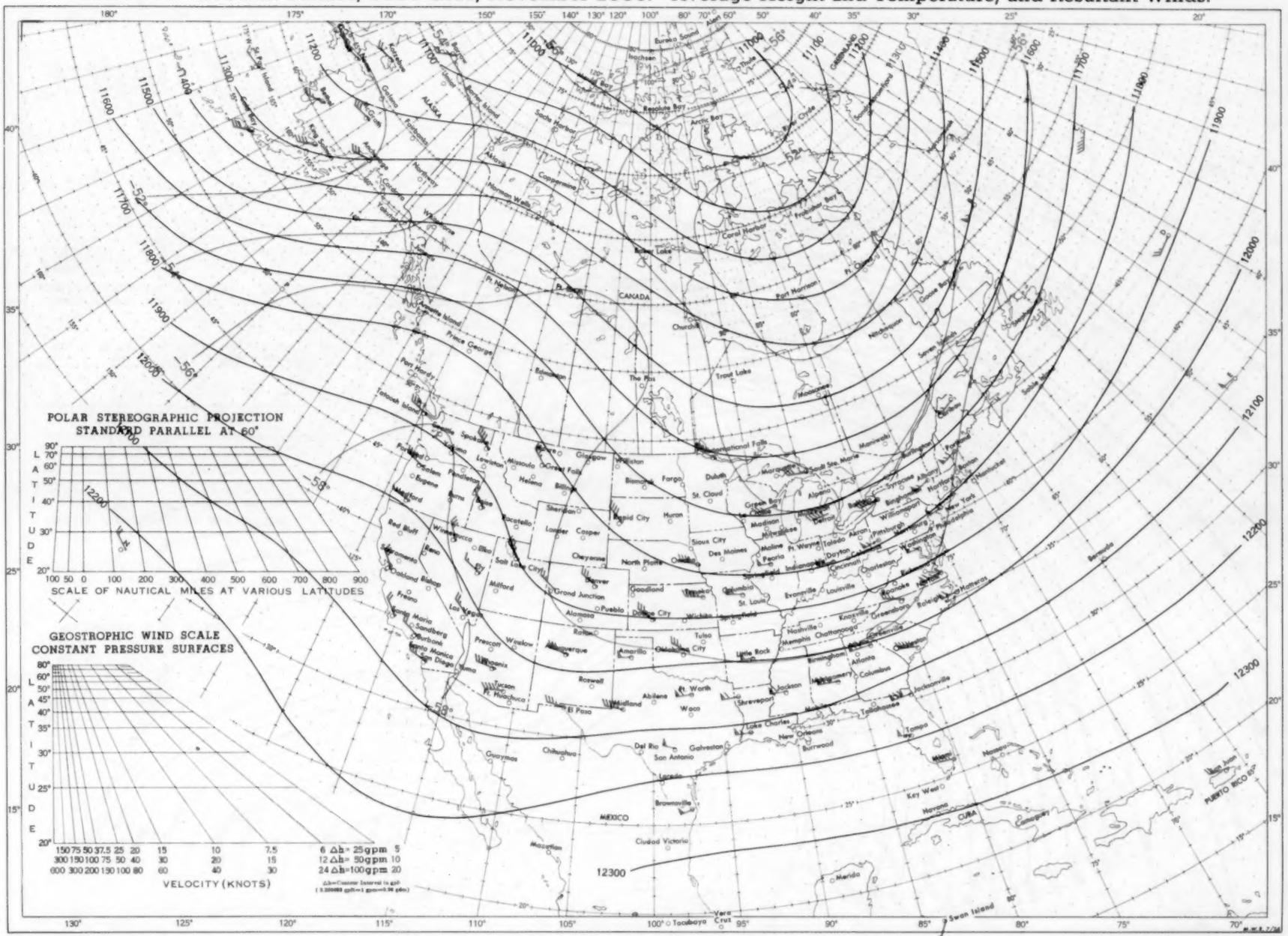

See Chart XII for explanation of map. All winds are from rawin reports.

Chart XVII. 100-mb. Surface, 0300 GMT, November 1956. Average Height and Temperature, and Resultant Winds.

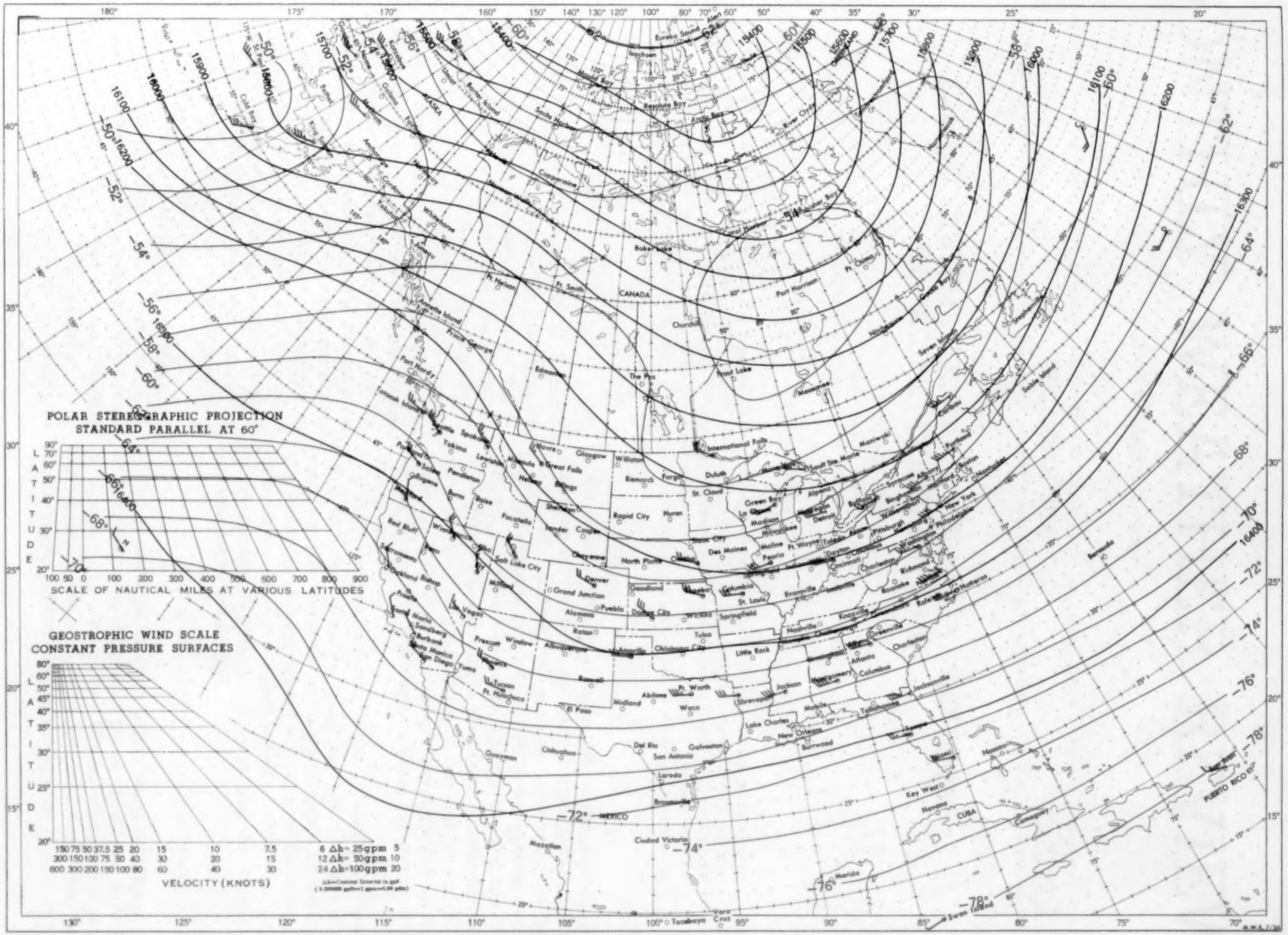

See Chart XII for explanation of map. All winds are from rawin reports.